NATIONAL AERONAUTICS AND SPACE ADMINISTRATION

Space Programs Summary 37-48, Vol. I

Flight Projects

For the Period September 1 to October 31, 1967

JET PROPULSION LABORATORY
CALIFORNIA INSTITUTE OF TECHNOLOGY
PASADENA, CALIFORNIA

November 30, 1967

NATIONAL AERONAUTICS AND SPACE ADMINISTRATION

Space Programs Summary 37-48, Vol. I

Flight Projects

For the Period September 1 to October 31, 1967

JET PROPULSION LABORATORY
CALIFORNIA INSTITUTE OF TECHNOLOGY
PASADENA, CALIFORNIA

November 30, 1967

SPACE PROGRAMS SUMMARY 37-48, VOL. I

Prepared Under Contract No. NAS 7-100
National Aeronautics & Space Administration

Preface

The Space Programs Summary is a bimonthly publication that presents a review of engineering and scientific work performed, or managed, by the Jet Propulsion Laboratory for the National Aeronautics and Space Administration during a two-month period. Beginning with the 37-47 series, the Space Programs Summary is composed of four volumes:

Vol. I. *Flight Projects* (Unclassified)

Vol. II. *The Deep Space Network* (Unclassified)

Vol. III. *Supporting Research and Advanced Development* (Unclassified)

Vol. IV. *Flight Projects and Supporting Research and Advanced Development* (Confidential)

Approved by:

W. H. Pickering, *Director*
Jet Propulsion Laboratory

Contents

PLANETARY–INTERPLANETARY PROGRAM

LUNAR PROGRAM

Contents (contd)

I. *Mariner IV* Project

PLANETARY–INTERPLANETARY PROGRAM

The *Mariner IV* Project is under the administrative cognizance of the *Mariner* 1967 Project Office, which also directs the *Mariner* Venus 67 Project and the residual activity of the *Mariner* Mars 1964 Project. Residual activity of the *Mariner* Mars 1964 Project consists primarily of continuing analysis of tracking data, publication of results by the principal investigators, and preparation of final reports. However, periodic detection, recording, and commanding activities involving the *Mariner IV* spacecraft have been assigned to the Deep Space Network. Elements of the experimental facilities at Goldstone Station (Venus and Mars Deep Space Stations) have been used to successfully communicate with the spacecraft. The DSN results will be published periodically in Vol. II of future Space Programs Summaries. *Mariner* Venus 67 Project activities are reported in the following Section II.

The objectives, authorized in December 1965, simultaneously with those for the Venus flight, have been established as:

The primary objective of the Mariner IV Project is to obtain scientific information on the interplanetary environment in a region of space further from the sun than the orbit of earth during a period of increasing solar activity in 1967, using the Mariner IV spacecraft still operating in orbit around the sun.

The secondary objectives are to obtain additional engineering knowledge about the consequences of extended exposure of spacecraft equipment in the interplanetary space environment and to acquire experience in the operation of a planetary spacecraft after a prolonged lifetime in deep space.

During the September–October reporting period the *Mariner IV* spacecraft was transferred to the roll inertial attitude control mode and reoriented so that the high-gain antenna would be positioned toward the earth. When the spacecraft transmitter was switched to the high-gain antenna, the ground-received signal strength increased 22.5 dB.

A second midcourse maneuver was performed on October 25 to determine if the propulsion system had survived its long-term storage. Since *Mariner IV* had been in outer space for more than 2 yr, the successful firing of its midcourse motor provided significant data applicable to future missions.

The spacecraft was left in data mode 2 (transmitting data at a rate of 33⅓ bits/s) so that a greater amount of engineering and scientific data could be obtained to further enhance the evaluation of the maneuver.

On October 26, the data rate was changed from 33⅓ to 8⅓ bits/s to enable the video storage subsystem to transmit one Mars picture back to earth. The spacecraft successfully transmitted the last half of picture 16, and the first half of picture 17.

II. *Mariner* Venus 67 Project

PLANETARY–INTERPLANETARY PROGRAM

A. Introduction

The *Mariner* Venus 67 Project is under the administrative cognizance of the *Mariner* 1967 Project Office, which is also responsible for the *Mariner* Mars 1964 Project and the *Mariner IV* Project (see Section I).

1. *Mariner* Venus 67 Project

The major task of the *Mariner* 1967 Project is the Venus flyby mission, named the *Mariner* Venus 67 Project. The following mission objectives have been established:

> *The primary objective of the Mariner Venus 67 Project is to conduct a flyby mission to Venus in 1967 in order to obtain scientific information which will complement and extend the results obtained by Mariner II relevant to determining the origin and nature of Venus and its environment.*
>
> *Secondary objectives are to acquire engineering experience in converting and operating a spacecraft designed for flight to Mars into one flown to Venus, and to obtain information on the interplanetary environment during a period of increasing solar activity.*

With the authorizing of this project late in December of 1965, and the launch opportunity occurring in June 1967, the period available to the *Mariner* Venus 67 Project for planning, design, test, and other flight preparation was 18 mo.

The single flight spacecraft, designated M67-2, was prepared by converting the spare spacecraft (MC-4) that was built for the *Mariner* Mars 1964 Project. An *Atlas-Agena D* launch vehicle was used to inject the spacecraft into a 127-day transit trajectory.

Seven scientific experiments were approved for the *Mariner* Venus 67 mission:

Experiment	Principal investigator
S-band radio occultation	Arvydas J. Kliore, Jet Propulsion Laboratory
Ultraviolet photometer	Charles A. Barth, University of Colorado
Dual-frequency radio propagation	Von R. Eshleman, Stanford University
Helium magnetometer	Edward J. Smith, Jet Propulsion Laboratory
Solar plasma	Herbert S. Bridge, Massachusetts Institute of Technology
Trapped radiation	James A. Van Allen, State University of Iowa
Celestial mechanics	John D. Anderson, Jet Propulsion Laboratory

The first experiment required the use of only the RF transmission subsystem on the spacecraft, and the last one utilizes only the tracking doppler data received from the

RF carrier. Of the remaining five experiments, four were accomplished with the existing instrumentation, with only minor modifications. Only the dual-frequency radio propagation experiment of Stanford University required the incorporation of a new scientific instrument into the payload.

Other changes to the basic spacecraft design were necessitated by the fact that the spacecraft will travel toward, rather than away from, the sun and also because conversions were made to accommodate revised encounter sequencing and science payload. In particular, modifications were needed in the following areas:

(1) Scientific data automation system.

(2) Antenna pattern and orientation.

(3) Thermal control.

(4) Solar panel configuration.

(5) Planetary sensors.

2. *Mariner V*

During the September–October 1967 reporting period, the *Mariner V* spacecraft continued to operate very satisfactorily.

On October 19, 1967, *Mariner V* encountered the planet Venus. The closest approach distance during the encounter phase was 2543 mi. Preliminary scientific findings are presented in the following paragraphs.

a. Plasma probe and helium magnetometer. Data from the plasma probe and the helium magnetometer show that while there is definite evidence for the interaction of the solar wind with Venus, the size of the interaction region is much smaller than for the earth, and larger than for the moon. The interaction seems to involve either the ionosphere of Venus, a weak planetary field, or both. Since there was no direct evidence for a planetary field, the field of Venus must lie somewhere between zero and 1/300 of the earth's field.

b. Trapped radiation detector. The trapped radiation detector, which measures electrons, protons, and x-rays, detected no energetic particles or radiation belts around Venus. The magnetic moment of the planet can therefore be presumed to be less than 1% that of the earth.

c. S-band occultation experiment. The effects of the neutral atmosphere, on the entry and exit sides of the planet, began at about 6130 km (radial distance from the center). The scale height in the upper neutral atmosphere was determined to be about 5.4 ± 0.2 km. Since the temperature at this height is unlikely to be greater than 230°K, the scale-height value indicates a maximum carbon dioxide abundance of 72 to 87% (if the other major constituent is nitrogen). An ionosphere with a peak electron density of 10^5 to 10^6 electrons/cm^3 (at a radial range of about 6175 km) was observed during exit occultation. Further analysis will be required to determine the density, temperature, and pressure in the lower atmosphere to the level at which the signal was lost.

d. Dual-frequency radio propagation experiment. The altitude of the ionosphere of Venus on the dark side of the planet has been determined to be about 100 km (scale heights range from 80 to several hundred kilometers). While the ionosphere of the lighted side of the planet is at about the same height as the dark side, it is several hundred times denser.

e. Celestial mechanics experiment. Determination of the astronomical unit, which is 92,955,640 ± 62 mi, agrees with recent values obtained by radar observations of Venus. The mass of Venus is 0.815003 ± 0.000018 the mass of the earth, and the earth is 81.2999 ± 0.0015 times as massive as the moon.

f. Ultraviolet photometer experiment. A hydrogen corona, which disappeared at an altitude of about 1,800 mi above the surface of Venus, was measured on the illuminated limb of the planet. This corona has a comparable hydrogen content and is as bright as that which surrounds the earth. No oxygen was detected in the vicinity of Venus. An unexpected ultraviolet emission was detected at the dark limb of the planet (may be the result of chemical reactions or particle bombardment).

B. Guidance and Control

1. Power Subsystem Flight Performance

The *Mariner V* spacecraft power subsystem operation through the launch, star acquisition, midcourse maneuver, and cruise phase has been completely nominal. The spacecraft electrical loads were transferred from ground power to internal power (the battery) 7 min prior to launch and operated from this source until the solar panels were sun-oriented some 38 min later.

After the transfer to the solar panel power source, the battery charging was started automatically and continued until the battery was again required during the midcourse maneuver. The battery was used for an additional 46 min during the midcourse maneuver when the pitch turn

caused a shading of one panel by the bus and shading between the solar panels and battery. At sun reacquisition after the maneuver the battery again began to charge and continued until the charger was turned off 13 days after launch. Approximately 5.5 A-h were used from the battery during launch and the midcourse maneuver.

Solar panel performance has been as predicted. A maximum of 226 W was provided by the panels in the maneuver mode just prior to the attitude turns. In the nominal cruise mode with the battery charger off and the RF switched to the traveling-wave tube power amplifier, the power drawn has been 178 W.

In flying a spacecraft from earth to Venus, the distance between the sun and the spacecraft decreases from approximately 150×10^6 to 108×10^6 km. The effect of this variation on both solar flux and solar panel temperature is illustrated in Fig. 1. For such an excursion it is characteristic that the open circuit voltage of a solar cell should decrease, and that the short circuit current should increase. *Mariner* V solar panels had zener diodes connected effectively across the output to limit the maximum panel voltage to 50 V. Near earth the panel voltage would exceed 50 V and as the distance to the sun decreased, this voltage would tend to decrease. However, the zener diodes masked this change until the panel voltage fell below the zener voltage. One other effect that can be noted in Fig. 1 is that the zener voltage decreases with an increase in temperature. This is observed to occur from launch + 50 days to the point where the zeners go off.

The power conditioning portion of the power subsystem has operated within predictions to date and no anomalies have been noted. Each of the commands sent to the power subsystem has been acted upon correctly by the power distribution module. The maneuver booster regulator has been turned on and off by the attitude control subsystem during star acquisition and the midcourse maneuver. The main booster regulator and main 2.4-kHz inverter have supplied the remainder of the spacecraft ac power requirements.

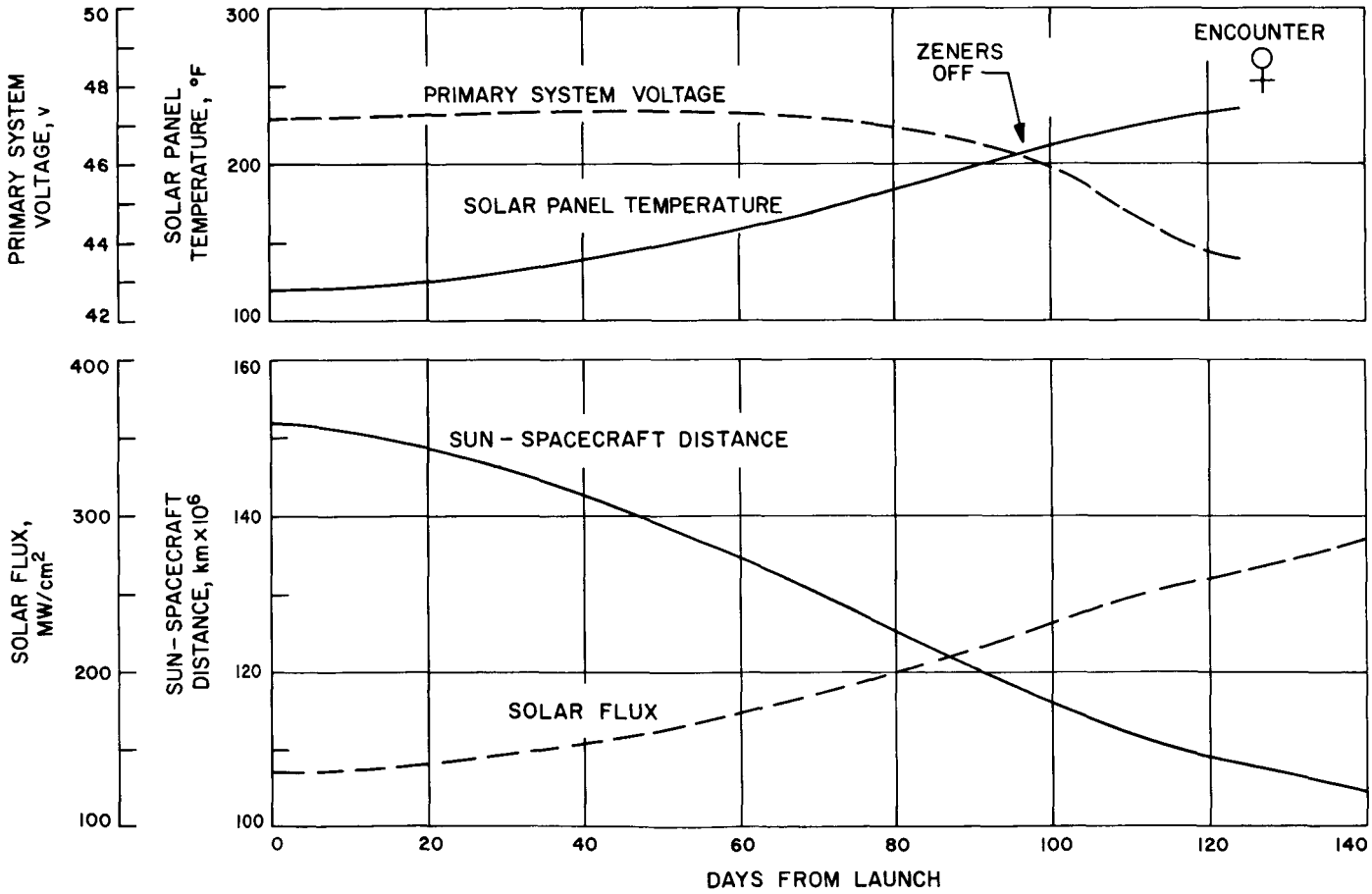

Fig. 1. Comparison of effects on the solar panel

III. *Mariner* Mars 1969 Project

PLANETARY–INTERPLANETARY PROGRAM

A. Introduction

The *Mariner* Mars 1969 Project was initiated in late December 1965 and formally tasked on February 1, 1966. The primary objective is to conduct two Mars flyby missions in 1969 to make exploratory investigations of the planet which will set the basis for future experiments—particularly those relevant to the search for extraterrestrial life. The secondary objective is to develop Mars mission technology.

The spacecraft design concept will be based on the configuration of the successful *Mariner IV* spacecraft, with considerable modifications to meet the 1969 mission requirements and to enhance mission reliability.

The launch vehicle will be the *Atlas/Centaur* SLV-3C as used for *Surveyor* missions. This vehicle, developed under contract for and direction by the Lewis Research Center by General Dynamics/Convair, has a single- or double-burn capability in its second stage and a considerably increased performance rating over the *Atlas D/Agena D* used in the *Mariner IV* mission.

Mariner Mars 1969 missions will be supported by the Eastern Test Range launch facilities at Cape Kennedy, the tracking and data acquisition facilities of the Deep Space Network, and other NASA facilities.

Six planetary-science experiments have been selected by NASA for the *Mariner* Mars 1969 missions; they are listed in Table 1.

Table 1. *Mariner* Mars 1969 scientific investigations

Experiment	Scientific investigator	Affiliation
Television	R. B. Leighton[a]	California Institute of Technology (CIT)
	B. C. Murray	CIT
	R. P. Sharp	CIT
	N. H. Horowitz	CIT
	J. D. Allen	Jet Propulsion Laboratory (JPL)
	A. G. Herriman	JPL
	R. K. Sloan	JPL
	L. R. Malling	Massachusetts Institute of Technology
	M. E. Davies	Rand Corporation
	C. Leovy	Rand Corporation
Infrared spectrometer	G. C. Pimentel[a]	University of California, Berkeley (UCB)
	K. C. Herr	UCB
Ultraviolet airglow spectrometer	C. A. Barth[a]	University of Colorado
	W. G. Fastie	Johns Hopkins University
Infrared radiometer	G. Neugebauer[a]	CIT
	G. Munch	CIT
	S. C. Chase	Santa Barbara Research Center
S-band occultation	A. J. Kliore[a]	JPL
	D. L. Cain	JPL
	G. S. Levy	JPL
Celestial mechanics	J. D. Anderson[a]	JPL

[a] Principal investigator.

The sixth Project Quarterly Review, combined with an experimenters' meeting, was conducted in October 1967. A number of design and breadboard tests—including, for example, testing of the scan platform thermal-control model (Fig. 1)—were conducted during the period. Fabrication of test models and equipment was continued, and manufacture of spacecraft subsystem flight-type hardware was begun. Spacecraft subsystem contracts covering the manufacturing phase have been definitized for all but seven contract efforts; in the latter cases, work is proceeding under letter contracts or other interim means.

The preliminary trajectory characteristics document, concerned primarily with the heliocentric and near-Mars phases, was published in the previous period; a companion volume, the near-earth trajectory-characteristics document, was published in this period. The standard mission was defined, together with a set of optional standard missions. A deep space instrumentation facility/spacecraft compatibility test facility, which will have its first application in *Mariner* Mars 1969 testing, was formally established and designated DSS 21. High rate data system developments are described in SPS 37-48, Vol. II, Section IV.

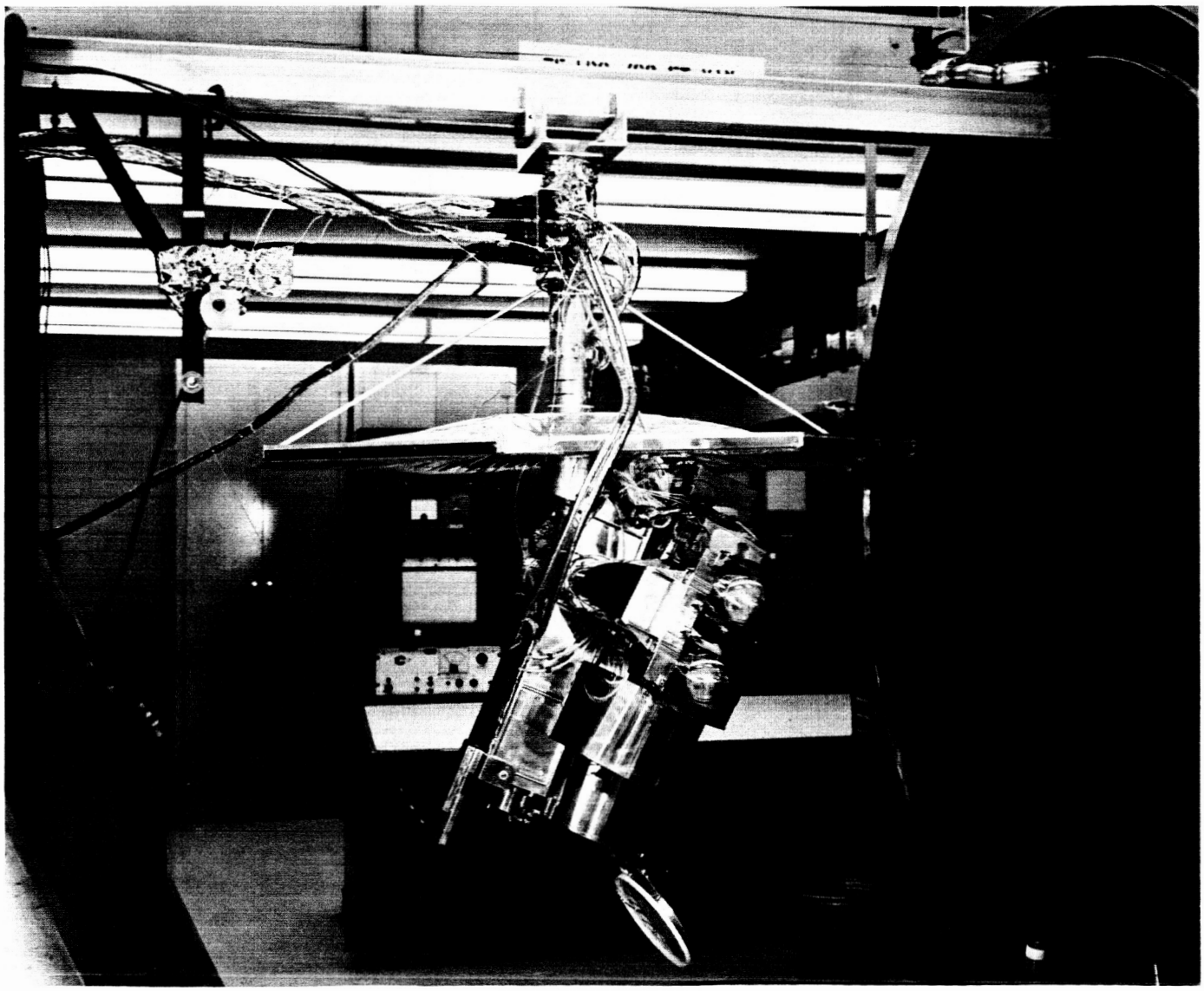

Fig. 1. Scan-platform thermal control model

B. Project Engineering

1. Alternate Far Encounter Plan Study

In an attempt to increase the value of the far encounter (FE) phase of the *Mariner* Mars 1969 mission, several alternate FE plans have been studied. Each plan that has been considered feasible will provide seventy-two or more FETV pictures.

Although the study included an examination of many possible alternate encounter plans, only the three most feasible are presented here. Selection of the optimum plan involves performing a tradeoff study between the necessary spacecraft design and operational changes and the value of science data returned.

The FE sequence, as presently planned, calls for eight FETV pictures to be taken on 4-h centers from $E - 40$ to $E - 12$ h. These eight pictures would be recorded on the first track of the analog tape, and the three remaining tracks would be used to store the near encounter pictures. All of the analog data would be returned in digital form subsequent to encounter. A deviation from this sequence in order to greatly increase the TV data return implies data playback prior to encounter, using the high-rate telemetry channel which transmits block-coded data at 16.2 kbps. Since the high-rate channel can only be used when the spacecraft is over Mars Station (DSS 14), data can be returned for only a few hours out of each day. It is interesting to consider the interactions among the spacecraft data storage, flight telemetry subsystems and antenna view periods on earth:

(1) TV pictures are stored on the analog tape recorder which has a capacity equivalent to about 1.575×10^8 bits.

(2) At 16.2 kbps, a full load of analog data can be returned in 2.7 h.

(3) For elevation angles greater than 25 deg, Goldstone stations view the spacecraft for 3.5 h, and the view period increases to 5 h for a 20-deg lower bound on elevation. This can be seen on Fig. 2, which is a graph of elevation angle as a function of time for each of the three assigned DSN stations.

If the playback period is 3 h, 21 h remain out of each day during which the analog tape can be filled. Given that the analog tape can store thirty-two pictures, the pictures will be recorded on approximately 40-min centers.

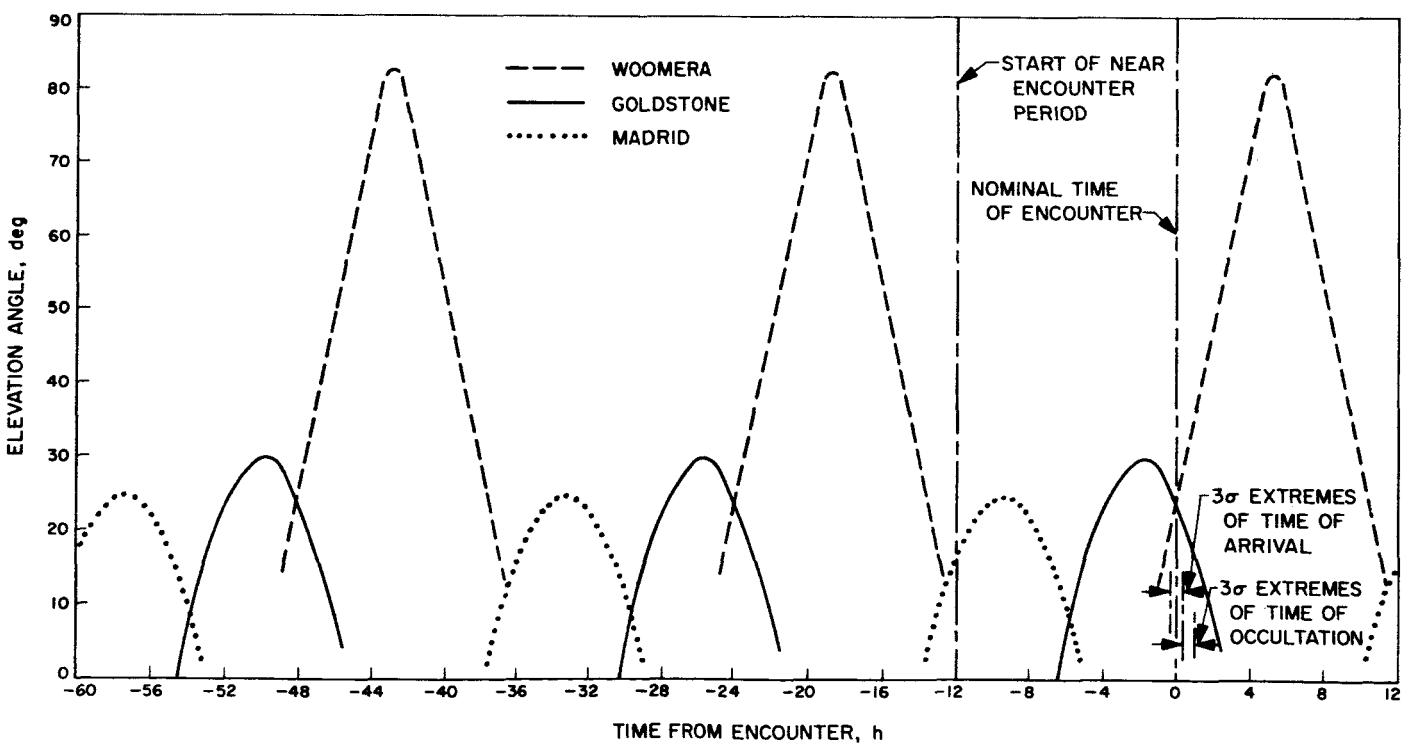

Fig. 2. Elevation angles vs time for the assigned DSN stations

In other words, thirty-two TV pictures can be recorded on the analog tape and retrieved at DSS 14 during each 24-h period.

Telecommunication studies show that the telemetry performance margin at the high data rate is above the sum of the negative tolerances (and increasing), starting 5 to 10 days before closest approach. These studies assume:

(1) Word error rate $\leq 10^{-2}$.

(2) DSS 14 used, at elevation angles greater than about 20 to 25 deg.

(3) Spacecraft traveling-wave-tube transmitter amplifier in the high-power mode.

Certain features of the mission tend to constrain data return from the FETV operations. First, the infrared spectrometer radiator plate must be exposed to deep space for 12 h prior to encounter for adequate cooling; therefore, the scan platform must be moved to the near encounter position at $E - 12$ h. The 128-word capacity of the central computer and sequencer (CC&S) memory is filled (at launch) under the present encounter plan; any alternate plan would entail inflight programming. For some trajectories, the cone angle to Mars exceeds the 165-deg maximum scan platform capability. However, this condition does not occur before $E - 2$ h, and does not affect the alternatives studied. The timing of encounter—closest approach at Goldstone zenith $+2$ h (± 20 min)—may constrain alternatives which depend on Goldstone visibility.

A summary of the alternate variations of plan B that have been considered feasible under these constraints is as follows:

(1) Plan B1. Accumulate and return two loads of tape in the 2-day interval $E - 72$ to $E - 24$ h. Record eight pictures on equal time centers on track 1 of the analog tape recorder from $E - 24$ to $E - 12$ h. Return the last eight pictures with the near encounter (NE) pictures, which are stored on tracks 2, 3, and 4, during the postencounter playback.

(2) Plan B2. Similar to plan B1, except that the last eight pictures stored on track 1 are accumulated from $E - 24$ to $E - 8$ h.

(3) Plan B3. Accumulate and return three loads of tape during the period $E - 72$ to $E - 1$ h. The last tapeload would be gathered from $E - 24$ to $E - 4$ h and returned during the next 3 h, leaving the analog tape "empty" at the beginning of NE.

A sequence for plan B1 is shown in Fig. 3. Plan B2 differs only in the third TV sequence of eight pictures, in which the pictures are taken at 137-min intervals until $E - 8$ h instead of ending at $E - 12$ h. Plan B3 is shown in Fig. 4. Figure 5 shows resolution per TV line of the narrow angle camera as a function of time before encounter. It serves as a demonstration of the increase in the amount of detail achievable as the period during which FETV pictures are gathered is prolonged.

The retrieval of seventy-two or more TV pictures prior to the NE period will certainly enhance the mission. In addition to the scientific value of obtaining a map of most of the surface of Mars, encounter plan B offers a significant increase in the confidence that the NE data recording sequence will be initiated at the proper time. The tape recorders are started when the data automation system receives CC&S N6 or discrete command (DC) -26 followed by narrow angle Mars gate (NAMG) -2 or TV planet in view (PIV). If the situation were such that N6 or DC-26 had been received, and if TV-PIV were to occur too soon (e.g., due to an unexpected response to visible radiation outside the TV field of view, as did occur on *Mariner IV*), the tape recorders would start too soon. The result would be a loss of a portion of the recorded dark side infrared radiometer, infrared spectrometer, and ultraviolet spectrometer data and some preterminator TV data. This possibility may be identified upon examination of the first tapeload of FETV data, which is retrieved between $E - 52$ and $E - 48$ h. The CC&S could then be reprogrammed such that at the time at which N6 is issued is delayed until very near to limb crossing.

It should be noted also that, as a bonus, Mars' moons will appear in many of the FETV pictures. This aspect of the alternate plans has not been considered in any detail. Further studies might include an examination of the amount of information which could be obtained as the picture-taking sequence is extended.

Spacecraft hardware implications of these alternative FE plans would be seen in the need to: (1) program additional operations in the CC&S memory; (2) incorporate minor changes in the data storage subsystem; (3) investigate the effects on the radio subsystem of the prolonged preencounter high-power and high-rate operations; and (4) the need for assurance of the reliability of TV and other subsystems whose scale of operation would be increased by these plans.

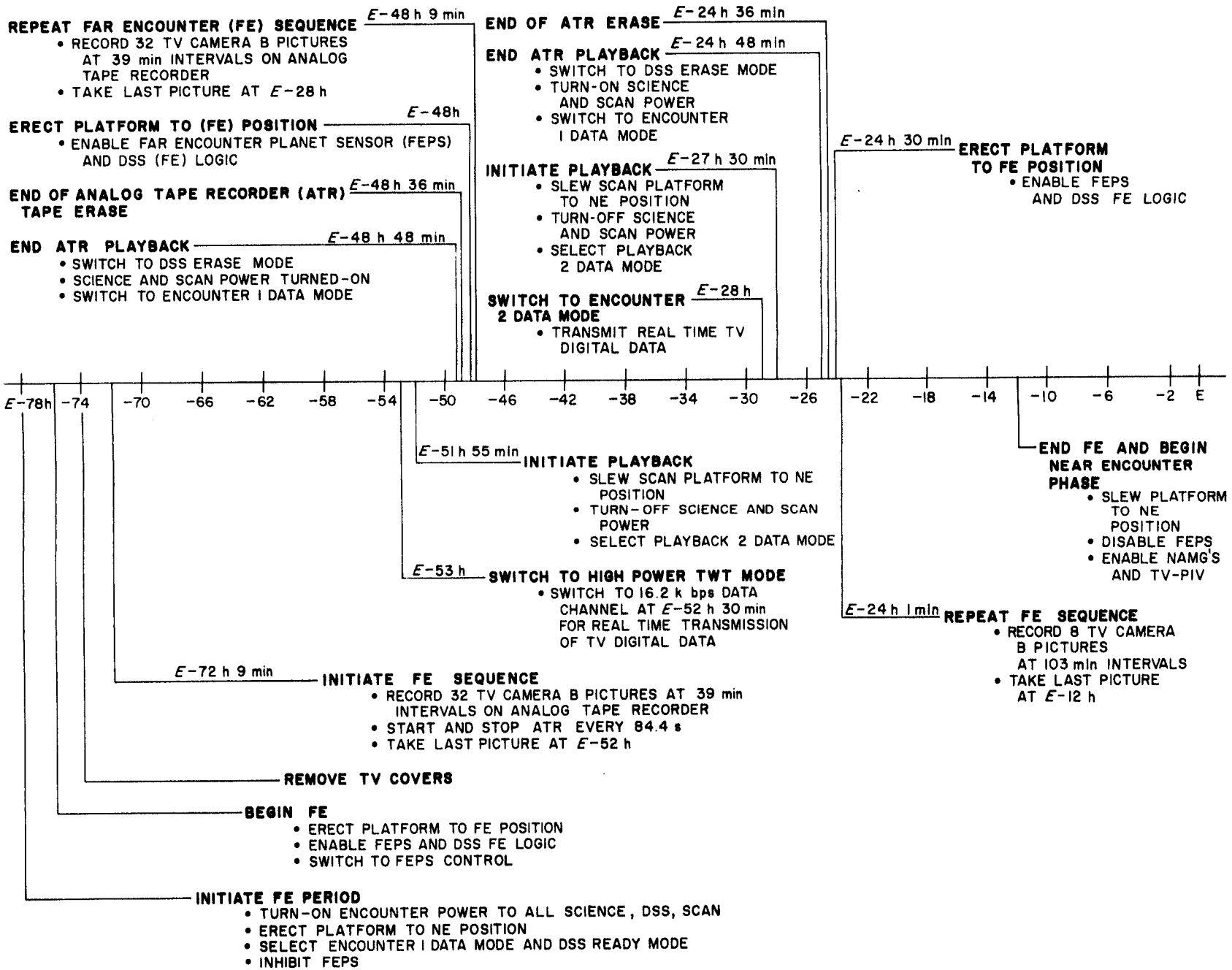

Fig. 3. Encounter sequence B1

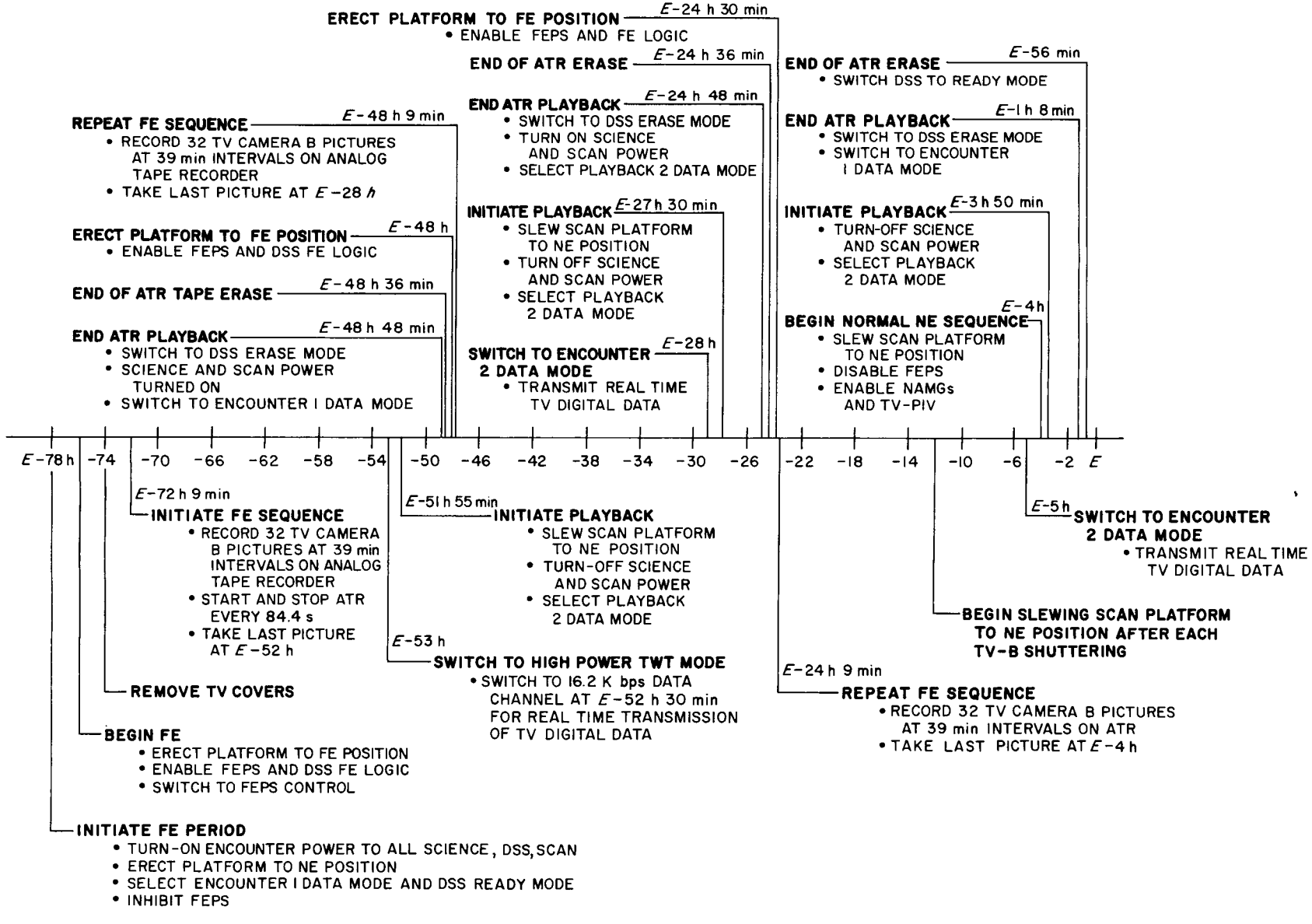

Fig. 4. Encounter sequence B3

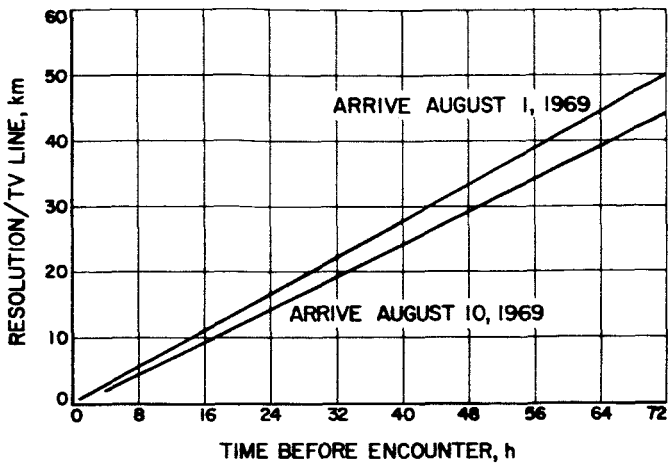

Fig. 5. Resolution vs time before encounter, camera B

C. Systems

1. Introduction

The technical areas in which the Systems Division supports the *Mariner* Mars 1969 Project have been previously identified in SPS 37-47, Vol. I, p. 24. Progress made in certain of those areas are covered in this subsection.

2. Mission Analysis (Documentation)

During the reporting period the first issue of the near-earth trajectory and the station view characteristics document was published. Graphical view period data are presented for several stations of the Deep Space Network, Manned Space Flight Network, and Air Force Eastern Test Range. The view period data contain the behavior of such parameters as rise and set times, slant range, range rate, elevation angle, and spacecraft location with respect to deep space station (DSS) stereographic projections. By using the latter, it is possible to identify the effects of ground mask and antenna look angle prelimits upon the actual view period for each DSS.

At the request of the project scientist to the mission analysis and engineering manager, a progressive effort is being carried out to provide instrument view data to the experimenters. Initial products of this effort consisted of Mars maps with fixed superimposed instrument tracks for representative encounter conditions. At the experimenters' meeting in October, data were presented which showed graphically the effect in latitude on the coverage swath for each instrument of variation in arrival date and time of day for the equatorial and polar-cap longitude options. This analog tool was devised for interim use in considering the scientific-coverage ramifications of various arrival-date options, pending the completion of the next step in the effort. This will be a more complete data package generated with the computer program PEGASIS (SPS 37-47, Vol. 1, p. 26, and below).

3. PEGASIS Status

Many of the output parameters have been checked through the use of conic computer programs. Further checkout of the algorithms will be accomplished by comparison with results from an integrated trajectory. The milestone dates for completing the trigger and search capabilities are November 10, and December 1, 1967, respectively. It is planned to provide a trajectory data package (using only PEGASIS) to the experimenters by January 1968.

4. Mission Analysis (Far-Encounter TV Plans)

During the spring quarter of 1967, a study was initiated to investigate the feasibility of returning a greater number of far-encounter TV (FETV) pictures. The far-encounter sequence nominally called for eight far-encounter TV pictures to be taken on 4-h centers from encounter minus 40 h ($E-40$) to $E-12$ h. These eight pictures would be recorded on the first track of the analog tape recorder and would be returned in digital form subsequent to encounter.

A deviation from this sequence in order to greatly increase the TV data return implies data playback prior to encounter using the high-rate telemetry channel, which transmits block-coded data at 16.2 kbps. A detailed discussion of several alternate FETV plans is given in Subsection III-B of this SPS. Several of the plans would return seventy-two or more pictures of Mars. Section III-B covers the interactions between the spacecraft data storage and flight telemetry subsystems, as well as certain spacecraft related constraints.

Figure 6 shows the longitudinal coverage of Mars as a function of time for both spacecraft, for FETV plan 3. In Fig. 6, it is assumed that the first spacecraft arrives August 1, 1969 and the second arrives August 10, 1969.

By cross-plotting TV resolution with sub-spacecraft longitude vs time before encounter, it is possible to obtain resolution as a function of longitude. Figure 7 shows "best" resolution/TV line as a function of sub-spacecraft

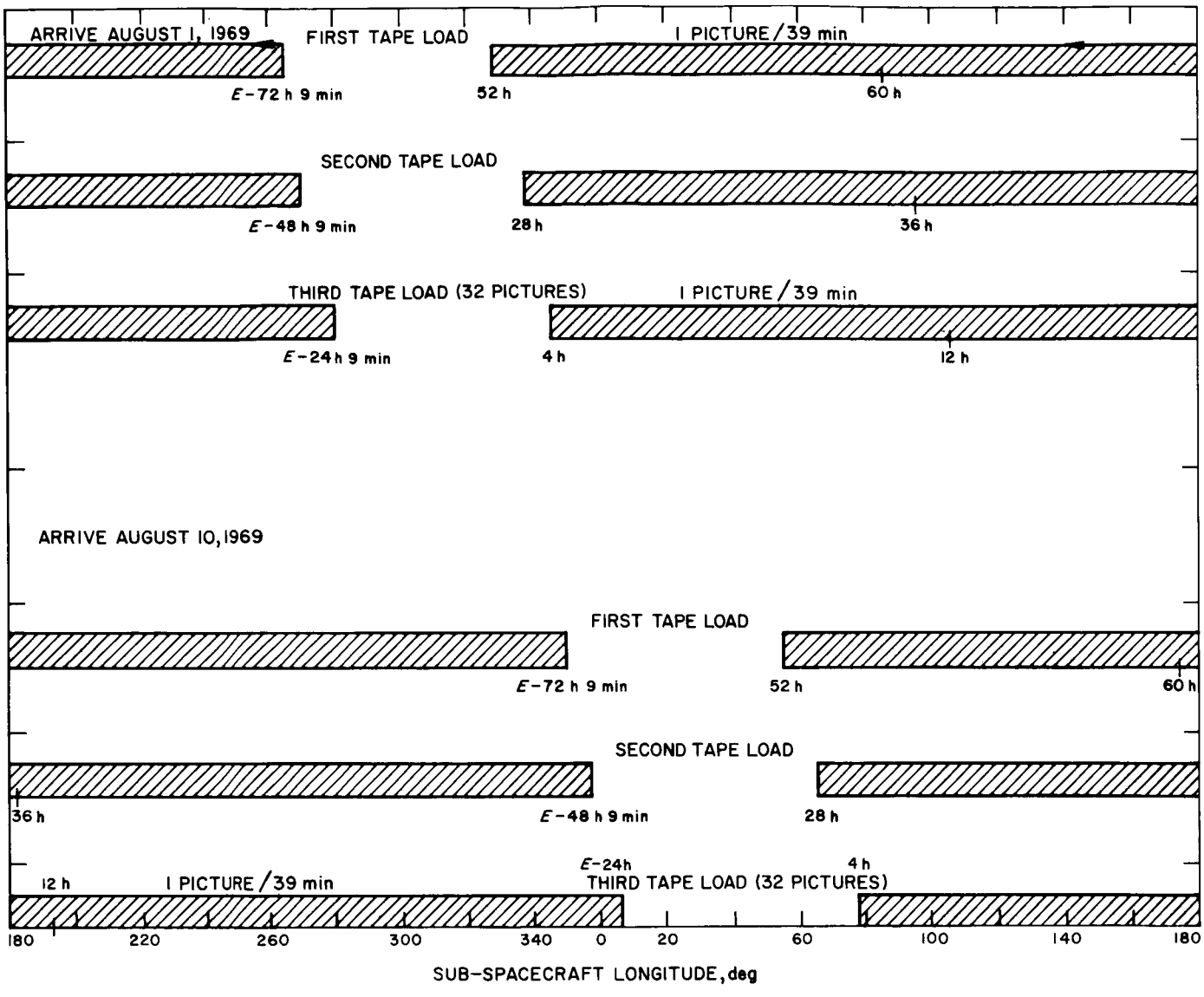

Fig. 6. Picture coverage of Mars (plan B_3)

longitude for an August 1 and an August 10 arrival. It is a composite of the two resolution functions for the two dates and is obtained by using the better resolution of the two. In general, this means using the resolution corresponding to the August 10, 1969 arrival, except when there is no TV coverage for that arrival, in which case the August 1 resolution is used. This explains the steps in resolution on Fig. 7.

The arrows on Fig. 7 indicate the direction in which the jumps in resolution are taken. It is seen that:

(1) There is a degrading jump in resolution at 55 deg longitude, corresponding to initiation of the first analog tape playback (at $E-52$ h) for the August 10 arrival and step back down at 357 deg.

(2) A degrading step occurs at a time corresponding to initiation of the second playback for the August 10 arrival.

(3) The rest of the steps result in degraded resolution and are caused by the completion of the accumulation of FETV data for the August 10 arrival.

The retrieval of seventy-two or more FETV pictures prior to the near-encounter phase will enhance the scientific mission return. There is also a greater probability that the Mars moons may appear in some of the pictures.

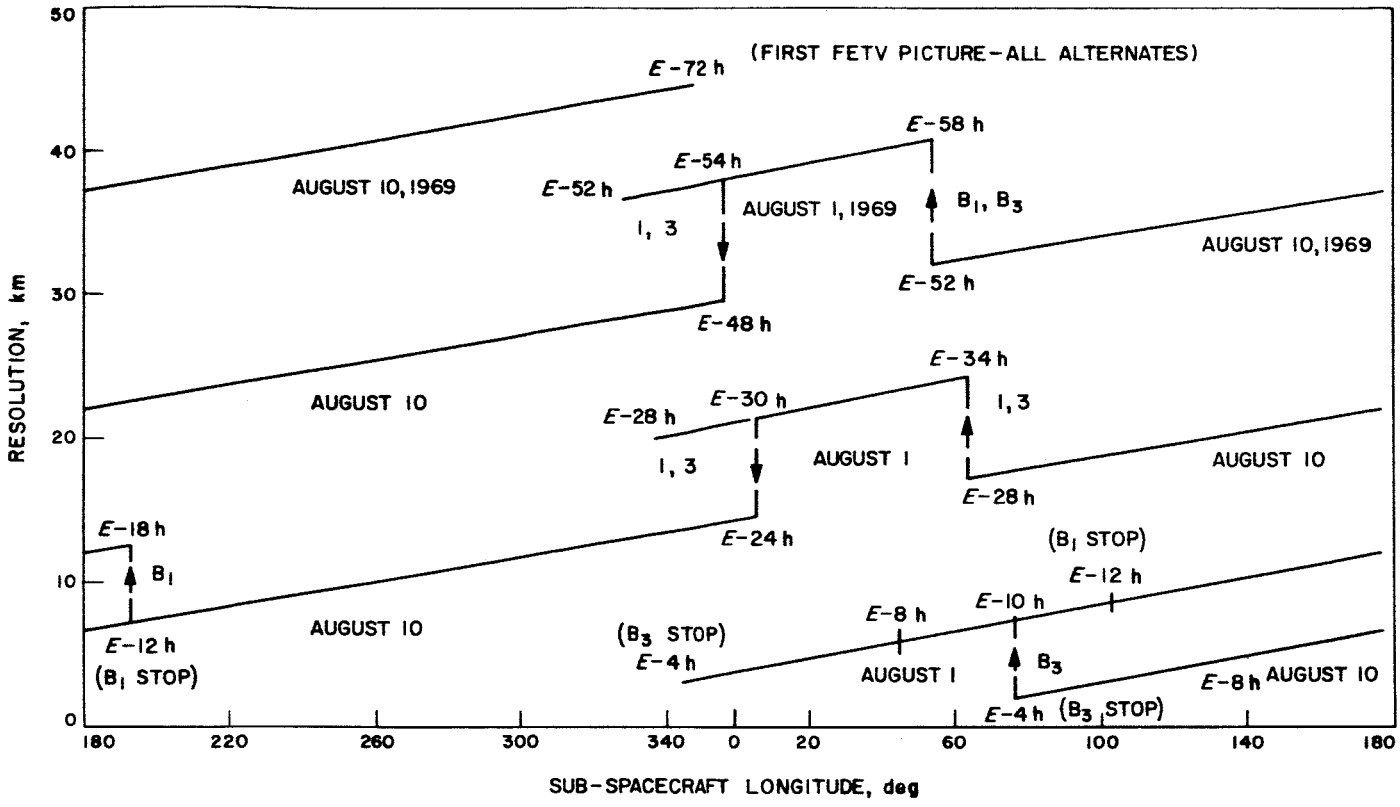

Fig. 7. Best resolution/TV line vs sub-spacecraft longitude

Some further work is necessary to make certain that the presence of certain spacecraft related constraints does not preclude the possibility of adopting one of the more ambitious FETV plans described in Section III-B.

5. Near-Encounter Orbit Determination Study

This study presents the orbit determination capability to be expected during the encounter phase of the *Mariner* Mars 1969 mission and evaluates this capability to determine whether the single precision orbit determination program (SPODP) can meet the desired accuracy of the UV spectrometer experiment.

Of all the experiments required to be performed during the *Mariner* Mars 1969 mission, the UV spectrometer pointing requirement is the most demanding on the encounter orbit determination. The UVS experimenter desires the slit alignment error (at 100 km above the bright limb) to be less than 3 deg with the probability of 0.9. This requirement translates into ± 250 km, 3σ, in the direction normal to the impact parameter and in the **R**, **T** plane.

A trajectory based on March 16, 1969 18:34:44.000 GMT injection, was used for this study. The arrival parameters are as follows:

(1) $\mathbf{B} = 7493.5$ km.

(2) $\mathbf{B}\cdot\mathbf{R} = 3252.6$ km.

(3) $\mathbf{B}\cdot\mathbf{T} = 6750.8$ km.

(4) $t_c =$ 04:55:19.951 universal time, August 10, 1969.

The 1σ physical constant uncertainties assumed for this study were:

$\sigma_{MM} = 6 \times 10^{-11}$ (mass ratio of Mars to sun)

$\sigma_{AU} = 100$ km (astronomical unit)

$\sigma_{Radius} = 10$ m (for each DSS)

$\sigma_{Longitude} = 0.0001$ deg (for each DSS)

$\sigma_{Range} = 300$ m/point (ranging system)

$\sigma_{Range\ rate} = 0.003$ m/s (60-s doppler sample)

a. Description of the study. A series of orbit solutions were calculated using only two-way doppler data from two tracking stations, of different lengths of data spans,

Table 2. Target statistics of different data spans

Target statistics	Data span					
	From $E-22$ days to $E-4$ h	From $E-12$ days to $E-4$ h	From $E-10$ days to $E-4$ h	From $E-7$ days to $E-4$ h	From $E-5$ days to $E-4$ h	From $E-3$ days to $E-4$ h
SMAA, km	243.45	247.43	249.16	253.10	256.85	265.81
SMIA, km	58.21	70.92	74.16	80.32	85.08	99.21
θ, deg	63.05	62.59	62.83	63.10	62.89	61.96
σ_t, s	3.439	3.801	3.941	4.203	4.376	4.903
$\sigma_{\mathbf{B}\cdot RT}$, km	218.61	222.06	224.24	228.62	231.89	239.20
$\sigma_{\mathbf{B}\cdot T}$, km	121.92	130.15	131.52	135.07	139.42	152.58
σ_{PB}, km[a]	243.40	247.34	249.09	253.06	256.78	265.63
P_z[b]	0.52	0.52	0.51	0.51	0.50	0.50

[a] σ_{PB} = The uncertainties in the direction perpendicular to the **B** vector.
[b] P_z = The probability of the slit alignment error equal to or less than 3 deg.

Table 3. Target statistics of doppler and range tracking[a]

Target statistics	Tracking time		
	From $E-5$ days to $E-3$ days	From $E-5$ days to $E-1$ day	From $E-5$ days to $E-4$ h
SMAA, km	543.54	230.19	194.06
SMIA, km	109.99	92.14	70.21
θ, deg	54.66	52.54	56.41
σ_t, s	13.79	7.59	3.11
$\sigma_{\mathbf{B}\cdot R}$, km	447.93	191.13	166.25
$\sigma_{\mathbf{B}\cdot T}$, km	326.94	127.95	122.26
σ_{PB}, km[b]	536.26	226.17	192.48
P_z[c]	0.26	0.55	0.62

[a] Doppler tracking from three stations and range unit from one station.
[b] σ_{PB} = The uncertainties in the direction perpendicular to the **B** vector.
[c] P_z = The probability of the slit alignment error equal to or less than 3 deg.

with starting epochs from $E-22$ days to $E-3$ days. All solutions have data from epoch to $E-4$ h. These orbit solutions show the effect of the length of orbit fitting span on the target statistics.

With the epoch at $E-5$ days, orbit solutions were computed with the last data point of each solution stopped at a different time moving toward encounter. Results were obtained for the following data configurations:

(1) Doppler data only (2 stations).

(2) Doppler data only (3 stations).

(3) Doppler and ranging data.

b. Results. Numerical results of this study are presented in Tables 2 and 3 and Figs. 8 and 9. From Table 2, it can be seen that there is only a small change in SMAA as the starting epoch is varied from 22 to 5 days before encounter. Therefore, all subsequent results are computed with an epoch at $E-5$ days. Table 3 illustrates the effect of the end of the tracking data span upon the orbit uncertainties. Some improvement continues to result as data are gathered closer to Mars.

Examining the orientation of the semimajor axis (SMAA), the SMAA is very nearly normal to the **B** vector. The ultraviolet spectrometer (UVS) requirement in the direction normal to the **B** vector is 250 km, 3σ. The best 1σ value, a conservative estimate for the SPODP, is 194.06 km. Thus the desired UVS alignment confidence level cannot be met by the SPODP with the assumed uncertainties in the physical constants and station locations used.

Figure 8 illustrates the 1σ error in the uncertainty ellipse SMAA in the **R**, **T** plane at Mars. At the starting epoch at $E-5$ days, no knowledge (infinite uncertainty in SMAA) of the orbit was assumed. This assumption was made in order to prevent the cruise orbit solution from biasing the near-Mars orbit solution.

Figure 9 illustrates the confidence level in meeting the UVS slit alignment with the SPODP, and assuming a 1-deg, 1σ, spacecraft error contribution to the total UVS alignment error. The desired confidence level of 0.9 cannot be guaranteed with the SPODP. Use of the more

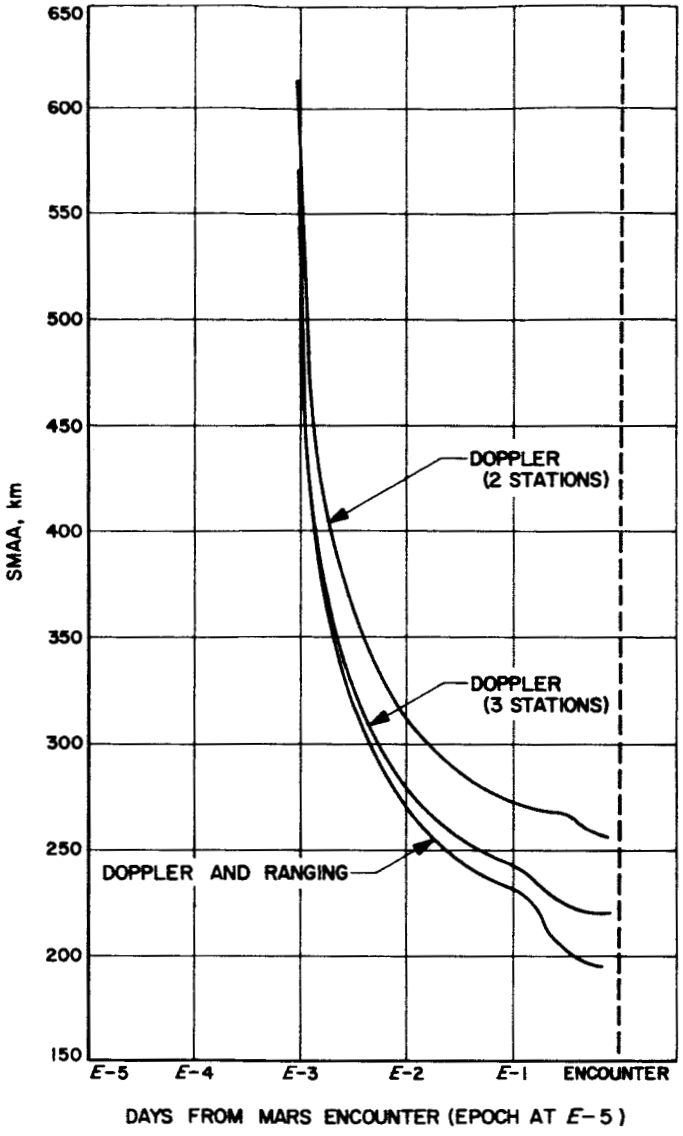

Fig. 8. Improvement in the SMAA uncertainty with time during the near encounter phase

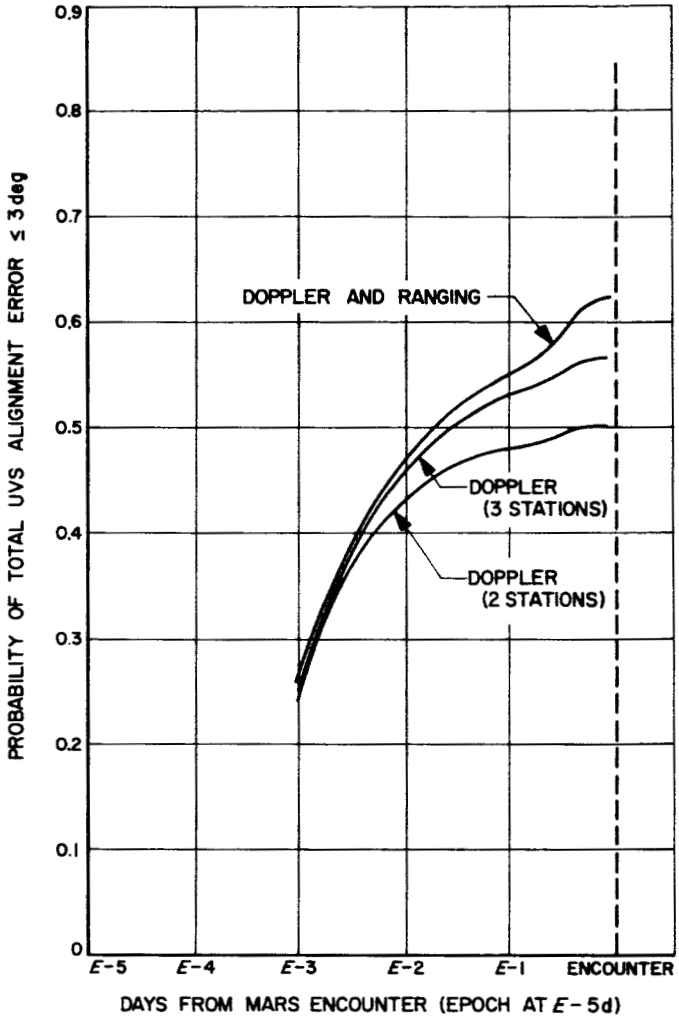

Fig. 9. Probability of meeting UVS slit alignment accuracy of 3 deg

sophisticated double precision orbit determination program (DPODP) would result in meeting the desired confidence level. The DPODP is under development for use during the *Mariner* Mars 1969 flight.

The conclusions of the near-Mars orbit determination study using the SPODP are:

(1) The orbit accuracy improves very little by moving the starting epoch back from $E - 5$ days.

(2) There is only a small improvement in the orbit uncertainty normal to **B** (and in the **R**, **T** plane) by extending the last data point from $E - 4$ to $E - 2$ h.

(3) The orbit determination accuracy is primarily limited by the station location errors and the "effective" tracking data quality.

(4) The SPODP cannot meet the UVS slit misalignment accuracy requirements to the required confidence level of 0.9.

6. Mission Operations Progress

During the reporting period, progress in mission operations design and documentation continued. The first issue of the Space Flight Operations Plan was published at the end of September 1967 (a preliminary version was distributed in June 1967). A revised edition is planned for release early in 1968.

Draft versions of the space flight operations test plan, the mission operations training plan, the spacecraft/mission operations system compatibility test plan, and the simulation RFP (phase II) were issued.

7. System Test Complex Data System

Significant progress for the months of September and October 1967 has been in the area of science subsystem test support scheduled to start November 6, 1967.

Design and construction of an interim J-box using *Mariner* Venus 67 components was completed. This unit allows for connection of all the science subsystem signals to the data input subsystem (DIS) portion of the system test complex data system (STCDS). The unit as constructed also permits two streams to be connected to the DIS for *Mariner* Venus 67 tests.

A number of interim modifications have been made to the DIS modules and to signal terminating circuits to permit compatible operation with the science subsystem. Final modifications will be installed in December 1967–January 1968, subsequent to the present group of tests.

Development of programs is proceeding and a final assembly of the November 6, 1967 configuration program will be available for verification the week of October 30. Standard processes and decommutation of the 66⅔-bps data stream will be available for tests commencing November 6.

The interfaces and software developed for science subsystem testing will be directly employed for spacecraft testing in the encounter mode. Most of the engineering test processes required for spacecraft testing have been defined, documented and are in some stage of implementation. The hardware needed to effectively use the two-computer complex of the STCDS has been designed and contracted for February 1968 delivery. An integrated system of display and logging entry for the test director's area has been specified and a contractor selected.

D. Guidance and Control

1. Solar Panel Development

A program leading to the fabrication and flight-acceptance qualification of *Mariner* Mars 1969 solar panels has been initiated with Electro-Optical Systems, Inc. Achievements to date include the design, development, manufacture, and test of prototype hardware (phase I). Completion of this phase will lead into a phase II program wherein one type-approval and ten flight panels will be fabricated and tested.

The *Mariner* Mars 1969 panels use N on P, 2 × 2 cm solder-dipped silicon solar cells and 20-mil-thick, 2 × 2 cm Corning 7940 fused-silica coverglasses with a blue interference coating filter similar to the type flown on *Mariner* Mars 1964.

The design configuration of the *Mariner* Mars 1969 solar panels was patterned after the basic cell layout that was successfully employed on *Mariner* Mars 1964 and *Mariner* Venus 67; however, some changes, such as the introduction of N on P, 2 × 2 cm solar cells and an improved solar cell interconnection, modify the design slightly. The improvement in cell interconnection includes the use of tin-plated kovar and a ribbon top contact for improved compliance.

An extensive solar cell submodule qualification test was conducted, the result of which indicates that the design changes result in a more easily fabricated and more rugged design than used on previous *Mariner* and *Surveyor* programs. A four-cell *Mariner* Mars 1969 submodule is shown in Fig. 10.

A sample panel program was conducted in the course of developing the *Mariner* Mars 1969 prototype panel to verify the electrical and mechanical performance of the various solar panel components at an assembly level before the fabrication and testing of a full-size panel. Further objectives of the sample panel program were to investigate the following interactions of solar cells and substrates: effect of bonding; effects of tab interconnections; effects

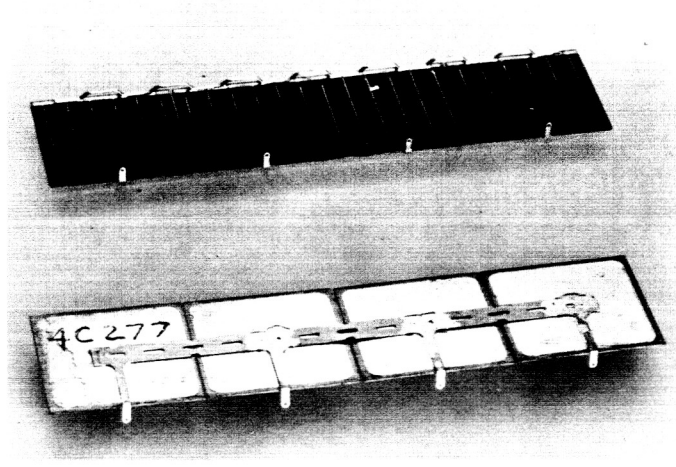

Fig. 10. *Mariner* Mars 1969 solar cell submodule

of substrate configurations; effects of the dielectric and adhesive; electrical performance of a voltage string; and effects of test environments. Test levels were employed similar to the type-approval levels anticipated for the full-size panel.

Six sample panels were fabricated and tested for mechanical and electrical performance. The panels were 1 ft² in area and were fabricated with aluminum substrates similar to the *Mariner* Mars 1969 panel configuration. Figure 11 shows a typical assembled sample panel. Various submodule design configurations were bonded to five panels. A sixth panel was later fabricated, using the selected submodule design described earlier.

The test results indicated that panel 6 passed all the flight-acceptance and type-approval levels anticipated for the *Mariner* Mars 1969 panels with no electrical or mechanical failure.

The preproduction prototype panel was fabricated utilizing a *Mariner* Venus 67 substrate, the use of which was required because of the unavailability of a *Mariner* Mars 1969-type structure. It is believed that the substrates are structurally similar; however, the *Mariner* Mars 1969 panel has 20.3 ft² of area available for cell bonding, compared to 10 ft² for *Mariner* Venus 67 substrate. The panel consists of three electrical sections, each section containing seventy-eight cells in series and nine cells in parallel. Minor problems were encountered during the fabrication phase. One area of concern was a delamination of a circuit board at three terminal locations. Investigation revealed that excessive heating during the soldering of wires to the boards caused the delamination. Temperature control methods are being introduced to eliminate this problem on future hardware.

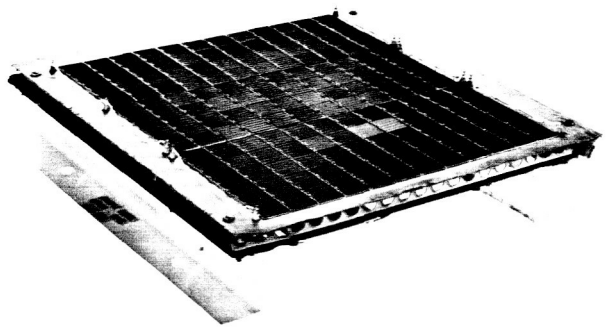

Fig. 11. *Mariner* Mars 1969 sample solar panel

Fabrication of the preproduction prototype panel was completed October 6, 1967. The panel was tested for electrical performance at Table Mountain, the JPL test site. Electrical performance of a typical section was reduced to space equivalent intensities and temperature, including a nominal 8% uncertainty due to temperature and intensity measurements. Results are tabulated below.

Intensity, mW/cm²	Temperature, °C	Maximum *P*, W
145	60	32.21
100	28	25.53
69	2	18.55

The panel is in process of being subjected to flight-acceptance and type-approval levels of environmental testing.

E. Telecommunications

1. Telecommunications Compatibility Test Facility

Prior spacecraft flight projects have verified the compatibility of spacecraft systems with deep space instrumentation facility stations by physically transporting spacecraft proof test model equipment to Goldstone and/or testing flight spacecraft at Cape Kennedy (DSS 71).

A new compatibility test facility is being developed by the Deep Space Network to allow compatibility testing at JPL. It will be called DSS 21. An interim version of this facility is under construction to support *Mariner* Mars 1969 and is scheduled for completion in January 1968. It includes a complete set of deep space station operations equipment, and communication networks linking the station with the spacecraft assembly facility (SAF), environmental test laboratory (ETL), RF subsystems laboratory, and the space flight operations facility (SFOF). DSS 21 will include a "clean screen-room" for housing spacecraft subsystems under test. Complete spacecraft will remain in SAF or ETL while being tested with the station. Compatibility tests will start with spacecraft subsystem breadboards and will continue throughout all phases of the test operations at JPL.

The station also allows for extensive testing of telecommunication performance. This is necessary for the *Mariner* Mars 1969 mission because of tight parameter tolerances and an associated smaller negative tolerance margin. Even

though design and performance analyses indicate a reduction in tolerance is feasible, experimental verification must demonstrate that the tight control of channel parameters is indeed practical and that such control can be maintained over the life of the *Mariner* Mars 1969 mission.

DSS 21 also provides a convenient location on premises for one set of the DSN multimission ground telemetry equipment being introduced for the first time on this mission. This new telemetry system is described in SPS 37-46, Vol. III. It consists of two SDS-920 computers and peripheral hardware. On past missions, the mission oriented ground telemetry system was included in each spacecraft system test complex. For *Mariner* Mars 1969, the DSS 21 based telemetry equipment will be used to check out each spacecraft during ETL tests and at least one SAF system test.

A complete series of operational tests is planned for the spacecraft and this facility. The first test, the initial design checks of spacecraft telemetry, command, data storage, and breadboards with available DSS 21 equipment, began during this report period. The second test scheduled is the initial spacecraft breadboard compatibility check with the new multimission telemetry hardware and development software. This test was also begun late in this period, and will continue throughout the month of December. The third test begins early in January. At that time, the actual *Mariner* Mars 1969 telemetry software will be tested with the new multimission ground telemetry subsystem.

The fourth test series covers the whole 1968 calendar year. It includes compatibility tests with each individual spacecraft during its shake test, vacuum temperature tests and at least one SAF system test. The command, high and medium-rate telemetry, ranging, and tracking channels will be checked. Also, during this period, each spacecraft radio subsystem ranging channel will be calibrated with the DSS 21 station. These tests are time limited because of other spacecraft test requirements and will be conducted as gross compatibility tests only.

The fifth test series will be similar to those conducted at Goldstone on previous *Mariner* and *Ranger* missions. It will include exhaustive compatibility tests between DSS 21 and telecommunications spacecraft subsystems before and after their assembly into the proof test model and flight spacecraft. These tests will begin in the spring and extend into the fall of 1968.

The sixth series of tests extend from mid-1968 to the beginning of 1969. They constitute final project buy-off of the real time telemetry software. SAF and DSN operational readiness tests with the spacecraft and SFOF will also be conducted. The seventh series—mission operations support tests—will include all tests conducted during Cape Kennedy and actual flight operations.

Development and design of DSS 21 will be reported by the DSN in future issues of the SPS, Vol. III. *Mariner* Mars 1969 testing operations will be reported in SPS Vol. I.

F. Propulsion

1. Propulsion and Pyrotechnics

a. Propulsion subsystem. The *Mariner* Mars 1969 propulsion subsystem generally resembles that employed in the *Mariner IV* and *V* missions. It is a constant-thrust liquid-monopropellant rocket engine with associated tankage, tubing, and valves. Jet vanes actuated through the spacecraft attitude control subsystem provide for thrust-vector-control attitude stabilization during the burning period. A dual-start (and -stop) capability provides for two trajectory correction maneuvers in the mission.

Principal subsystem components consist of a high-pressure gas reservoir, a pneumatic pressure regulator, a propellant tank and propellant bladder, and a rocket engine. The pressurizing gas is nitrogen; the monopropellant is anhydrous hydrazine. The engine contains a quantity of a spontaneous catalyst to initiate and maintain the decomposition of the propellant. Two parallel sets of start and shutoff squib-actuated valves in the nitrogen and fuel lines provide the two-maneuver capability. Welded and brazed tubing and fittings are used wherever possible to minimize leakage during the relatively long (maximum 250 days) storage period, as are metal seals, rather than elastomer seals, where welding and brazing are impossible.

A schematic of the subsystem is given in Fig. 12. Figure 13 is a photograph of the equipment, being manufactured under contract by TRW Systems, Inc., Redondo Beach, California.

Prototype testing of the rocket engine has been completed and all test results appear favorable. Data reduction is continuing. All documentation has been completed for flight release. Fabrication of rocket engine and regulator parts for the proof test model (PTM) were started in late July, 1967. The phase II fabrication effort was formally

PRESSURE TRANSDUCERS

- P_1 NITROGEN TANK
- P_2 PROPELLANT TANK
- P_3 THRUST CHAMBER

TEMPERATURE TRANSDUCERS

- T_1 PROPELLANT TANK
- T_2 NITROGEN TANK

1 ROCKET ENGINE
2 PROPELLANT ORIFICE
3 PROPELLANT INLET FILTER
4 PROPELLANT VALVE, START 1
5 PROPELLANT VALVE, START 2
6 PROPELLANT VALVE, SHUTOFF 1
7 PROPELLANT VALVE, SHUTOFF 2
8 FILL VALVE, PROPELLANT
9 PROPELLANT TANK
10 PROPELLANT BLADDER
11 PRESSURIZATION VALVE, NITROGEN
12 PRESSURE REGULATOR, NITROGEN
13 NITROGEN FILTER
14 NITROGEN VALVE, START 1
15 NITROGEN VALVE, START 2
16 NITROGEN VALVE, SHUTOFF 1
17 NITROGEN VALVE, SHUTOFF 2
18 FILL VALVE, NITROGEN TANK
19 NITROGEN TANK

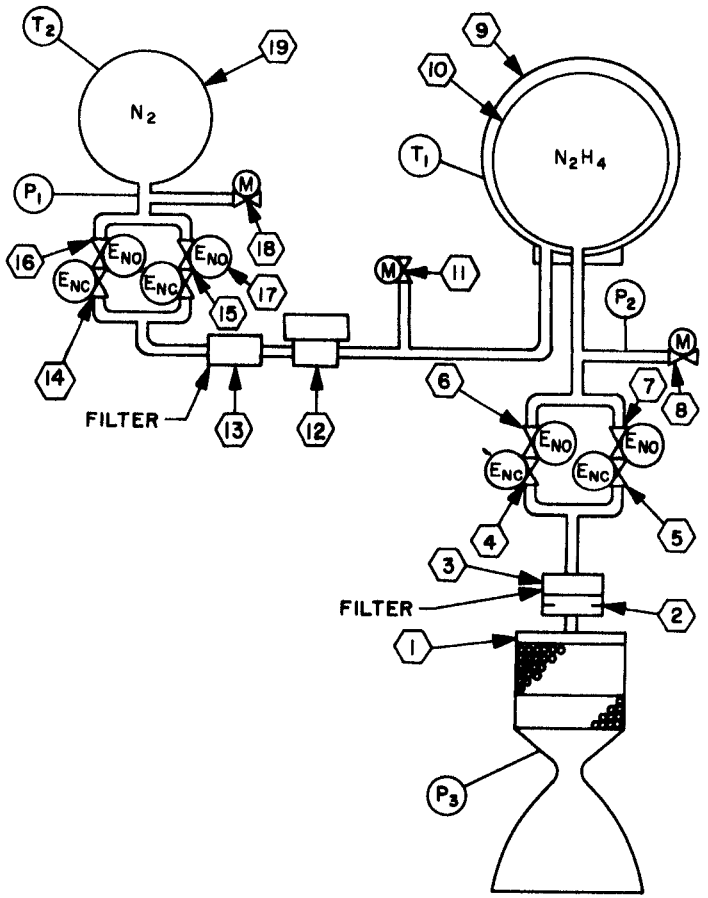

- E_{NO} 2 WAY VALVE, EXPLOSIVELY ACTUATED, NORMALLY OPEN
- E_{NC} 2 WAY VALVE, EXPLOSIVELY ACTUATED, NORMALLY CLOSED
- M 2 WAY VALVE, MANUALLY ACTUATED
- 10 COMPONENT NUMBERS (TYPICAL)
- FILTER
- PRESET REGULATOR
- ORIFICE, PROPELLANT
- P_1 INSTRUMENTATION NUMBERS (TYPICAL)

Fig. 12. Propulsion subsystem schematic

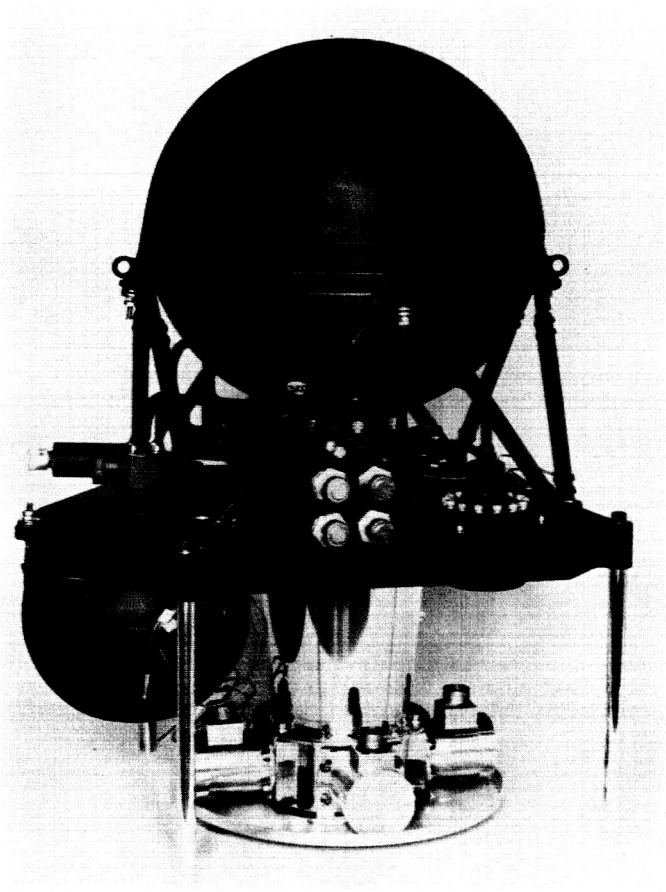

Fig. 13. Propulsion subsystem temperature control model

begun August 28, 1967. During this period the temperature control model shown in Fig. 13 was completed by the contractor and delivered to JPL. The delivery of the developmental test model (DTM) is expected shortly. Fabrication of all the PTM hardware has started. Delivery of the PTM for type-approval testing is expected January 2, 1968. The pacing items are the pressure transducers and the regulator.

It is expected that type-approval testing will be completed by January 15, 1968 with refurbishment of the system (replacement of squib-actuated valves) being completed by the contractor before February 1, 1968. Type approval and flight acceptance tests of component hardware has started with testing of the nitrogen and propellant tanks.

b. Pyrotechnic subsystem. The *Mariner* Mars 1969 pyrotechnic subsystem is involved in the performance of the following flight events:

(1) Spacecraft separation.

(2) Solar panel deployment and scan platform unlatching.

(3) Propulsion thrust initiation and termination.

(4) Infrared spectrometer cooldown and motor start.

Separation is effected through two mechanically redundant two-squib release devices which are actuated by the launch vehicle firing unit. Solar panel deployment is accomplished by 4 two-squib pinpullers. The scan platform is unlatched by a squib valve, the propulsion system contains eight squib valves (start and shutoff for nitrogen and fuel for two maneuvers), and the infrared spectrometer is started by two squib valves. The squib-operated valves each contain one dual-bridgewire squib.

The squib-firing power storage and switching and command control are performed redundantly by two identical pyrotechnic control units, which also provide for prelaunch analytic testing and inflight diagnostic telemetry. Squib-firing energy is accumulated by charging capacitor banks. Simple redundancy is provided in the duplication of pyrotechnic control units and the use of either dual-bridgewire squibs or dual-squib pinpullers.

A simplified schematic of the subsystem is shown in Fig. 14, with the exception of the spacecraft release devices. This shows the sources of command input and the output to the squibs, infrared spectrometer (IRS) motor and flight telemetry subsystem. The pyrotechnic control unit is being developed and manufactured under contract by Electro-Optical Systems, Inc., Pasadena, California. The valve squibs are manufactured by Hi-Shear, Inc., Torrance, California.

During this period fabrication of the two prototype pyro control units (PCU) was completed. During engineering test, several errors in both the prototype flight hardware and the laboratory test set (LTS) were found. These errors were corrected and compatibility tests with the two flight units and the LTS have been completed. The units are now in the formal testing, which precedes potting. The testing to date has shown no evidence of any major design problems though some redesign of the main circuit board is being accomplished to improve the fabrication and the tie-down of the cable bundles. This circuit board is shown in Fig. 15.

Fabrication started October 17, 1967 on the proof test model (PTM) PCUs. Based on the October 17 date, PTM fabrication is scheduled for completion by December 15,

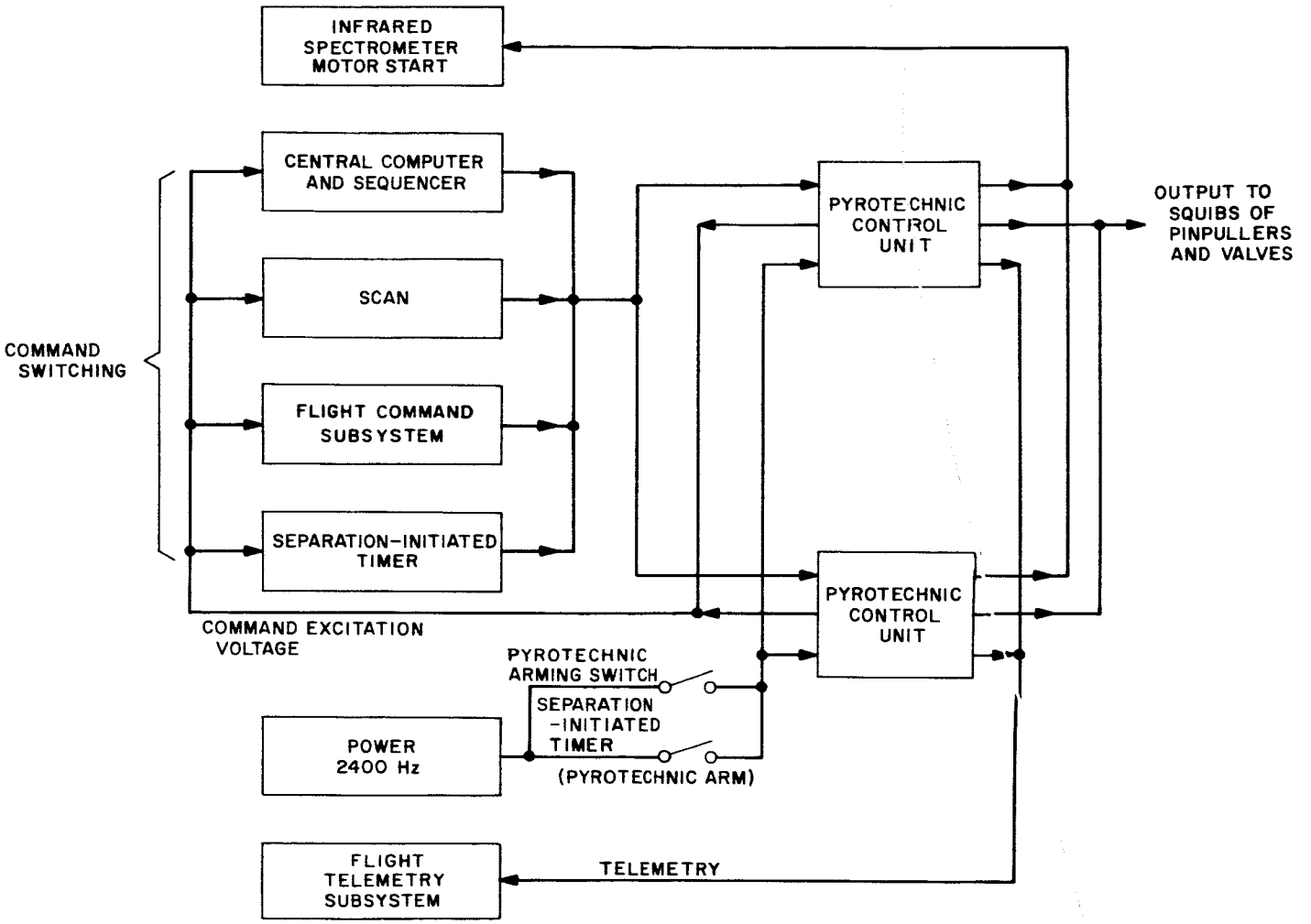

Fig. 14. Pyrotechnic control subsystem

1967. Functional tests will be completed by December 20 and type-approval testing by January 12, 1968 for delivery to the spacecraft assembly facility by January 15. This schedule is very tight, and in the event of any problems delivery to SAF may be delayed. If that occurs the prototype PCUs can be substituted for early testing.

Hi-Shear, Inc. delivered 129 valve squibs September 15, 1967. Fabrication of the second lot of 71 squibs has been started. Evaluation testing has been completed on the pinpuller squib and the spacecraft release device and squib. Requests for quote have been prepared and are ready for release for both items.

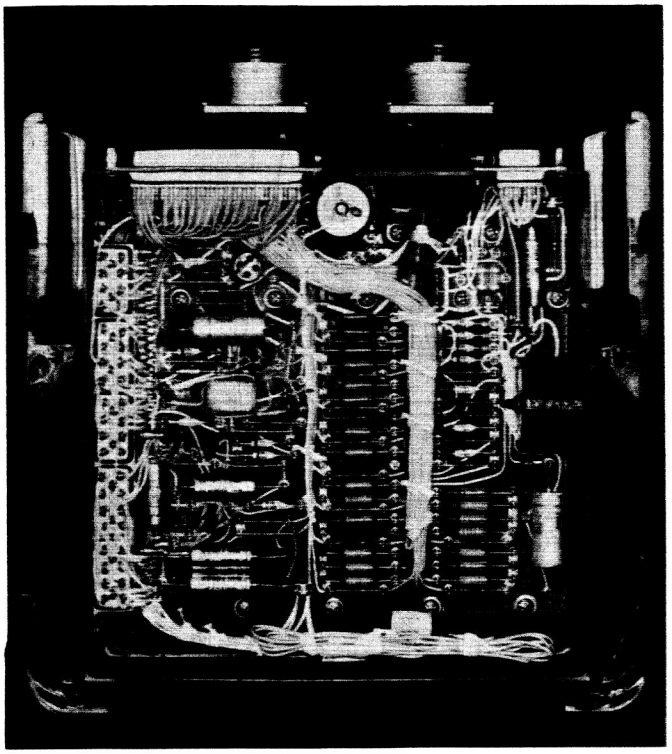

Fig. 15. Pyrotechnic control unit prototype

IV. *Voyager* Project

PLANETARY-INTERPLANETARY PROGRAM

A. Introduction

1. Status

All phase B (preliminary design) activities of the *Voyager* Project have been closed out, and the initiation of phase C (system design) has been suspended. All *Voyager* interplanetary missions have been indefinitely postponed. Material in Subsections B and C represents effort performed prior to the phase B close-out.

2. Objectives

The primary objective of the *Voyager* program had been to carry out scientific investigations of the solar system by instrumented, unmanned spacecraft which would fly by, orbit, or land on the planets. Emphasis was placed on acquisition of scientific information relevant to the origin and evolution of the solar system; the origin, evolution, and nature of life; and the application of this information to an understanding of terrestrial life. The primary objective of the *Voyager* missions to Mars was to obtain information relative to the existence and nature of extraterrestrial life; the atmospheric, surface, and body characteristics of Mars and the planetary environment by performing automated experiments on the surface of, and in orbit about, the planet. A secondary objective was to further our knowledge of the interplanetary medium between the planets Earth and Mars by obtaining scientific and engineering measurements while the spacecraft was in transit.

3. Project Plan

All *Voyager* missions were to be conducted as events of an integrated program in which each individual flight formed a part of a logical sequence in an over-all technical plan of both lander and orbital operations. The *Voyager* design would provide for the carrying of large scientific payloads to the planet, the telemetering of a high volume of data back to Earth, and long useful lifetimes in orbit about the planet and/or on the planetary surface. Hardware was to be designed to accommodate a variety of spacecraft, capsule bus, and lander science payloads, mission profiles, and trajectories. Particular emphasis was to be given to simple and conservative designs, redundancy wherever appropriate, and a comprehensive program of component, subsystem, and system testing.

4. Technical Description

Two identical planetary vehicles were to be launched by a single *Saturn* V launch vehicle. Each complete planetary vehicle was to consist of a flight spacecraft, flight capsule bus, and surface laboratory. Science experiments were to be conducted from the orbiter during descent and on the planet surface. The sterilized flight capsule bus was to be designed for separation from the flight spacecraft in orbit, for a Mars impact trajectory, for entry into the Mars atmosphere, for descent to the surface, and for soft-landing the surface laboratory, with surface lifetimes of months. The surface laboratory was to contain all power, sequencing, and communications for the conduct of surface operations.

B. Space Sciences

1. Soil Organic Matter, its Sampling and Analysis, With the Total Analytical Fractionation of Chlorella 71105 Used as a Model Scheme Preliminary to Application to Soil

a. Introduction. The soil organic analysis (SOA) program is a support program for the pyrolysis-gas chromatography and mass spectrometry (GC/MS) instrumental analysis effort. The GC/MS effort is to analyze barren desert soils: (1) for organic compounds in general, and (2) for "life-related" compounds, if it is found feasible to do so. The SOA program will support the main program by chemically characterizing all the types of organic matter found in terrestrial desert soils.

b. The two great categories of soil organic matter. Operationally, soil organic matter falls into either of two great categories: (1) that easily extractable (EE) by organic solvents, and (2) that hydrolytically "extractable" (HE) by acids or bases. The EE material is a very complex mixture of fairly intact compounds from living systems or their little-altered remains, as for example, the green pigments extractable from soils or rocks by acetone (Refs. 1 and 2). The EE material, though complex, may be analyzed by chromatographic means; the main body of this article will deal with a model experimental approach to the task. In marked contrast, the HE material occurs in soil and rock as a high polymer of uncertain structure which is apparently derived from higher plant tissue by secondary processes. Thus, HE material ("humic acid," "kerogen") can be analyzed imperfectly only by degradative attack (Refs. 3, 4, and 5). It is important to note with respect to pyrolysis that "extracted" and subsequently reconstituted "humic acid" is not the same compound as that found *in situ*. There is no method known for extracting all the organic matter from mineral soils (Ref. 6), and there is always an "unextractable" organic residue "humin" present.

c. Organic trace analysis. EE material may be thought of as "primary" with respect to living soil systems, while HE material is derived or "secondary" material. The analysis is complicated by the fact that a typical barren desert soil may contain 0.1% or less of total organic carbon (Ref. 7) (1 mg/g) of which only 0.01% (10μg/g) is EE material. We are thus dealing with trace biochemical organic analysis. This sampling problem is somewhat analogous in its extreme difficulty to that met in sampling for marine plankton (Ref. 8).

d. Pyrolysis and the importance of the type of sample chosen. The pyrolysis sample may consist of either whole soil or an extract (HE or EE) of it. It may also consist of derivatives of any of these, prepared *in situ* or otherwise. The exact type of sample to be chosen depends on matters outside the scope of this article, such as sample handling systems. Let us, however, consider the types of samples to be chosen for pyrolysis as they affect the complexity of the process and thus the interpretation of data from the instrumentation train. First, consider that a 1-g sample of a whole typical barren sandy desert soil will consist largely of a great amount of heterogeneous surface, 0.4–0.8 m^2/g (Ref. 9) which is "coated" lightly with about 0.1% of organic matter. This amounts to only about 2 mg/m^2 of surface. The pyrolysis of the organic matter in a gram of such whole soil will thus be affected by the catalytic effect of the complex and greatly heterogeneous mineral surfaces present. Further, since the organic matter present is mostly the little understood polymeric "humic acid" or "kerogen" (Refs. 10, 11, and 12) (only hydrolytically "extractable"), it is reasonable to expect that there will be some difficulty in interpreting the data so as to reveal the parent structures from which the pyrolysate is derived. If one is seeking evidence of life in the soil by means of the traces of cells or relatively unaltered EE cellular material present, it will be recalled that this occurs only at the 0.01% (20 $\mu g/m^2$) level. Of course, it is a great over-simplification to speak of EE matter "coating" a surface at this level. Evidently, whole soil samples will introduce the important variable of heterogeneous surface catalysis into the pyrolysis process (Ref. 13).[1] This situation is complicated by the fact that soils show extreme point-to-point variation

[1]Adamcik, J. A., *Studies on the Pyrolysis-Gas Chromatography of Organic Compounds*, Section 326 Internal Section Report. Jet Propulsion Laboratory, Pasadena, Calif., 1966.

within a sample so that there is no such thing as a "standard" soil.

Second, consider the 1 mg of HE fraction from the 1-g sample. It may be pyrolyzed either as the solution in which it was "extracted" or as the precipitate ("humic acid" or "kerogen") obtained on neutralization of the solution or as volatile derivatives (trimethylsilyl ethers) of either. The HE pyrolysis data would probably be less ambiguous than that from whole soils because of the lack of surface catalysis effects. In this case, we again have the problem that the nature of the parent structure is poorly understood (Refs. 4 and 10) so that we are always dealing with polymers of relatively unknown structure. Because barren deserts without higher plants would have soil "humic acid" based on non-lignified algae or fungi, this might be quite different from "ordinary" humic acid.

Third, consider that the 10 μg or so of EE material from the 1 g of soil can be pyrolyzed either in solution or after removal of the solvent. This sample would provide the least ambiguous pyrolysis data because it would be made up of reasonably intact or monomeric "life related" structures such as the altered chlorophylls. Even here, however, the "synergistic" effect of the many components present in the complex EE mixture would probably introduce some ambiguity into the course of the pyrolysis.

This discussion of course implies that (1) complete extraction and handling of the soil fractions without introduction of artifacts is possible and (2) that the instrumentation train is of sufficient sensitivity to characterize at least "most" of the compounds present. The problem of integrating the pyrolysis data so as to permit an unambiguous interpretation in terms of life originally present in the soil is outside the scope of this article (Ref. 14). An important third implication in this discussion is that one can effectively disrupt the cell walls of the soil microflora-or-fauna during the extraction step and thus ensure "complete" extraction.

e. Operational tasks of the SOA program. The soil organic analysis program thus has two main tasks:

(1) The immediate preparation of a number of humic acids (HE material) from desert soils for other workers on the program to analyze by means of pyrolysis/GC/MS. Because there is no "standard" method of effecting this preparation, one will have to be arbitrarily chosen. The choice will be arbitrary because: (1) "humic acids" are artifacts of the particular method chosen; they are secondarily derived products which are reconstituted as complex polymers on neutralization of the hydrolytic extracts of native soil; (2) thus the merit of the method chosen depends not on the "quality of the product," (which is of unknown structure) but only on the total yield; and (3) no method exists which recovers all the organic matter of mineral soils (Ref. 15). Once the preparation method is chosen, this task will be routine.

(2) The complete analysis of the EE material into functional group classes and individual compounds. The remainder of this article will detail the planned analytical attack on the EE soil material. Such material is amenable to chromatographic analysis because it is non-polymeric, and is extracted as a true solution. This task is not routine.

f. Sampling. We should perhaps re-emphasize the point that such analyses of barren desert soils fall into the category of organic trace analysis. In view of this, let us consider the following diagram:

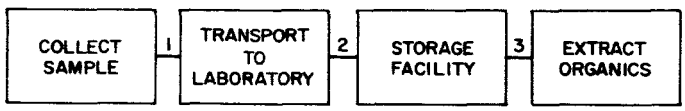

The blocks correspond to the traditional trace analysis steps: collection, fractionation, analysis. It is clear that contaminating artifacts can be introduced into the sample at any step in this sequence as from tools, soil bags (Ref. 16), air conditioning systems (Ref. 17), laboratory environment (Ref. 18), or extraction solvents. Samples should, therefore, be collected in clean all glass or Teflon–FEP vessels, and all extraction solvents should be freshly distilled before use.

g. The extraction problem and the complexity to be expected of EE material. The extraction of material from biological tissue is an empirical matter—there is no general method of choice. The specialized investigator usually selects an extractant which takes up a given class of compounds "preferentially," and the rest of the sample is discarded. Such solvents as the chloroform/methanol 2/1 (by volume) mixture of Folch, as discussed in Entenman's review (Ref. 19), appear to be of general utility for the extraction of all non-polymeric compounds from animal tissue because they are able to break the tissue lipoprotein complexes present. Because soil is a unique system of fresh and autolyzed animal and plant cells attached somehow to a damp mineral matrix, this solvent shows promise.

In a previous study, we found that most simple polar solvents extracted about the same proportion of organic

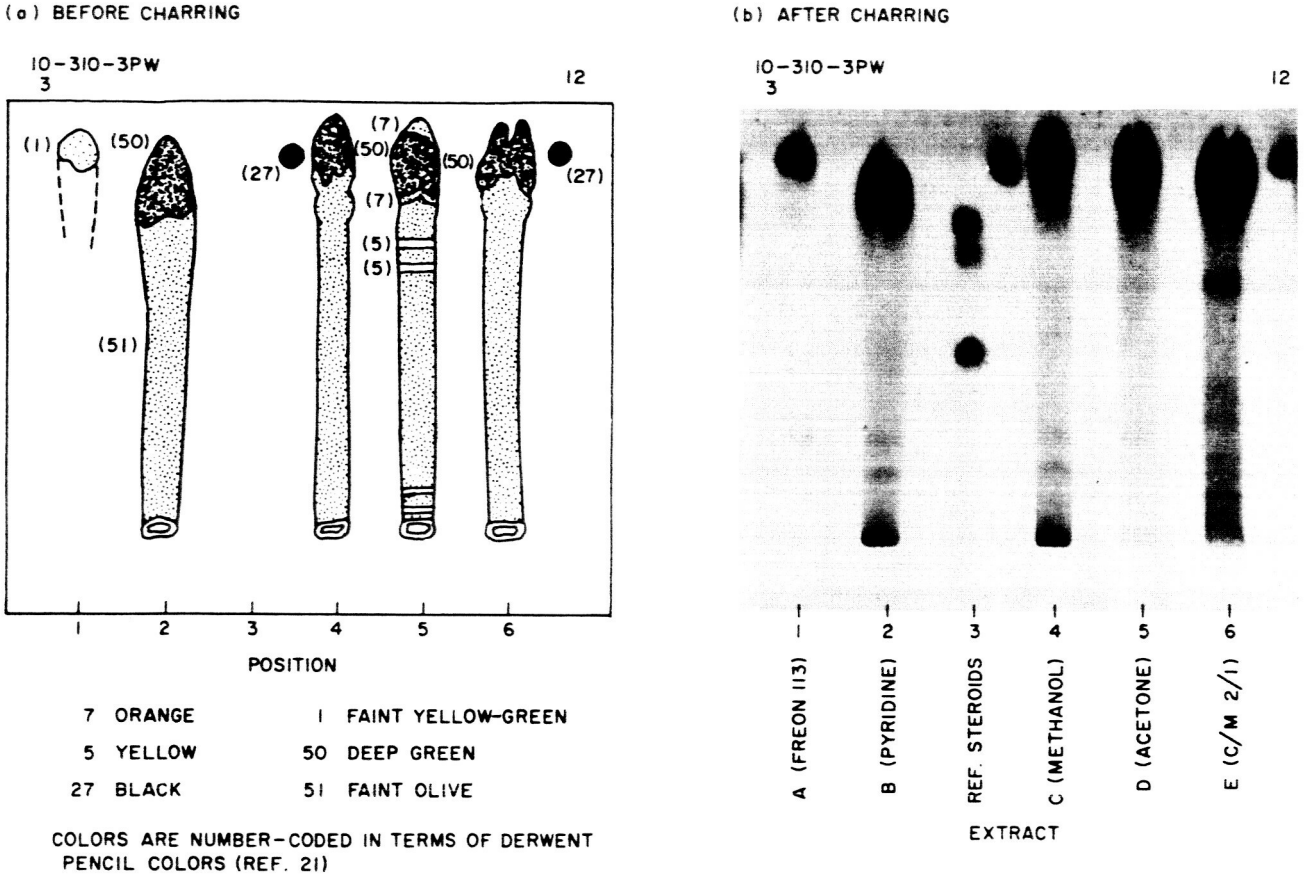

Fig. 1. One-dimensional TLC on the adsorbent silica gel plain/Corning high-purity porous glass/magnesium silicate 1/3/1 (w/w) developed in a steroid system, chloroform/methanol/water 188/12/1 (v/v), (Ref. 20) and charred after spraying with 50% aq. H_2SO_4

matter from algal crust soil. Figure 1 (a thin-layer chromatogram, TLC, Ref. 20) will suggest the nature of the EE mixture extracted from such soil by blenderization with the solvents listed. (Extracts of soil 1-5 (algal crust) were applied at positions 1, 2, 4, 5, and 6 in the following amounts, respectively: 120, 450, 450, 550, and 700 μg. Reference steroids were applied at the 25-μg level at position 3 as follows: cholesterol, androsterone, and corticosterone. Azulene was applied at the 15-μg level between positions 3 and 4 and to the right of position 6.) Several significant features can be seen from Fig. 1; let us present a conclusion first, then a discussion for each:

(1) The mixture extracted can be made simple if poor (and, therefore, selective) solvents such as Freon 113 are used. This solvent extracted only about one third as much material as did the others, but the relatively simple mixture appeared to consist only of hydrocarbons, waxes, and other neutral lipids.

(2) The soil matter is not very greatly altered or at least not polymerized because it is soluble in organic solvents. The fresh plate showed "peacock feather" patterns of green and orange pigments which means (not surprisingly in this case) that plants (algae) and their remains are present in the soil. We have seen such poorly separated pigment "feathers" in all soils examined thus far (Cameron collection numbers 1-2, 3-1, 6-1, 17-1, 62-1, 73, 76-1, 142, and 301). This suggests that we are dealing with an ubiquitous (and mostly autolyzed) algal population in desert soils. Extracts of live algae show the presence by TLC only of clearly separated bands of unaltered pigments.

(3) TLC alone cannot fully resolve such a complex mixture of related polar compounds. Because the green pigments on the plate form long streaks, they probably represent a family of structurally similar compounds (Refs. 1 and 2). The TLC system operates by means of functional group hydrogen bonding to the silanol groups of the adsorbent so that compounds with the same general molecular shape and number of H-bonding functional groups will run together. Parenthetically, TLC is a rapid,

versatile method of great value in comparing great numbers of mixtures. Whether the separations are complete or not, the pattern of separation in itself is a "fingerprint." Its value may be made great by the use of diagnostic spray reagents (Ref. 21) (i.e., ninhydrin) and by selective removal of compounds from the plate for chemical or spectral study.

(4) We must decide: (1) whether to use a poor (selective) solvent, such as Freon 113, to extract a part of the soil material which is relatively simple (Waksman's "proximate analysis" approach) (Ref. 6) in the number and kind of compounds present, or (2) whether to use the "best" solvent (or mixture) to extract all the extractable material.

h. Criteria for extracting EE matter. Because a biochemical analysis is of limited value if only part of the data is included, we shall try to extract all the EE material from the soil. It may be necessary to use a sequence of solvents to accomplish this, such as acetone followed by chloroform/methanol 2/1, so that the subsequently pooled extracts will contain "all" of the extractable native material from the soil. We shall then have a mixture of compounds which will range in solubility from the water-soluble free amino acids to the hydrocarbon-soluble plant waxes. This extraction procedure is not yet complete.

This entire extract will then be fractionated according to the protocol of Rouser, as shown in Fig. 2 (Ref. 22,

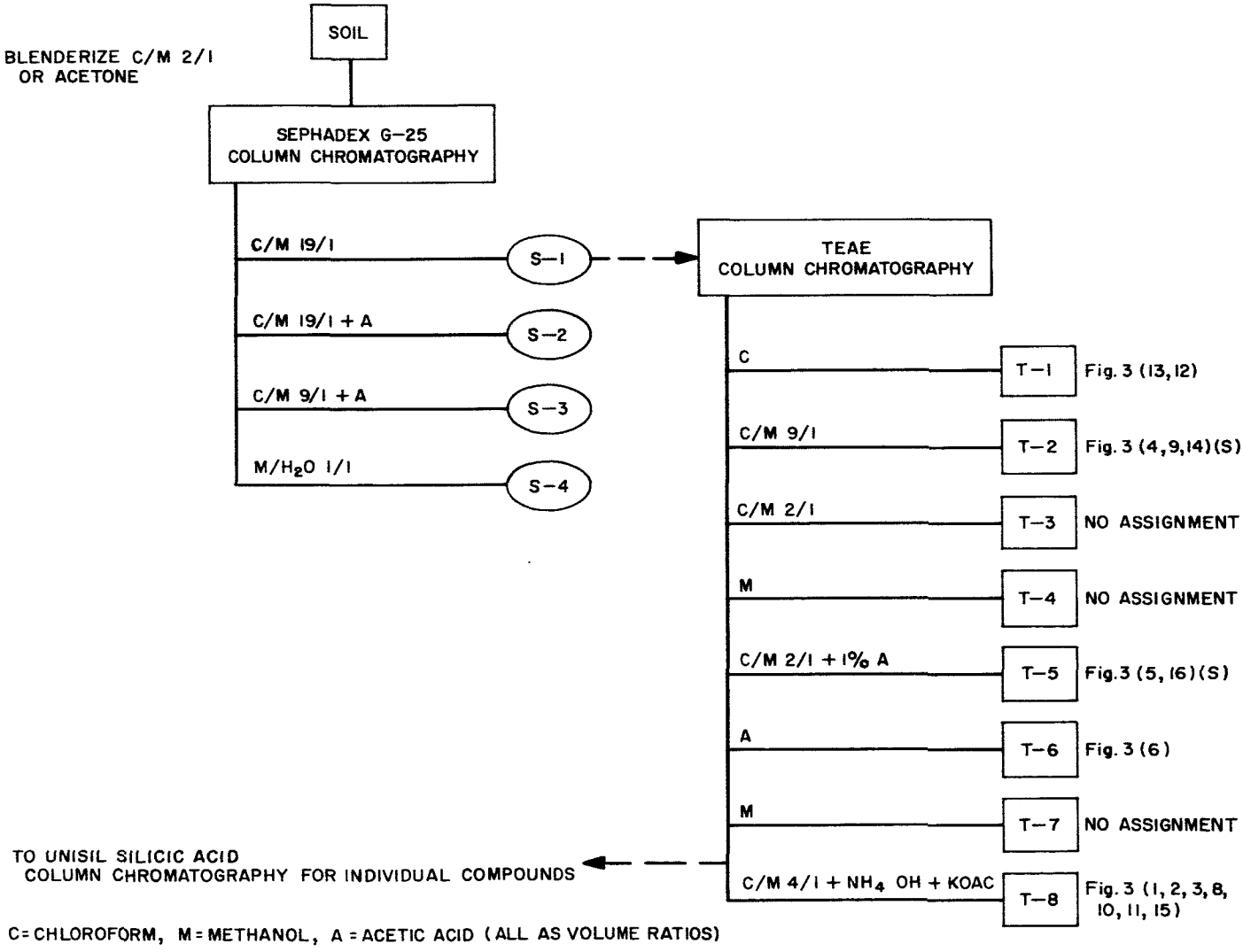

Fig. 2. Overall analysis scheme for EE soil organic matter with some partially speculative class assignments for typical lower plant compounds (coded S) as well as known typical classes, all in terms of the structures shown in Fig. 3

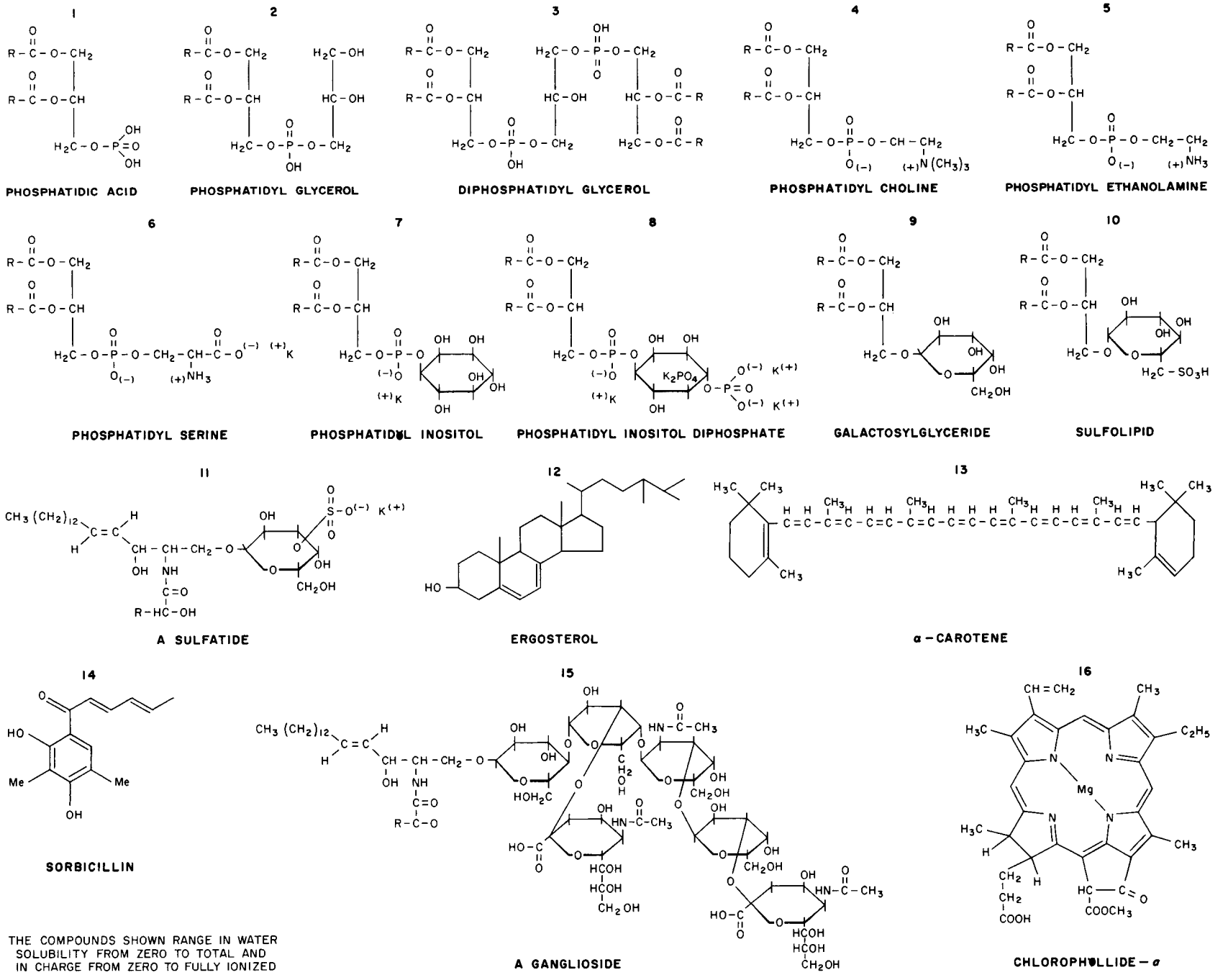

Fig. 3. Some typical natural products which have been placed in the scheme shown in Fig. 2

23, 24). He devised this scheme in order to separate brain lipids, a mixture of compounds of great diversity such as cholesterol (hexane-soluble) and the gangliosides (water soluble). The only other great-group analytical scheme we know of is that proposed by Degens and Reuter, but its chief value lies in the subfractionation of hydrolysates (Ref. 25). Figure 3 lists some arbitrarily chosen typical structures as they place in the scheme.

This scheme is general and might be used to resolve any complex organic mixture because it uniquely: (1) first separates the mixture into classes of different water solubility by means of gel filtration; (2) then separates each class into ionic, neutral, or zwitterions by means of triethylamino-ethylcellulose (TEAE) anion exchange chromatography in a nonaqueous medium; and (3) finally resolves each class into small fractions by means of silicic acid (hydrogen-bonding/partition) chromatography. TLC will be used to monitor all these fractions for heterogeneity by means of systems able to "place" the entire polarity spectrum of compounds (water soluble through hydrocarbon solubles).

This analytical approach has a number of unique features:

(1) The scheme first isolates great polarity groups such as lipid solubles and water solubles by means of Sephadex column chromatography, then each of these is subfractionated separately by means of ion exchange chromatography in nonaqueous media. An example of this latter chromatographic mechanism is as follows:

TEAE, hydroxide form, packed in a chloroform/methanol mixture

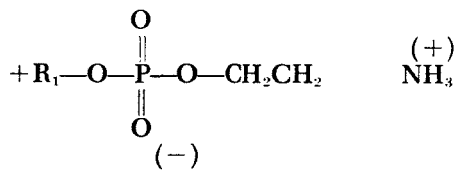

a typical ionic lipid, phosphatidyl ethanolamine, (PE), yields upon exchange

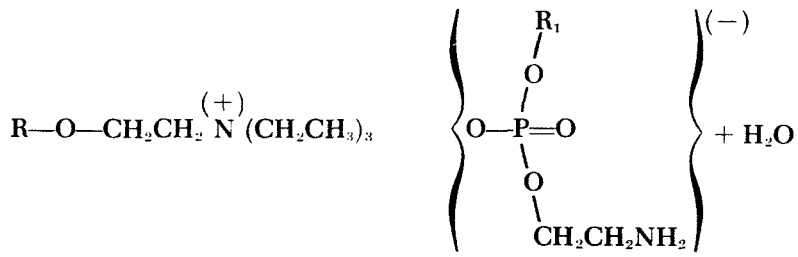

and the PE is then eluted only with an acid, such as acetic:

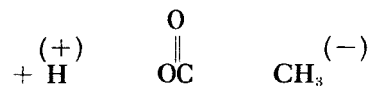

to yield the resin with the free compound

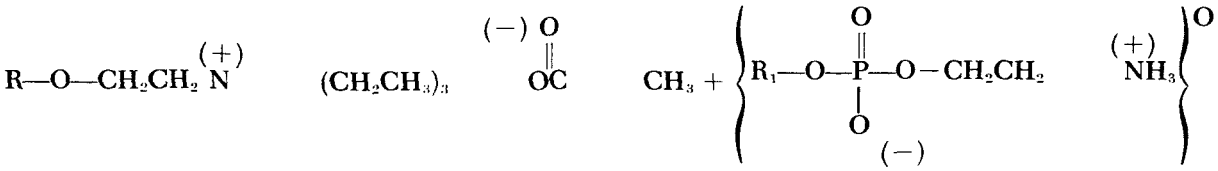

TEAE, acetate form

free PE

Thus, TEAE cellulose operates in a sort of "go-no-go" manner to separate compounds by means of neutral, acid, and basic solvent gradients in nonaqueous media.

(2) The column procedures will isolate large amounts of native material quantitatively. All the extractable material will place somewhere in the scheme without regard to its solubility properties. If derivatives for gas chromatography (e.g., trimethylsilyl ethers of sugars) are desired, they can be made without great concern for interfering materials. Columns are easily protected from light and, with air-free solvents used, the procedures minimize artifact formation. In general, most natural product separations require that the material be kept free of operational artifacts by working on it in the cold under ultrapure nitrogen and under dim or red light.

(3) The column fractions are to be quantitated by means of a Cahn microbalance weighing of aliquot residues (Ref. 26). Qualitative identification will be made conventionally by means of analytical and preparative TLC and by a combination of spectrographic techniques, such as IR, MS, and NMR[2] (Refs. 27 and 28). In general, two-dimensional TLC will be used to monitor the column fractions. Two-dimensional TLC gives better resolution than one-dimensional, permits the recognition of more components, and is relatively simple, rapid, and suited to the comparative study of complex mixtures.

(4) A special feature of great importance is the minimal exposure of such labile compounds as the carotenoids to disturbance by the "adsorbents." These and other natural products are altered by even short exposures to silicic acid (Ref. 29).

We may note that Fig. 1 implicitly suggests the need for such a sophisticated analytical attack on the EE mixture. The mixtures which we extract from soil contain a great number of reasonably intact photolabile pigments as well as numerous oxygen-labile "lipids."

i. The fractionation of Chlorella. Because algae are ubiquitous terrestrial life forms and because we have seen their green pigments in all soil samples examined thus far, we decided to test the analysis scheme of Fig. 2 on an alga. We carried out this work in the laboratory of Dr. George Rouser at his kind suggestion in order to learn his methodology. A large stock of the thermophilic alga *Chlorella pyrenoidosa Tx-71105* (Sorokin and Myers, 1953) was available as a freeze-dried mass culture product (Refs. 30 and 31). We felt that these cells which had been inadvertently thawed once were nevertheless acceptable for a test of the analytical scheme because antarctic or desert algal populations would probably consist of material which was greatly autolyzed. As an example of the complexity to be expected of such a mixture of oxidized and autolyzed plant material, we cite the work of Thirkell and Tristram (Ref. 32). These investigators found numerous chlorophyll pigments and alteration products in air-milled lucerne which they subjected to silicic acid column chromatography. They did not identify the products.

j. Experimental method. 24.9 g of frozen Chlorella 71105 were extracted in a nitrogen atmosphere by blenderizing with the solvents listed below at medium speed in a Waring blender fitted with a Polytron head.[3] The cells were blenderized with 0.75 mg of 2,6-di-tertbutyl-*p*-cresol (BHT), an antioxidant, and 0.25 g (1%) of magnesium carbonate in order to reduce alteration and pheophytinization of the chlorophylls. A sample of the frozen cells, 6.444 g in weight, lost 2.051 g of water on freeze-drying (31.8%) so that 17.0 g dry weight of tissue were actually blenderized. This also corresponds to a cell count of 2.1×10^{12} cells per gram of frozen tissue made for us by Mr. Frank A. Morelli. Mr. Morelli also observed that the cells were generally of intact appearance. All extractions were carried out in the cold (10–15°C) under dim white light (one well-shaded 60-W bulb 15 ft away) and under high-purity nitrogen which contained less than 8 parts/10^6 of oxygen. All solvents were freshly redistilled before use and showed a zero solvent blank.

The extraction sequence used was: chloroform/methanol 2/1 (20 vols.) (twice), chloroform/methanol 2/1 (10 vols.), chloroform/methanol 1/2 (10 vols.), and chloroform/methanol 7/1 saturated with concentrated aqueous ammonia (10 vols.) (Ref. 26). Solvent volumes are expressed as ml/g of frozen fresh algae. Filtration after each extraction was done under nitrogen with an "M" porosity sintered glass filter. The combined neutral extracts were concentrated separately from the ammonia extract in order to prevent base alteration of the chlorophylls. The neutral and the ammonia extracts were each concentrated separately to a small volume in the cold under nitrogen using a Buchler rotary evaporator. Water was displaced by repeated addition of chloroform and azeotropic concentration with care to avoid evaporation to dryness. After removal of ammonia from the last fraction was complete, the moist residues (black-green solids) were all combined

[2]IR = infrared; MS = mass spectrometry; NMR = nuclear magnetic resonance.

[3]Bronwill Scientific Division, Rochester, New York.

into a small volume of chloroform/methanol 2/1 which contained 5% water by volume. This represented the "total sample" of extractable material.

It should be stressed that this extraction procedure recovers water solubles (sugars, free amino acids) as well as the chloroform/methanol-soluble "lipids." The weight per ml and the total weight of the extract were determined by weighing the solids obtained from 50–200 μl of solution. The sample was placed in a small (about 6 mg) aluminum pan, dried at 75°C for 2 min, cooled for 2 min over KOH pellets in a desiccator, and quickly weighed on a Cahn microbalance. Tare weights on the empty pans were determined similarly. This quantitation method was used for all subsequent column fractions (Ref. 26).

The bright green insoluble cake which represented the algal cell walls weighed 6.5 g after desiccation over KOH beads *in vacuo*. The "total sample" of cell extracts (1.51 g or 6.1% of the frozen cells) was taken nearly to dryness under nitrogen, and as much as would dissolve in chloroform/methanol 19/1 was applied to a Sephadex G-25 (coarse bead) column, 2.5-cm ID by 30 cm high, freed of "fines" before use. The exact protocol shown in Fig. 2 was followed with the sample residue rinsed into the column with new solvent at each change. The appearance of these fractions and those from subsequent column runs are given in Table 1. In this way, the entire "total sample" was applied to the column (which was said to have a column volume, or CV, of 42 ml). After recovery, the fractions were transferred to small all glass storage vessels by means of the following solvents: Sephadex 1 dissolved in chloroform/methanol 9/1, Sephadex 2 in chloroform/methanol 2/1 with 1% water, Sephadex 3 in methanol, and Sephadex 4 in methanol/water 1/1. The quantitative recoveries are also given in Table 1.

TLC separation of the fractions was effected on an adsorbent composed of 9 parts of Silica Gel plain (no binder) plus one part of magnesium silicate slurried into 0.01N KOH (20 g/60 ml of solution) and spread with a Desaga spreader set at 0.25 mm. The adsorbent was air-dried and heat-activated just before use at 120°C for 20 min, cooled in air for 3 min, equilibrated in a flowing stream of air saturated with water vapor for 5 min, and spotted immediately. This protocol was observed for all subsequent TLC chromatography. Spotting was done unavoidably in air and under normal laboratory illumination. The TLC systems and their applications have been described (Refs. 22, 23, 24, and 26).

Table 1. Columns run, description of fractions, and recoveries

Sephadex columns[a]					
Fraction	**Wt, mg**	**Recovery, % of total**	**No. and TLC[b]**	**Remarks**	
S-1	1215	80.3	20 (39, 40)	Emergent front orange; fraction olive green	
S-2	196	12.9	11 (55, 52)	Faint green due to inadvertent spill	
S-3	62	4.1	3 (55)	Colorless (S-3 and S-4)	
S-4	41	2.7	—	—	
		Total recovery: 1513 mg = 100.9%			
TEAE column[c]					
Fraction	**Wt, mg**	**Recovery, % of total**	**λ max, mμ (in ether)**	**Remarks (color no.)[d]**	**No. and TLC[b]**
T-1	127	38.9	413, 443, 469, 663	Emergent front orange (9,50)	5 (46)
T-2	23.3	7.1	452, 642	Emerald green (46) chlorophyll-*b*	11 (45, 56)
T-3	105	32.1	408, 667	Olive green (51)	6 (47)
T-4	26.1	8.0	409, 665	Olive green (51)	4 (48)
T-5	28.0	8.6	408, 665	Green (49)	5 (50)
T-6	6.2	1.9	399, 666	Green (49)	13 (49)
T-7	0.1	—	—	Colorless	—
T-8	11.5	3.5	—	Nearly colorless	24 (51)
		Total recovery: 327 mg = 99.4%			

[a] Sephadex G-25 coarse bead, 2.5-cm ID × 30 cm high, packed in methanol/water 1/1 v/v and cycled twice through the elution scheme (Fig. 2). One column volume (CV) = 42 ml.

[b] Apparent number of components first, then TLC plate reference number in parentheses.

[c] TEAE, Brown Paper Co. Selectacel Standard Type 20, 12 g dry weight, packed in glacial acetic acid to a height of 21 cm in a 2.5-cm-ID column. One column volume (CV) = 75 ml. Remove acetic acid by 3 CV (225 ml) methanol, then put in OH^- form by 4 CV 0.1N KOH/methanol, then 8 CV methanol wash, then 4 CV chloroform/methanol 1/1, and 4 CV chloroform.

[d] Derwent pencil color (Ref. 21).

The nature of the classes of compounds represented in these fractions is indicated by Fig. 4 (lower half of illustration). The colors number-coded in the sketch represent those of "Derwent" colored pencils, as used by Reio (Ref. 21). The plates were sketched as they appeared visually, then sprayed with formalin/concentrated H_2SO_4 3/97 (v/v) and charred to reveal the colorless components. In plate 55 the beef brain standard mixture at position 6 contains the following compounds, read in order from the origin: two gangliosides (15), sphingomyelin plus phosphatidyl serine (6), two sulfatides (11), lecithin (4), phosphatidyl ethanolamine (5), two cerebrosides and finally cholesterol at the front. The numbers in parentheses refer to the structures listed in Fig. 3.

Figure 4 shows that: (1) fraction 1 contains most of the pigments; (2) fraction 2 contains only traces of pigments; and (3) the other two fractions are colorless and fraction 3 probably contains water-soluble salts and saccharides.

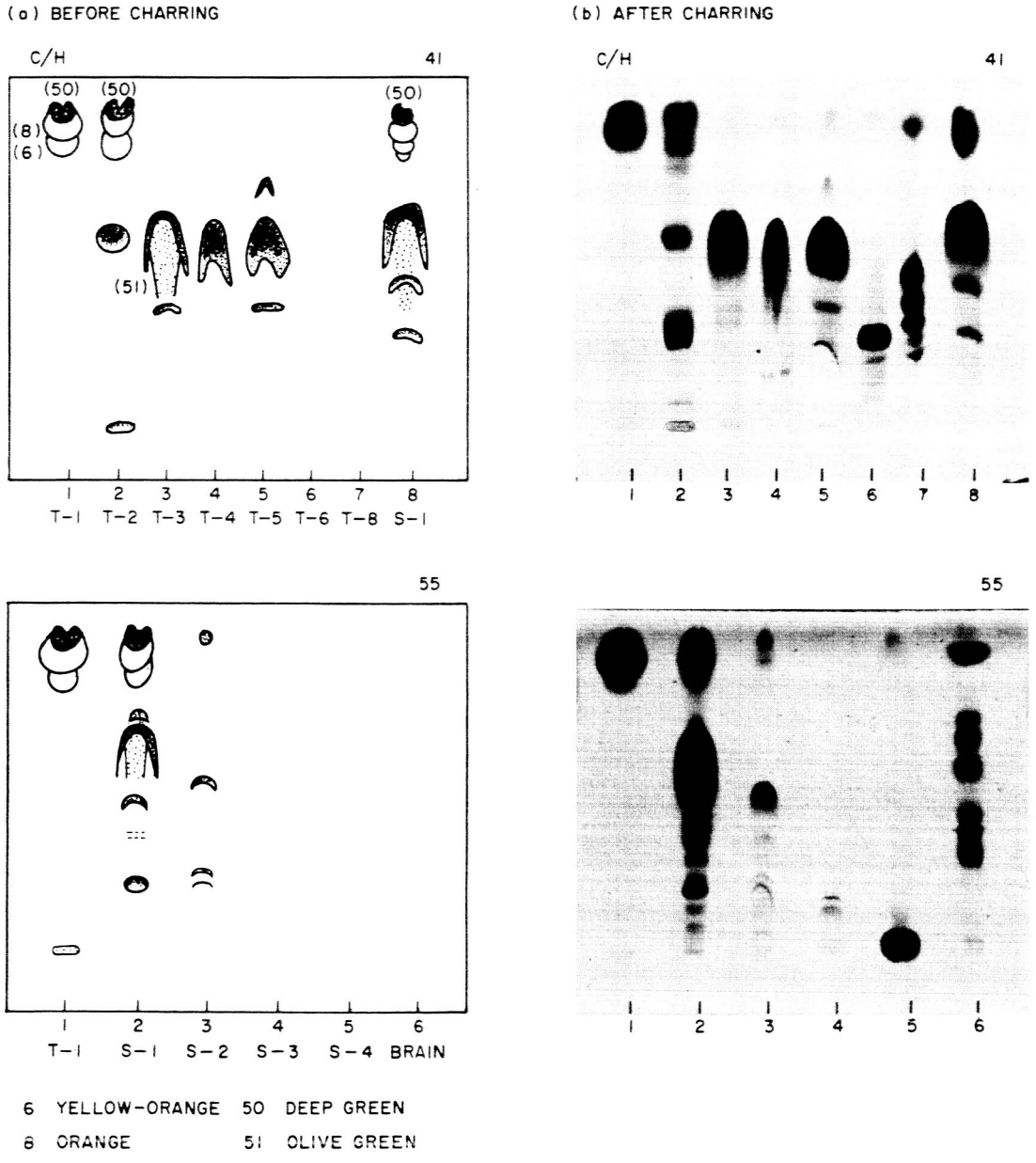

Fig. 4. One-dimensional TLCs on the adsorbent silica gel plain/magnesium silicate 9/1 (w/w) (spread in 0.01M KOH) and developed in chloroform/methanol/water 65/25/4 (v/v)

k. TEAE column chromatography. At this writing only the first Sephadex fraction (S-1) has been subjected to TEAE cellulose anion exchange chromatography. A TEAE column, 2.5-cm ID and 21 cm high (CV = 75 ml), was packed in the manner described for DEAE (Ref. 22) and converted to the hydroxyl form. A sample of 300.0 mg of fraction S-1 was applied in 2 × 3 ml of chloroform and the column eluted at 3 ml/min in accordance with the plan of Fig. 2. We followed this protocol rigidly because the object of this effort was to place the algal fractions in the scheme as designed by Rouser. However, as the TEAE chromatogram developed, a number of pigment bands appeared, as sketched in Fig. 5, coded in terms of Derwent pencil colors as before (Ref. 21). We did not attempt to collect each band separately, and the bands were pooled as described in Table 1.

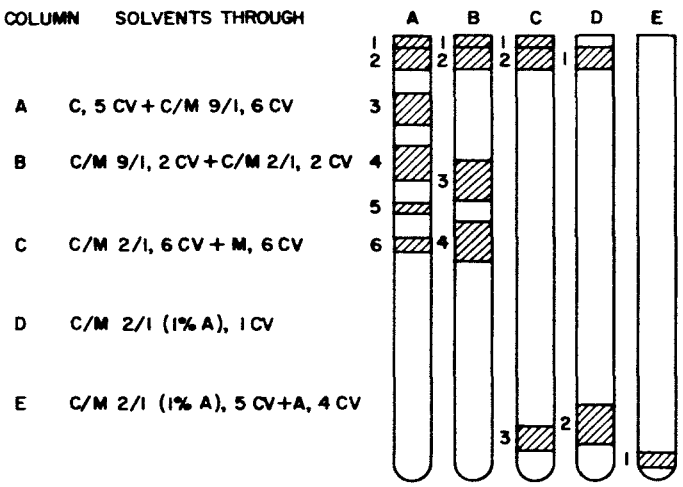

Fig. 5. Schematic diagram showing appearance of TEAE column during development

The column fractions were evaluated by (1) spectrophotometry and (2) TLC.

l. Spectrophotometry of the Chlorella pigments in either solution. Aliquots of the TEAE fractions collected (Table 1) were taken nearly to dryness under HP-grade nitrogen, and the residues were quickly extracted into peroxide-free ether. Spectra in ether obtained by means of a Cary Model 14 spectrophotometer are shown in Fig. 6. Carotenoid pigments and (probably) chlorophyll-*a* appeared in the first fraction (T-1), pure chlorophyll-*b* appeared in the second (T-2), and what appears to be pheophytin-*a* appears in fractions T-3, T-4, and T-5. The spectrum of fraction T6, eluted with glacial acetic acid, does not correspond to that of any described chlorophylloid pigment.

This separation is quite different from that reported for the TLC or paper chromatography of such pigments. Ordinarily, the order of migration is: pheophytins-*a* then -*b*, chlorophylls-*a* then -*b*, and finally, the chlorophyllides (Refs. 33 and 34). The structure of pheophytin-*a* and the diagram shown in Fig. 7 will serve as a point of speculative discussion as to the nature of the TEAE separation. The molecule easily loses magnesium to form the nonacidic pheophytin, and it can also lose the phytol (7e) and the carboxymethyl (6e) groups to form acidic compounds. These acidic compounds probably represent bands 2 and 1, respectively, of Fig. 4 if we assume that they were fixed to the column as carboxylate anions. We may expect to find a very complex mixture of such pigments in soil because there are at least 8 native chlorophylls (including the poorly characterized bacteriochlorophylls) and because innumerable isomerization reactions occur with each molecular species (Ref. 35). Even fresh Chlorella has recently been reported to possess a host of tetrapyrrole pigments (Ref. 36).

The TEAE column technique is strikingly effective in separating the acidic alteration products of the chlorophylls from the native pigments. The method should thus find wide general application for such problems as the soil pigment separations. The one-dimensional TLC characterization of the TEAE column fractions is given in Fig. 4, with Sephadex-1 for comparison. The TLC figure confirms that: (1) TEAE-1 contains only mixed pigments and neutral non-polar compounds such as triglycerides; (2) TEAE-2 contains only one chlorophyll pigment (Chl-*b*) with traces of carotenoids and numerous polar colorless unknowns; (3) TEAE-3 and -4 contain the same chlorophyll; and (4) TEAE-5 and -6 each contain a chlorophyll different from the others. Only a single two-dimensional TLC separation of one TEAE fraction (Fig. 8) is presented in order to give a further indication of the complex nature of the Chlorella 71105 Sephadex-1 mixture. The mixture of polar "lipids" shown is made up entirely of unknowns. The two-dimensional plates were dried under a flowing stream of nitrogen between dimensions for 8 min in very dim light. Two-dimensional TLC, although less rapid than one-dimensional TLC, shows better resolution of complex mixtures and thus permits more positive

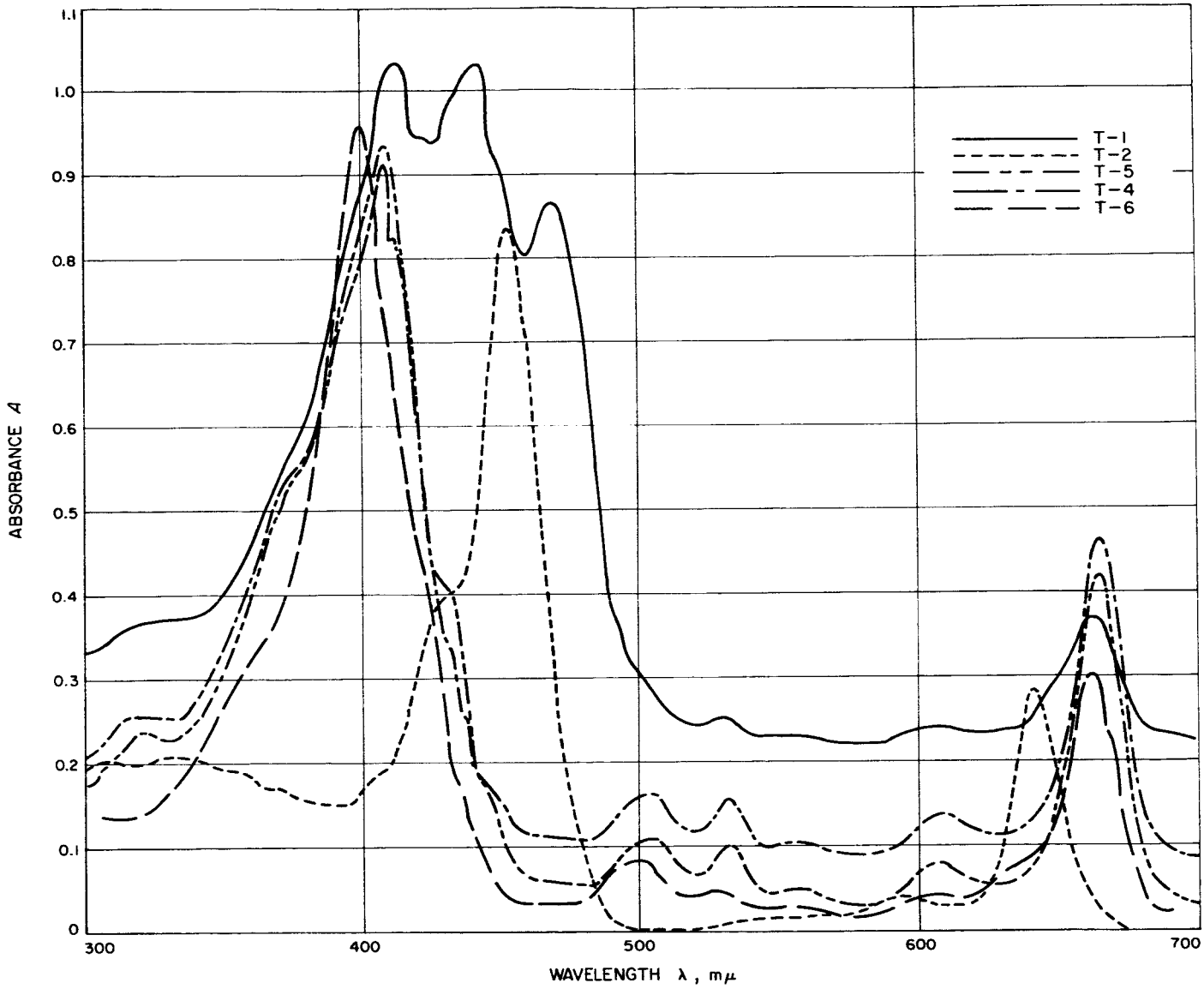

Fig. 6. Visual absorption spectra in diethylether of TEAE column fractions ether-soluble portions

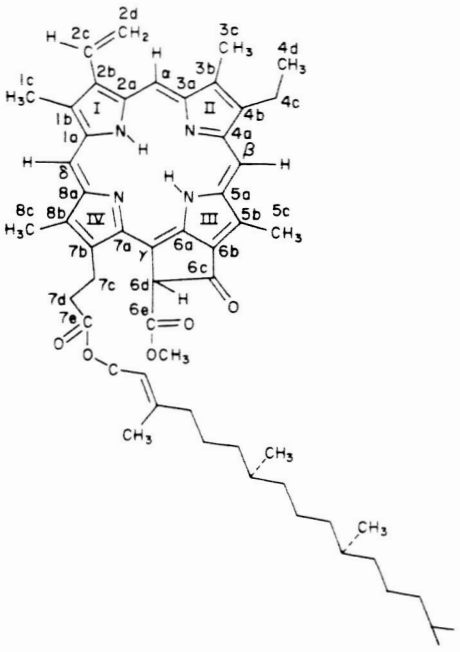

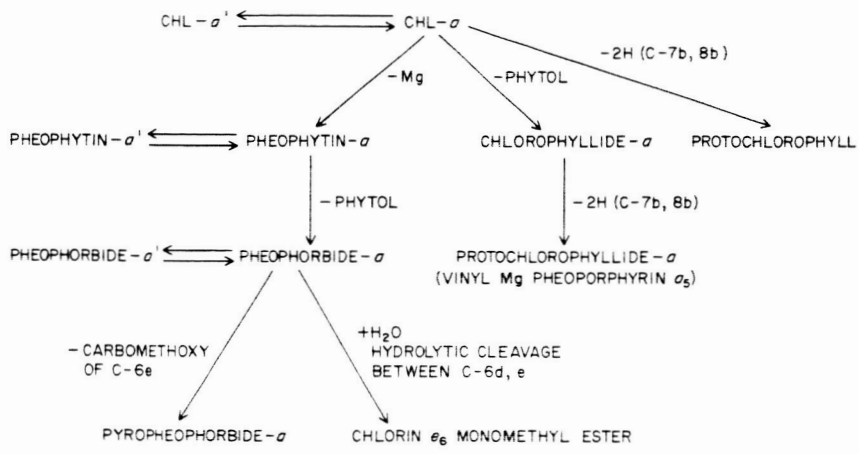

Fig. 7. Pheophytin-*a* and some of its possible alteration products (Ref. 35, Chap. 1)

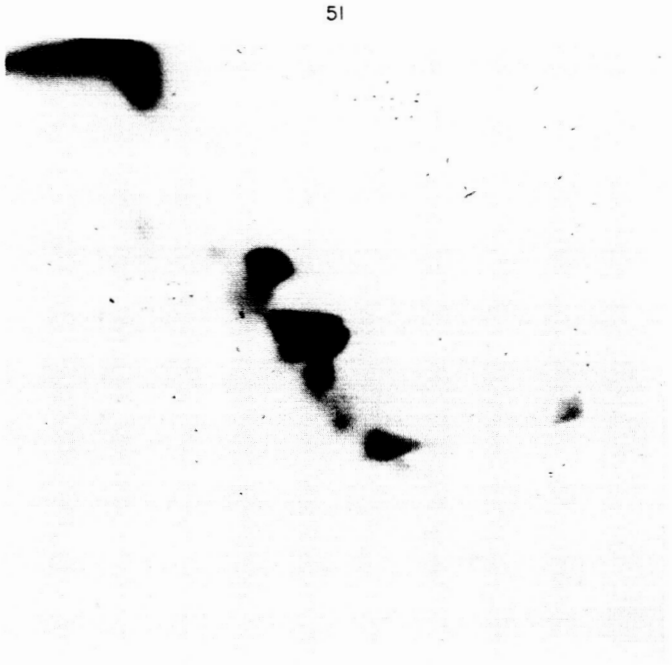

Fig. 8. A two-dimensional TLC separation of TEAE column fraction 8 effected on the same adsorbent as for Fig. 4

CHLORELLA 71105, 400 μg,
40 μl TEAE-8, $HCHO/H_2SO_4$
SILICA GEL PLAIN + 10% $MgSiO_3$
Δ 120°C, 20 min, COOL 30 min

$C/M/H_2O$
65/25/4

$BuOH/HAc/H_2O$
60/20/20

ON THE ORDER OF 20–24 COMPONENTS ARE PRESENT
SUBSEQUENT TO CHARRING

identification of components. In all cases, the plates were sprayed with Le Rosen's reagent (40% formalin/concentrated sulfuric acid 3/97 v/v) then heated at 180°C for 30 min to reveal the colorless compounds. The two-dimensional TLC studies of the other TEAE fractions confirm that the Sephadex-1 fraction of algae is indeed quite complex, although the TEAE-1 fraction appears to consist only of pigments (Refs. 37 and 38). Other TLC systems for pigments (Refs. 37 and 38) could be used to completely resolve the Sephadex-1 pigments, and the individual components could then be characterized by the techniques of carotenoid chemistry. This will be the subject of future work with algal crust soil in view of the fact that such strongly "life-related" pigments appear to be ubiquitous in the EE matter of soils. One should be able to detect their pyrolysis products, such as the ionenes (Ref. 39), even in whole soil pyrolyzates.

2. The Readily Extractable Organic Matter of Soil 1-4, an Algal Crust Desert Soil From Thermal, California

Soil organic matter consists chiefly of a complex polymer, "humic acid," which requires acid or base hydrolysis for its isolation (Refs. 40 and 41). The "humic acid" may contain in its structure altered and derived life products such as DNA[4] bases (Ref. 42). However, one would not usually expect to recover unaltered and thus readily recognizable "life-related" compounds from this fraction, but it is reasonable to expect recovery of such compounds from simple solvent extracts of soils. For example, one would expect that chlorophylls would be found in alcohol extracts of soils, since they are in extracts of sediments (Ref. 1). Such simple solvent extracts should contain the most chronologically recent unaltered cellular products present in the soil. Therefore, the yield of material extracted by several solvents applied to algal crust soil from Thermal, California was examined. The soil was collected free of bag contamination in June of 1966. It was extracted under nitrogen in a small stainless-steel Waring blender fitted with Teflon fittings. All solvents used were redistilled reagent grade, except the Freon 113 which was refrigeration grade. All containers used in the extracting were washed with solvent before use. Extracts were concentrated almost to dryness at 15–20°C under nitrogen in dim light, by means of a Buchler flash evaporator. A thin layer chromatography plate of the extracts is shown in Fig. 1. Most of the extracted material consists of chlorophyll residues as shown by its red fluorescence under ultraviolet irradiation and by development of a transitory brown color when sprayed with methanolic KOH (Molisch test). We have tentatively identified cholesterol in the chloroform/methanol 2/1 extract on the basis of its color response to 50% aqueous sulfuric acid (Ref. 43). As shown in Table 2, all the solvents except Freon 113 were about equally effective in extraction ability by removing about 0.1% of the available "total organic matter." The Freon extract contained a very simple mixture—a trace of chlorophyll (or pheophytin-*a*), a wax, and two sterols.

Table 2. Yield of total extractable Soil 1-4 organic matter by various solvents

Solvent	Yield, mg/kg	Remarks
Freon 113	3.63	Pale yellow
Pyridine	39.2	Olive green
Methanol	34.8	Olive green
Acetone	58.0	Olive green
Chloroform/methanol	24.6	Olive green (flocs)

A subsequent two-dimensional TLC study based on the systems of Rouser (Ref. 44 and 45) showed that only minor traces of polar lipids such as phosphatides were present in the extracts. However, one cannot rule out the possibility that absorption and denaturation losses of labile compounds may have occurred in the difficult extraction step.

Carotenoids were extracted from soil (Refs. 1 and 40) under nitrogen in red light by means of the techniques of carotenoid chemistry (Refs. 38 and 46). Because all soils examined showed the presence of pigments which are key compounds in photosynthetic organisms, we felt that this "life-related" class of compound deserved careful examination. The carotenoids were examined by means of column chromatography and spectrophotometry by Mr. Michael White and Dr. Henry Yokoyama at the U.S.D.A. Laboratory in Pasadena, California. A tentative assignment, on the basis of spectral evidence only, is as follows: β-carotene (8%), "astaxanthin" (21%), X (58%), X_2 (trace), X_3 (3%), and X_4 (11%). This work requires larger samples in order to provide fractions for co-chromatography, IR, NMR,[5] and elemental analysis. The very simple pattern of compounds resembles that of a marine environment. The soil sample came from an area 5 mi east of Thermal, California, which was an arm of the Gulf of California within recent geological time (Ref. 48). The total yield, on the basis of β-carotene's specific extinction in petroleum ether of 2500, was 300 mg/kg of soil.

[4]DNA = deoxyribonucleic acid.

[5]IR = infrared; NMR = nuclear magnetic resonance.

R. E. Cameron in Table 2, Ref. 7, cites "total organic matter" at 4500 mg/kg for this equivalent soil, number 1.

3. Programmed Linear Pyrolysis in Organic Detection

a. Introduction. Differential thermal analysis (DTA) studies concerning the detection of life-related compounds have led to the development of a programmed linear pyrolysis technique of investigation of the kinetics of dynamic organic pyrolysis.

In the majority of analytical organic pyrolyses that have been accomplished in conjunction with gas chromatography, flash or very rapid pyrolysis has proved to be the most reproducible method. This conclusion is in part a result of the nature of the gas chromatographic technique rather than the reproducibility of the kinetics of such pyrolyses. The reason the technique has such a strong influence on the manner of pyrolysis is because the reaction products must be introduced rapidly to prevent overlapping of the gas chromatographic peaks, or to prevent changes or interactions in the reaction products before analysis.

The other extreme in pyrolysis, which was used extensively before the implementation of modern instrumentation, is the pyrolysis of a sample at a fixed temperature for sufficient time for complete reaction to occur. The reaction products are trapped during equilibration and introduced into a gas chromatograph at some later time.

Since the above modes of programming do not yield analytical information concerning processes occurring during the pyrolysis, a linear heating rate program, intermediate between flash and equilibrium pyrolysis, has been investigated.

b. Objective of the general study. The objective of the over-all study is to examine all aspects of sample heating; specifically, the study of those processes occurring in the sample as a result of heating. In order to determine factors which affect the sample during a linear programmed dynamic pyrolysis the following aspects are being investigated:

(1) Which type of reactions with the carrier gas (oxidizing, reducing, or inert) yield the greatest amount of information concerning both the organic material and the inorganic substrate.

(2) Effects of heating rate from flash to equilibrium pyrolysis.

(3) Effects of flow rate and residence time in the pyrolysis furnace.

(4) Effects of sample configuration, dynamically swept sample or diffusion into the carrier stream.

(5) Effects of the inorganic substrate on the organic yield.

c. Objective of this phase of the study. A portion of this objective is to determine the nature and extent of the information that can be gained directly from the sample reactions and their undifferentiated gaseous products, and further, how this information can best be obtained; either as a specific experiment, or how this information can be applied to optimize the functional specifications of any experiment that uses sample heating as a necessary part of its implementation.

d. Objective of instrument configuration. Desert soils which contain only a minor amount of organic material were considered most applicable to conditions which might be encountered in Martian soils. Therefore, the high sensitivity of the hydrogen flame ionization detector was employed to analyze the distribution and the relative magnitude of the yield of organic effluent with respect to the sample temperature.

The instrumental configuration is analogous to a gas chromatograph with an empty column, in which the temperature at which products are introduced into the carrier is determined, rather than the retention *time* of a component in the carrier. The instrumentation has the following physical configuration (Fig. 9):

(1) The furnace is a standard DTA instrument using an effluent gas analysis thermal head that is programmed at 80°C/min up to 1000°C.

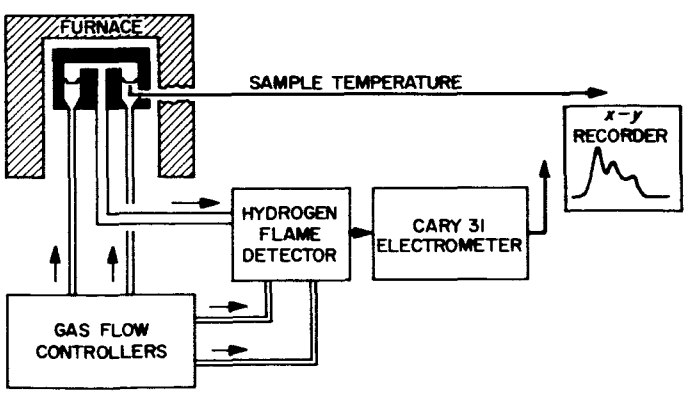

Fig. 9. Organic effluence analysis instrumentation

(2) The column is represented by a 6-in. length of tubing held at 250°C to prevent sample condensation.

(3) The detector is a hydrogen flame ionization detector of special design (SPS 37-44, Vol. IV, pp. 236–239) to allow the use of any type of carrier gas with rapid start-up and large thermal and flow cycling of the carrier.

(4) The carrier is hydrogen, air, or helium at 60–90 cm^3/min.

e. Instrument configuration. A standard R. L. Stone Company DTA instrument was used with an effluent gas analysis thermal head, type 12CR2S. The sample is contained on a ¼-in.-diameter platinum dish, 0.001 in. thick. The sample dish and the reference dish containing a thermally inert substance (aluminum oxide) are supported by ring thermocouples in identical black body cavities of the thermal head which is dynamically swept with 60–90 cm^3/min of carrier gas. Approximately 6 in. of tubing heated to 250°C connects the thermal head to a hydrogen flame ionization detector.

Several flame detectors were evaluated for use; however, the special requirements of the instrumentation and the manner in which it was used required the development of a special flame detector for convenience and flexibility. Some of the requirements are as follows:

(1) Rapid programming resulted in a maximum of 20 min for analysis time. Sample insertion interrupted carrier gas flow. This would extinguish the flame and allow back flushing of hydrogen into the sample chamber with the normal detector arrangement in which the sample and the carrier gas are premixed with the hydrogen before entering the detector jet.

(2) The high-temperature palladium ring seal used on the sample chamber required a minimum pressure drop in the carrier gas system.

(3) A wide variety of carrier gases was used, inert and reactive, and with a considerable variation in flow rate.

Preliminary investigation indicated that it was desirable to use the maximum heating available to approximate in part the rapid kinetics obtained in the pyrolysis used with gas chromatography. Therefore, the DTA furnace was programmed by application of full power, which resulted in a linear program of approximately 80°C/min to 600°C. Above this temperature the heating rate gradually decayed in a smooth manner to approximately 20°C/min at 1000°C.

Since nearly all reactions were observed at temperatures below 600°C, the high-temperature nonlinearity is not considered critical for this investigation.

The total organic effluence as a function of sample temperature was plotted on an x-y recorder with the output of the flame detector plotted on one axis and the temperature of the sample dish on the other axis.

f. Results of instrument with desert soils. Figure 10 indicates the general response of various desert soils from the JPL soil collection (Ref. 48), pyrolyzed with helium as the carrier gas. All desert soils analyzed yielded effluence programs that were characteristically different in detail. The base lines of the curves are offset vertically for maximum clarity.

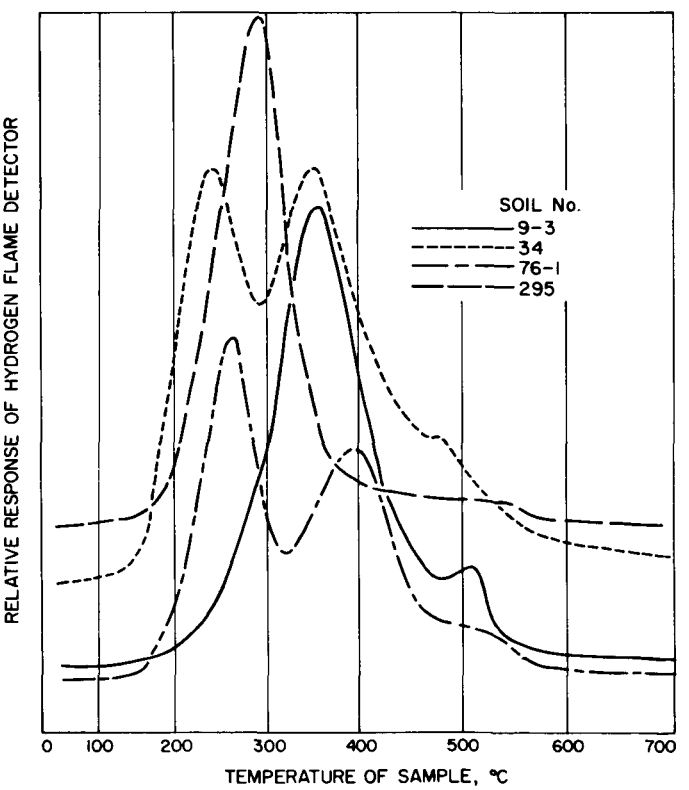

Fig. 10. Total organic effluence of various desert soils with respect to linear programmed sample temperature

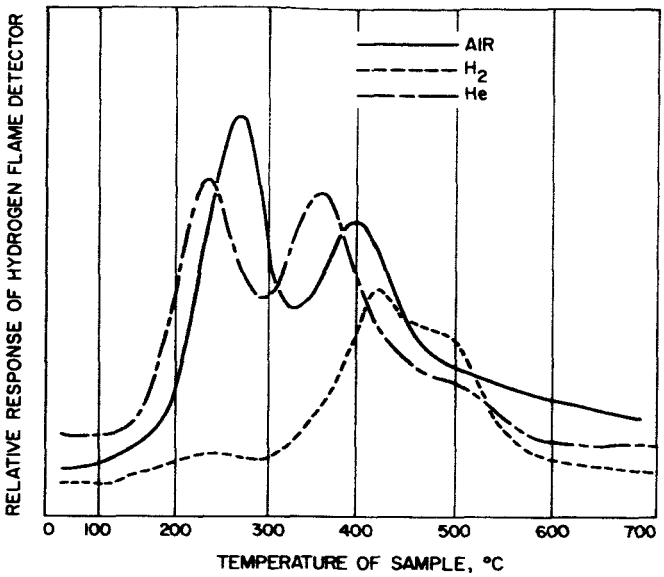

Fig. 11. Variation of effluent pyrolysis temperature with different carrier gases (desert soil #34)

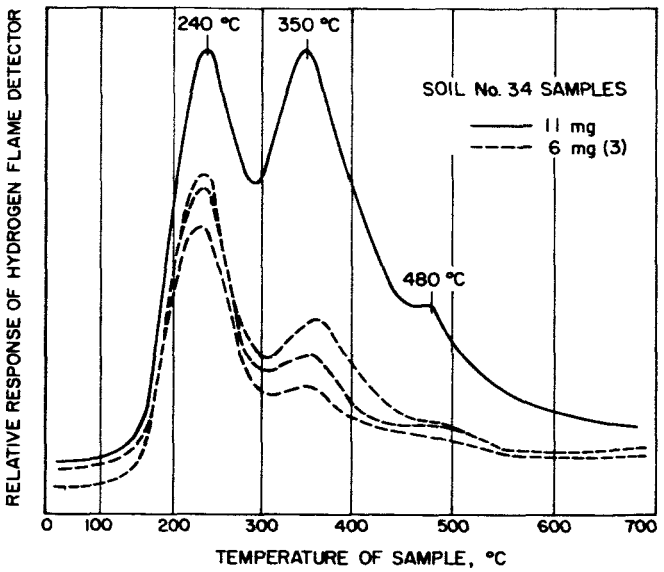

Fig. 12. Reproducibility of programmed linear pyrolysis with helium carrier gas (desert soil #34)

Figure 11 shows the effect of different carrier gases. The curve for hydrogen has been attenuated by a factor of ten, since the total response is much greater using hydrogen as the carrier gas. The peaks of maximum effluence are also shifted to higher temperatures.

The reproducibility of the curves from any single desert soil was considered to be good using helium as the carrier gas. However, with hydrogen and air as carriers, reproducibility was degraded somewhat due to the added complexity of the oxidation reduction reactions.

The relative magnitude of the ratio of the peak heights in any one type of curve is variable with repeated analysis. This indicates that sampling error is relatively high due to the very minor amount of organic material present in these soils. Figure 12 of desert soil #34 shows this variability especially well in that the relative peak heights of the 240- and 350-deg peaks were generally obtained as shown for the 6-mg samples, regardless of sample size. However, in the peak configuration shown for the 11-mg samples these two peaks were nearly equal in magnitude and the 480 peak is sharply defined; whereas, it is very broad in the 6-mg samples. The two weight ranges are included in Fig. 12 only to separate the two types of curves since many 6-mg samples yielded a curve configuration identical to the 11-mg sample shown in the figure.

g. Conclusions. The programmed linear pyrolysis instrumentation readily shows that considerable information can be gained from the reactions that are proceeding during pyrolysis:

(1) The total effluence program provides an organic detection scheme that is extremely sensitive, and more quantitative than sampling techniques for very small amounts of organics randomly distributed on an inorganic matrix; and when combined with DTA, the program provides considerable information concerning the nature of the inorganics as well.

(2) Desert soils yield total effluence programs that are characteristically different in fine detail: distinctive but not definitive.

(3) Different carrier gases do not appear to change the effluence program sufficiently to indicate that pyrolysis conditions alone necessitate a specific carrier gas. Mass spectrometry or other instrumental constraints may show such is necessary.

(4) The effluence program does not give sufficient qualitative information as to conditions of pyrolysis to allow definitive answers as to the optimum rate of pyrolysis yielding the most characteristic product since the resolution of this question rests upon interpretation of the mass spectrometry data.

C. Project Engineering

1. Transmission of Solar Radiation to the Surface of Mars

a. Introduction. One phase of research in support of the preparation of environmental requirements for the *Voyager* program involves the estimation of solar irradiance at the Mars surface. To determine—with precision—the fraction of solar energy incident on the top of the Martian atmosphere that penetrates to the surface level, a detailed knowledge of the atmospheric gaseous and aerosol composition, distribution, and the vertical temperature and pressure profiles is required. In addition, accurate absorption functions appropriate to the atmospheric pressures and absorber path lengths on Mars must be known. Unfortunately, since this information is currently unavailable, a crude approximation must be attempted.

Carbon dioxide and nitrogen are assumed the principal constituents of the Mars lower atmosphere. Above the tropopause, CO_2 photochemistry results in vertical distributions of CO, O_2, and O. Upper atmospheric calculations[6] indicate that virtually all ultraviolet solar energy below $\lambda = 0.1925$ μm is absorbed before penetration to the surface. This investigation considers the atmospheric transmission to be influenced only by CO_2 infrared absorption and multiple gas molecular scattering.

b. Infrared absorption. It is assumed that carbon dioxide is the only absorber in the near-infrared. Absorption by the ν_3 band at 4.3 μm and the significant overtone and combination bands listed in Table 3 were examined on the basis of Roach and Houghton's studies (Refs. 49 and 50) of absorption in the earth's stratosphere. The results of both studies were extended here to the atmospheric pressures and CO_2 optical path lengths appropriate to Mars.

[6]By F. Marmo of GCA Corp., Bedford, Mass., in a personal communication, Aug. 1967.

Table 3. Carbon dioxide bands—Goody (1964)

Band, μm	Limits, cm^{-1}
1.4	6650–7250
1.6	6000–6550
2.0	4750–5200
2.7	3480–3800
4.3	2160–2500
4.8	1980–2160
5.2	1870–1980

Results of other reported studies were the basis for a suggestion by Roach that solar absorption by carbon dioxide in the atmosphere could be fitted by two empirical relations:

$$A = \int A_\nu \, d\nu = cm^{1/2} p^k$$

for weak absorption bands, when $A < A_c$

$$A = C + D \log m + K \log p$$

for strong absorption bands, when $A \geqq A_c$, where A is the absorber band area in wave numbers (cm^{-1}), A_c the critical band area above which the strong absorption band expression becomes applicable, p the total pressure based on the Curtis–Godson approximation (Ref. 51), m the absorber optical path length (cm-atm), and c, k, C, D, K are empirically determined constants. Three Mars atmospheric models were considered in this analysis, as shown in Table 4. The absorption band areas computed from Roach's data were converted to fractional transmissions through the relation $T = 1 - 1/\Delta\nu \int A_\nu \, d\nu$ (where $\Delta\nu$ is the width of the absorption band), as listed in Table 5.

Table 4. Mars atmospheric models

Model	Surface pressure P_0, mbar	CO_2, % by volume	CO_2 path length m, cm-atm
I	5	100	6.7×10^3
II	7	100	9.5×10^3
III	21	27	10.5×10^3

Table 5. Infrared transmission functions

Band, μm	Bandwidth $\Delta\nu$, cm^{-1}	Roach			Houghton		
		Model I	Model II	Model III	Model I	Model II	Model III
1.4	600	0.990	0.986	0.977	0.99	0.99	0.98
1.6	550	0.988	0.984	0.974	0.99	0.99	0.98
2.0	450	0.875	0.822	0.757	0.93	0.91	0.83
2.7	320	0.472	0.384	0.300	0.58	0.52	0.42
4.3	340	0.510	0.483	0.433	0.56	0.53	0.47
4.8	180	0.932	0.907	0.859	—	—	—
5.2	110	0.975	0.969	0.949	—	—	—

Similarly, absorption band areas were calculated from the data of Houghton for the models in Table 4, and converted to fractional transmissions, as listed in Table 5. Houghton's data consist of curves of integrated absorption plotted against either the pressure–path length product pm or its square root $(pm)^{1/2}$ for each CO_2 band.

c. Molecular scattering. Using Rayleigh's law, molecular scattering, which accounts for the extinction of solar energy in the Mars atmosphere between 0.1925 and 1.0 μm, can be calculated for a clear cloudless sky with no aerosols. The scattering phase function, which describes the probability of scattering in any direction, is given by $P(\phi) = 3/4(1 + \cos^2\phi)$. Assuming single scattering only, the monochromatic transmission function, which represents the sum of the energy transmitted and scattered in the downward hemisphere, is given by $T_\lambda = 1/2 + 1/2e^{-\tau_\lambda}$, where τ_λ is the total monochromatic optical depth of the Mars atmosphere. For the sun at the zenith,

$$\tau_\lambda = \int_0^\infty \beta_\lambda(z)\,dz,$$

where β_λ is the volumetric scattering coefficient. For molecular scattering by a mixture of k component gases,

$$\beta_\lambda = \frac{32}{3}\frac{\Pi^3}{\lambda^4}\sum_{j=1}^{k}\frac{(N_j - 1)^2}{n_j},$$

Table 6. Optical depths for molecular scattering

Model	Surface pressure, mbar	Composition		Optical depth $\tau_\lambda/\tau^*_\lambda$
		% N_2	% CO_2	
I	5	0	100	0.167
II	7	0	100	0.233
III	21	73	27	0.415

where N_j is the refractive index of gas j, and n_j the number density. Coulson and Lotman (Ref. 52) give the optical depths τ^*_λ at the surface of Mars for an 85-mbar 94% nitrogen atmosphere. These are scaled to an atmosphere having a mixture of nitrogen and carbon dioxide by the following relationship:

$$\tau_\lambda = \tau^*_\lambda\left[\frac{(N_{CO_2} - 1)^2}{(N_{N_2} - 1)^2}\frac{p_{CO_2}}{85} + \frac{p_{N_2}}{85}\right]$$

where p_{CO_2} and p_{N_2} are the partial pressures of CO_2 and N_2, respectively. The three atmospheric models listed in Table 4 were examined. Optical depths were calculated and summarized in Table 6.

Transmission functions for each model were calculated as summarized in Table 7.

The combined absorption and scattering transmission functions for the three models of the Mars atmosphere are shown in Fig. 13. The scattering functions have been extrapolated below 0.25 μm.

d. Conclusions. To estimate the solar irradiance arriving at the Mars surface, the irradiance at the top of the atmosphere corresponding to the appropriate sun–Mars distance should be multiplied by the transmission function (Fig. 13). It should be emphasized that the scattering processes in the Mars atmosphere are most likely dominated by the aerosol content. The treatment of this problem is a very difficult task, but it is required before a more precise description of the Mars atmospheric transmission spectra can be developed.

Table 7. Scattering transmission functions

λ, μm	τ^*_λ	Model I		Model II		Model III	
		τ_λ	T_λ	τ_λ	T_λ	τ_λ	T_λ
1.0	2×10^{-2}	0.334×10^{-3}	1.0	0.466×10^{-3}	1.0	0.83×10^{-3}	1.0
0.8	5×10^{-2}	0.835×10^{-3}	0.9995	1.16×10^{-3}	0.9995	2.07×10^{-3}	0.9990
0.6	1.5×10^{-2}	0.25×10^{-2}	0.9990	0.35×10^{-2}	0.9985	0.622×10^{-2}	0.9970
0.5	3×10^{-2}	0.50×10^{-2}	0.9985	0.7×10^{-2}	0.9965	1.25×10^{-1}	0.9935
0.4	8×10^{-2}	1.34×10^{-2}	0.9935	1.86×10^{-2}	0.9910	0.332×10^{-1}	0.9835
0.35	1.5×10^{-1}	0.25×10^{-1}	0.9875	0.35×10^{-1}	0.9830	0.622×10^{-1}	0.9695
0.3	2.7×10^{-1}	0.45×10^{-1}	0.9775	0.63×10^{-1}	0.9695	1.12×10^{-1}	0.9460
0.25	6×10^{-1}	1.0×10^{-1}	0.9475	1.4×10^{-1}	0.9345	2.49×10^{-1}	0.8900

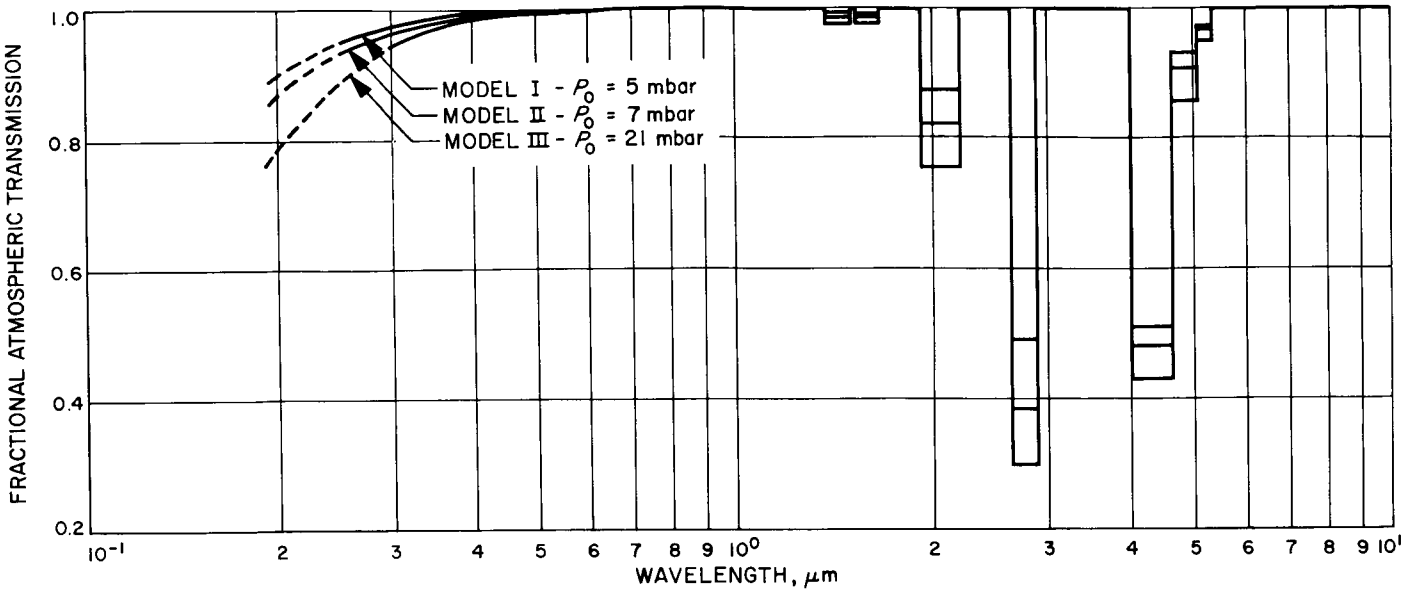

Fig. 13. Fractional transmission in the Mars atmosphere for a clear, cloudless day with the sun at the zenith

References

1. Orr, W. L., Emery, K. O., and O'Grady, J. R., "Preservation of Chlorophyll Derivatives in Sediments off Southern California," *Bull. Am. Assoc. Petr. Geol.*, Vol. 42, No. 5, pp. 925–962, 1958.

2. Orr, W. L., and O'Grady, J. R., "Determination of Chlorophyll Derivatives in Marine Sediments," *Deep-Sea Res.*, Vol. 4, pp. 263–271, 1957.

3. Finkle, B. J., "Soil Humic Acid as a Hydroxypolystyrene: a Biochemical Hypothesis," *Nature*, Vol. 207, No. 4997, pp. 604–605, 1965.

4. Keefer, R. F., *Chromatographic and Spectrographic Analyses of Soil Organic Matter Extracts*, Ph.D. Dissertation 64-7028. University Microfilms, Inc., 1963 (JPL Library Document 148144).

5. Keefer, R. E., Himes, F. L., and Mortensen, J. L., "Evidence Indicating the Presence of Loosely-Bound Phenolic Groupings in Soil Organic Matter Extracts," *Soil Sci. Soc. Am.*, Proc. 30, pp. 415–416.

6. Marshall, C. E., *The Physical Chemistry and Mineralogy of Soils*, Chap. 4. John Wiley & Sons, Inc., New York, 1964.

7. Cameron, R. E., and Blank, G. B., *Soil Organic Matter*, Technical Report 32-433, p. 9, Table II. Jet Propulsion Laboratory, Pasadena, Calif., May 23, 1963.

8. Braarud, T. (Discussion Leader), "Technical Problems in Sampling," in *Marine Biology II, Proceedings of the Second International Interdiscussion Conference, Princeton, N. J., 1962*. New York Academy of Sciences, New York, 1966.

References (contd)

9. Baver, L. D., *Soil Physics*, Third Ed., p. 12, Table III. John Wiley & Sons, Inc., New York, 1956.

10. Jacquin, F., "Contribution á L'étude des Processus de Formation et D'évolution de Divers Composés Humiques," Thesis, Faculté des Sciences. *Bull. L'École Nat. Super. Agron.*, Nancy, France, 1963.

11. Swain, F. M., "Geochemistry of Humus," in *Organic Chemistry*, Chap. 4. Edited by J. A. Breger. The MacMillan Co., New York, 1963.

12. Nagar, B. R., "Examination of the Structure of Soil Humic Acids by Pyrolysis-Gas Chromatography," *Nature*, Vol. 199, pp. 1213–1214 (1963).

13. Vango, S. P., Oyama, V. I., and Wilson, E. M., *Applications of Gas Chromatography to the Analyses of Organics, Water, and Adsorbed Gases in the Lunar Crust*, Technical Report 32-107. Jet Propulsion Laboratory, Pasadena, Calif., April 25, 1961.

14. Parker, P. L., et al., "Fatty Acids in Eleven Species of Blue-Green Algae: Geochemical Significance," *Science*, Vol. 155, pp. 707–708, 1967.

15. Marshall, C. E., "The Physical Chemistry and Mineralogy of Soil," Chap. 4. John Wiley & Sons., Inc., New York, 1964.

16. Bauman, A. J., Cameron, R. E., Kritchevsky, G., and Rouser, G., "Detection of Phthalate Esters as Contaminants of Lipid Extracts From Soil Samples Stored in Standard Soil Bags, *Lipids*, Vol. 2, No. 1, pp. 85–86, 1966.

17. Blumer, M., "Contamination of a Laboratory Building by Air Filters," *Contam. Control, Am. Assoc. Contam. Control*, Vol. 4, pp. 13–14, 1965.

18. Rouser, G., Kritchevsky, G., Whatley, M., and Baxter, C. F., "Laboratory Contaminants in Lipid Chemistry: Detection by Thin-Layer Chromatography and Infrared Spectrophotometry and Some Procedures Minimizing Their Occurrence," *Lipids*, Vol. 1, No. 2, pp. 107–112, 1966.

19. Entenman, C., "General Procedures for Separating Lipid Components of Tissue," *Methods in Enzymology*, Vol. 3, p. 299. Academic Press, New York, 1957.

20. Bennett, R. D., and Heftmann, E., *J. Chromatography*, Vol. 9, pp. 348–352, 1962.

21. Reio, L., "A Method for the Paper-Chromatographic Separation and Identification of Phenol Derivatives, Mould Metabolites, and Related Compounds of Biochemical Interest, Using a Reference System," *J. Chromatography*, Vol. 1, pp. 338–373, 1958.

22. Rouser, G., et al., "Lipid Composition of Beef Brain, Beef Liver, and the Sea Anemone: Two Approaches to Quantitative Fractionation of Complex Lipid Mixtures," *J. Am. Oil Chemists Soc.*, Vol. 40, No. 9, pp. 425–454, 1963.

23. Siakotos, A. N., and Rouser, G., "Analytical Separation of Nonlipid Water Soluble Substances and Gangliosides From Other Lipids by Dextran Gel Column Chromatography, *J. Am. Oil Chemists Soc.*, Vol. 42, pp. 913–919, 1965.

References (contd)

24. Feldman, G. L., Feldman, L. S., and Rouser, G., "The Isolation and Partial Characterization of Gangliosides and Ceramide Polyhexosides From the Lens of the Human Eye," *Lipids*, Vol. 1, pp. 21–26, 1966.

25. Degens, E. T., and Reuter, J. H., "Analytical Techniques in the Field of Organic Geochemistry," in *Advances in Organic Geochemistry, Proceedings Milan, 1962*. Edited by V. Colombo and G. D. Hobson. The Macmillan Co. (Pergamon Press), New York, 1964.

26. Rouser, G., et al., "Variations in Lipid Composition of Human Brain During Development and in the Sphingolipidoses: Use of Two-Dimensional Thin-Layer Chromatography," in *Inborn Disorders of Sphingolipid Metabolism*. Edited by S. M. Aronson and B. W. Volk. Pergamon Press, New York, 1966.

27. Meinwald, Y. C., Meinwald, J., and Eisner, T., "1,2-Dialkyl-4(3H)-Quinazolines in the Defensive Secretion of a Millipede (Glomeris Marginata)," *Science*, Vol. 154, pp. 390–391, 1966.

28. Silverstein, R. M., Rodin, J. O., and Wood, D. L., "Sex Attractants in Frass Produced by Male Ips Confusus in Ponderosa Pine," *Science*, Vol. 154, pp. 509–510, 1966.

29. Strain, H. H., Sherma, J., and Grandolfo, M., "Alteration of Chloroplast Pigments by Chromatography With Siliceous Adsorbents," *Anal. Chem.*, Vol. 39, pp. 926–931, 1967.

30. Casey, R. P., et al., "Mass Culture of *Chlorella* 71105," Paper 44, *Twenty-second Annual Meeting of the Institute of Food Technology*, Miami Beach, Florida, 1962.

31. Lubitz, J. A. (General Dynamics Corp., Electric Boat Div., Groton, Conn.), "The Protein Quality, Digestability, and Composition of *Chlorella* 71105," Technical Report 61-535. Aeronautical Systems Division, Wright-Patterson Air Force Base, Ohio, 1961.

32. Thirkell, D., and Tristram, G. R., "The Isolation of Leaf Components. II." *J. Sci. Food Agric.*, Vol. 14, pp. 488–495, 1963.

33. Lynn Co, D. Y. C., and Schanderl, S. H., "Separation of Chlorophylls and Related Plant Pigments by Two-Dimensional Thin-Layer Chromatography," *J. Chromatography*, Vol. 26, pp. 442–448, 1967.

34. Bogorad, L., "Chlorophylls," in *Physiology and Biochemistry of Algae*, Chap. 23. Edited by R. A. Lewin. Academic Press, New York, 1962.

35. Strain, H. H., and Svec, W. A., *The Chlorophylls*, Chap. 2. Edited by L. P. Vernon and G. R. Seelcy. Academic Press, New York, 1966.

36. Michel-Wolwertz, M. R., and Sironval, C., "On the Chlorophylls Separated by Paper Chromatography From Chlorella Extracts," *Biochim. Biophys. Acta*, Vol. 94, pp. 330–343, 1965.

37. Hager, A., and Meyer-Bertenrath, T., "Extraction and Quantitative Determination of Carotenoids and Chlorophylls of Leaves, Algae, and Isolated Chloroplasts With the Aid of Thin-Layer Chromatography," *Planta (Berlin)*, Vol. 69, pp. 198–217, 1966.

References (contd)

38. Yokayama, H., and White, M., "Citrus Carotenoids VI. Carotenoid Pigments in the Flavedo of Sinton Citrangequat," *Phytochemistry*, Vol. 5, pp. 3456–3468, 1966.

39. Day, W. C., and Erdman, J. G., "Ionene: A Thermal Degradation Product of Beta-Carotene," *Science*, Vol. 141, p. 808, 1963.

40. Mortenson, J. L., *Chemistry of the Soil.* Edited by F. E. Bear. Reinhold Publishing Corp., New York, 1965.

41. Mathur, S. P., and Paul, E. A., "A Microbiological Approach to the Problem of Soil Humic Acid Structures," *Nature*, Vol. 212, p. 646, 1966.

42. Rosenberg, E., "Purine and Pyrimidines in Sediments From the Experimental Mohole," *Science*, Vol. 146, No. 3652, p. 1680, 1964.

43. Heftmann, E., Ko, S-T, Bennett, R. D., "Response of Steroids to Sulfuric Acid in Thin-Layer Chromatography," *J. Chromatography*, Vol. 21, pp. 490–494, 1966.

44. Rouser, G., et al., "Analytical Fractionation of Complex Lipid Mixtures: DEAE Cellulose Column Chromatography Combined With Quantitative Thin Layer Chromatography," *J. Am. Oil Chemists' Soc.*, Vol. 41, pp. 836–840, 1964.

45. Rouser, G., et al., "Determination of Polar Lipids: Quantitative Column and Thin Layer Chromatography," *J. Am. Chem. Soc.*, Vol. 42, pp. 215–227, 1965.

46. Goodwin, T. W., "Carotenoids" in *Modern Methods of Plant Analysis, Volume* 3, pp. 272–311. Springer-Verlag Publishing Co., New York, 1955.

47. Longwell, C. R., "Lake Cahuilla," in *Geology of Southern California*, Chap. V, Sect. 9. Bulletin 170, State of California Division of Mines, 1954.

48. Cameron, R. E., Blank, G. B., and Gensel, D. R., *Desert Soil Collection at the JPL Soil Science Laboratory*, Technical Report 32-977. Jet Propulsion Laboratory, Pasadena, Calif., Oct. 15, 1966.

49. Roach, W. T., "The Absorption of Solar Radiation by Water Vapour and Carbon Dioxide in a Cloudless Atmosphere," *Quart. J. Roy. Meteorol. Soc.*, Vol. 87, pp. 364–373, 1961.

50. Houghton, J. T., "The Absorption of Solar Infrared Radiation by the Lower Stratosphere," *Quart. J. Roy. Meteorol. Soc.*, Vol. 89, pp. 319–331, 1963.

51. Goody, R. M., *Atmospheric Radiation*, Oxford University Press, London, 1964.

52. Coulson, K. L., and Lotman, M., "Molecular Scattering of Solar Radiation in the Atmosphere of Mars," *J. Geophys. Res.*, Vol. 68, No. 20, pp. 5681–5688, Oct. 15, 1963.

V. *Surveyor* Project

LUNAR PROGRAM

A. Introduction

The landing of *Surveyor VI* ensured the success of the *Surveyor* Project objectives, which were to obtain information in support of the *Apollo* manned lunar landing program. Seven missions were planned and the results of three of these missions were reported in prior issues of the Space Programs Summaries.

Mission D was conducted from July 14, 1967 (day 195 GMT) through July 18, 1967 (day 199). Lift-off was at 11:53:29 GMT, with a launch azimuth of 103.82 deg. Due to the relatively small miss distance, about 150 km from the initial targeted aiming point of 1°20′W and 25′N in Sinus Medii, a decision was made to execute the midcourse correction at approximately launch plus 39 h. After a successful midcourse correction, calculations indicated that the landing probably would be within 9 km of the aiming point. All operations of the spacecraft were nominal, and no errors were indicated. The retroengine sequence mode was commanded on at 01:56 GMT, July 17 (day 198), and main retroengine ignition occurred at 02:01:58 GMT. However, the spacecraft signal was lost abruptly at 02:02:41 GMT. Estimated time of touchdown was 02:05:01 GMT. Efforts to recontact *Surveyor IV* were continued through July 18 (day 199). Then, because every feasible recovery technique had been tried, mission D was terminated.

The transit phase of mission E commenced September 8, 1967 (day 251) with the lift-off of *Surveyor V* at 07:57:01 GMT at a launch azimuth of 79.517 deg. Normal preprogrammed spacecraft events occurred successfully and in proper sequence. Without a midcourse correction, the trajectory would have provided a miss distance of 46 km from the landing site of 0.83°N and 24°E, within the Sea of Tranquility. Following a successful midcourse correction at 01:45:02 GMT, September 9 (day 252), the new aiming point was defined as 0.917°N and 24.083°E. However, following premidcourse helium release, the regulator failed to lock up the propellant tank pressure, which resulted in a gradual helium tank pressure decay.

Due to this pressure decay, a decision had to be made whether to: (1) fire the retroengine in order to place the spacecraft in an earth orbit to obtain TV pictures of the earth and collect alpha scattering data; or (2) redesign the terminal descent sequence and attempt a soft landing on the moon. As more test and analytical data were obtained advancing the possibility of a soft landing, the decision was made in favor of a soft landing. Subsequent orbit computations predicted the landing site to be in unfavorable terrain. Therefore, it was decided to perform another midcourse maneuver and thus return to the landing site originally targeted. The second midcourse maneuver returned the spacecraft to a landing point of 1.5°N

and 23.19°E, a miss of only 30 km from the initial site. The flight of *Surveyor V* skidded to a halt on a slope of approximately 20 deg inside a small crater, about 30 ft in diameter and 5 ft deep, at 00:46:45 GMT, September 11 (day 254), in the Sea of Tranquility.

During the first lunar day, *Surveyor V* returned 18,006 excellent pictures and accumulated 93.5 h of valuable alpha scattering experiment data. The first attempt to conduct a static firing test of spacecraft vernier engines on the moon was completely successful. The 0.55 s firing of all three engines resulted in slight movement of the alpha scattering sensor head. Preliminary analysis of the lunar surface data indicates that the surface material in the vicinity of the spacecraft is composed of basaltic rock, similar to that found in various places on earth. The spacecraft was shut down for the lunar night on September 27, when the last command was sent at 06:35:58 GMT.

The mission E lunar operations for the second lunar day began at 08:07:34 GMT, October 15 (day 288). Activated by a command from DSS 42 (Canberra, Australia) lunar operations continued until 20:20 GMT, November 1 (day 305), when they were terminated, and the spacecraft entered its second lunar night. During the second lunar day more than 1,000 pictures were received, which, after enhancing, were of good quality. Alpha scatter data were also obtained, but because of the operational noise the data were deemed more suitable for engineering evaluation of the instrument than for science data.

Mission F began with the lift-off of *Surveyor VI* at 07:39:01 GMT, November 6 (day 310), on a launch azimuth of 82.995°. A midcourse correction for a 1°8′W and 0°25′N lunar target was successful. Premidcourse trajectory computations indicated an approximate miss distance of 120 km SE of the original aiming point. *Surveyor VI* ended the transit phase at 01:01 GMT, November 10 (day 314), landing almost vertically about 6.4 km west of the aiming point in Sinus Medii. Lunar operations began with all systems operating nominally.

B. Systems Engineering

1. Surveyor V Helium Regulator Failure

Surveyor V experienced a malfunction in the helium pressurization subsystem during flight to the moon. The malfunction occurred at the time of helium pressurization of the vernier propulsion subsystem, just prior to the midcourse correction. After the midcourse correction it was noted that the helium pressure was decreasing at a greater than normal rate; review of the data suggested the helium regulator had an internal leak, increasing the downstream pressure and allowing the relief valves to vent to space. Subsequent vernier engine firings failed to correct the internal leak.

The spacecraft system performance capabilities were analyzed and the terminal descent phase of the mission was redesigned during the remainder of the transit phase. The spacecraft performed the terminal descent and landed successfully.

Subsequent analysis of the flight data substantiated that the loss of helium high pressure was caused by an internal helium leak in the helium regulator that allowed the downstream pressure to rise beyond the crack pressure of the oxidizer or fuel system relief valves, venting the helium into space.

The *Surveyor* project has reviewed the data and the results of special failure mode tests in order to determine the cause of the failure. It was concluded that the most likely cause was contamination on the helium regulator valve seat. Such contamination could result in an internal leak through the regulator, causing the outlet pressure to increase to a level that would cause the fuel or oxidizer relief valve to vent into space.

The flight integrity of the SC-6 helium system has been demonstrated by tests, the exhaustive review of SC-6 and -7 quality assurance records, the verification of system cleanliness by particle counts implemented on SC-6 during the vernier propulsion system functional tests (including the 6-h regulator lockup performed last in the test sequence), and the elimination of regulator back flow. The SC-7 procedures have been changed to incorporate the above additional tests and test sequences as part of the normal spacecraft testing.

C. Flight Control System

Testing was performed on the *Surveyor* S-9 structural test vehicle to determine the attitude loop transfer functions, including the elastic structural response. The S-9 was suspended such that suspension frequencies were less than 0.5 Hz. The force inputs were from Stevens ST 10 permanent-magnet field shakers attached at each of the vernier engine dummy masses. The outputs were instrumentation accelerometers and flight control electronics thrust commands.

Testing was performed on the retrorocket and post-retrorocket release configurations. Figure 1(a) shows the gain for the inputs of engines 1 and 2 out of phase (as seen on *Surveyor IV*) for low level input of 2 lb zero to peak. Figure 1(b) is for inputs at a higher level of 10 lb zero to peak. No rolloff is included in these plots for engine transfer functions. The resultant change in gain indicates that a limit rather than an instability cycle operation exists.

Closed-loop tests (flight control electronics connected to shaker input) showed a limit cycle at 40 Hz and amplitude 6 to 7 lb peak to peak. This was with engines 1 and 3 out of phase and for a 3-dB system gain increase. The potential frequencies (having sufficient gain) of oscillation from open-loop tests were 18, 23, and 28 for engines 1 and 2 out of phase and 40 Hz for engines 1 and 3 out of phase; 40 Hz must have had the correct phase for the components on S-9. Another vehicle engine transfer function and electronics might have had the correct phase at one of the other frequencies.

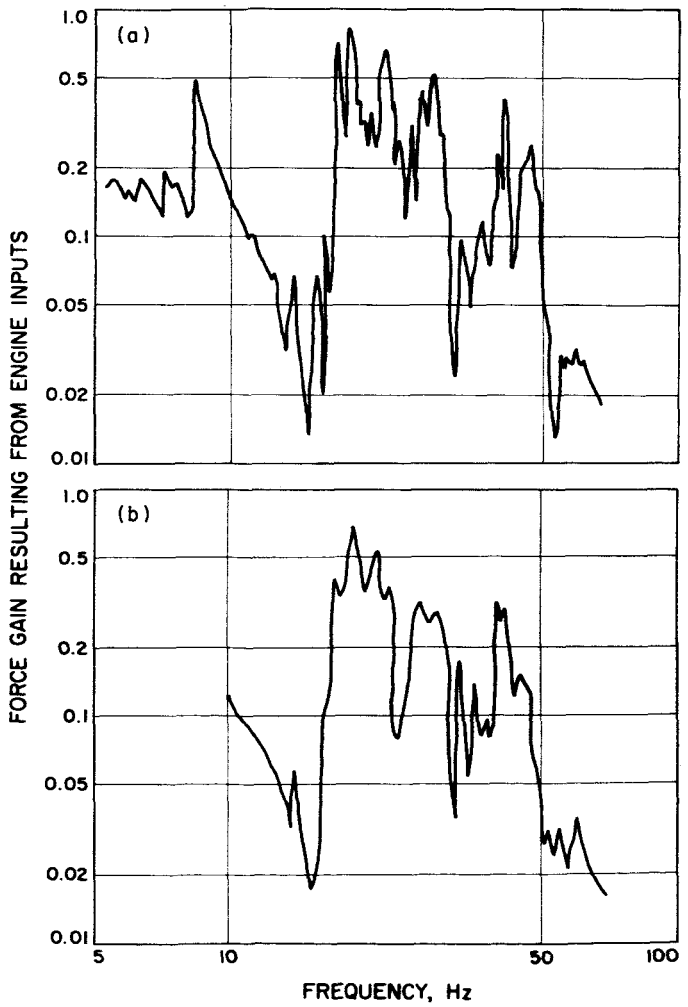

Fig. 1. Input gains: (a) lower level; (b) higher level

Manufacturing effort on the radar altimeter doppler velocity sensor during the report period was limited mainly to the production of the Y-1 and Y-2 signal data converters (SDC), rework of a production SDC, klystron power supply modulator (spacecraft spares for SC-6 and -7), and retest of SC-6 and -7 flight hardware, as required.

Manufacturing effort on the flight control system for the report period has been confined to the rework of a chassis of the flight control sensor group (+29-V thrust phase power) and other minor tests, as required.

D. Thermal Engineering[1]

Surveyor V was launched at 07:57 GMT September 8, 1967 and touched down on the moon at 00:47 GMT September 11, 1967. The transit phase of the mission was marked by excellent thermal performance despite several nonstandard vernier engine firings. All temperatures were nominal.

The vernier engine anomaly during SC-6 solar thermal vacuum (STV) testing, described in SPS 37-47, Vol. I, p. 107, was found to be due to a variable joint conductance between the engine barrel and the extension cone. This variability was demonstrated by a test program at JPL. Because the variability of the joint conductance could result in out-of-tolerance temperatures in flight, the engine was removed from the spacecraft.

E. Propulsion

1. Introduction

Propulsion for the A-21 configuration spacecraft is provided by a liquid propellant vernier rocket system and a solid propellant retrorocket engine. The latter provides primary deceleration during descent to the moon. The vernier system is used for midcourse maneuver, attitude control during retrorocket engine firings, and terminal descent.

2. Main Retroengine

a. Surveyor IV. After the *Surveyor IV* failure and subsequent investigation by the technical review board, the

[1]Prepared by JPL Technical Section 355.

board recommended that further investigation be conducted with respect to the retroengine. A team comprised of specialized personnel reviewed records in their respective specialty areas to determine if the retroengines were being fabricated in a reproducible manner. Static test data, X-rays, process techniques, trouble and failure reports, material review board records, and pressure vessel design criteria were reviewed in detail. Changes were recommended that can be expected to improve the process control and result in a better rocket engine. The fact that 47 engines have been fired with no out-of-specification test results, coupled with the rejection of engines that would be expected to display abnormal results, added to the conclusion that the engine fabrication is a controlled process.

During the investigations, certain discrepant items were disclosed that could possibly affect the suitability of retroengine A21-29 for flight use on SC-6. These items were investigated and the conclusions reached are as follows:

(1) Pyrogen threads. The no-go gage entered the pyrogen boss 75% of the thread depth. Computations were made assuming this entire 75% thread depth contributes nothing to the pyrogen support, resulting in a minimum margin of safety of 0.38 with a safety factor of 1.25. Further analyses confirm adequate safety margin.

(2) Surface voids. Surface voids were observed in the propellant grain. Burning surface progression due to the voids will cause premature exposure of the case to high temperature exhaust gases near propellant burnout. Thermal analyses indicate a 300°F temperature increase with a 0.5-in. void depth and a 140°F temperature increase with a 0.25-in. void depth. The estimated void depth in A21-29 is 0.37 in. Neither of these temperatures will be detrimental to the structural integrity of the case.

(3) Case weld mismatch and weld quality. An extensive investigation was conducted in this area. The principal elements of this investigation were: (1) survey of case manufacturing and performance records; (2) evaluation of weld strength, using tensile samples taken from a retroengine case of similar mismatch properties; and (3) hydro-burst of a case of similar mismatch properties. Based on the results of these investigations, coupled with the fact that the case has passed hydro proof tests twice, it was concluded that the case is satisfactory for flight use.

(4) Insulation groove. During X-ray examination at the Air Force Eastern Test Range (AFETR), a discontinuity in insulation density was detected in a region 0.3-in. aft of the case girth weld, extending for a length of 16 in. in a direction parallel to the weld. This region was X-rayed a second time to gain better definition of the discontinuity. It was concluded that the maximum width of the groove is 0.030 in. at the case interface and 0.060 in. at the propellant interface. Groove density is very similar to that of the liner. It is concluded that the groove is filled with either liner or Thixon-1209. Thixon-1209 is the most likely. A thermal model was constructed where the notch was 0.100 in. in cross section and a minimum of 0.005 in. of liner at the case interface (nominal value of liner thickness for this engine is 0.012 in. based on measured liner weight).

Results of thermal analysis indicate that a maximum temperature rise due to the groove is 330°F. This degrades the ultimate strength of ladish D6AC steel

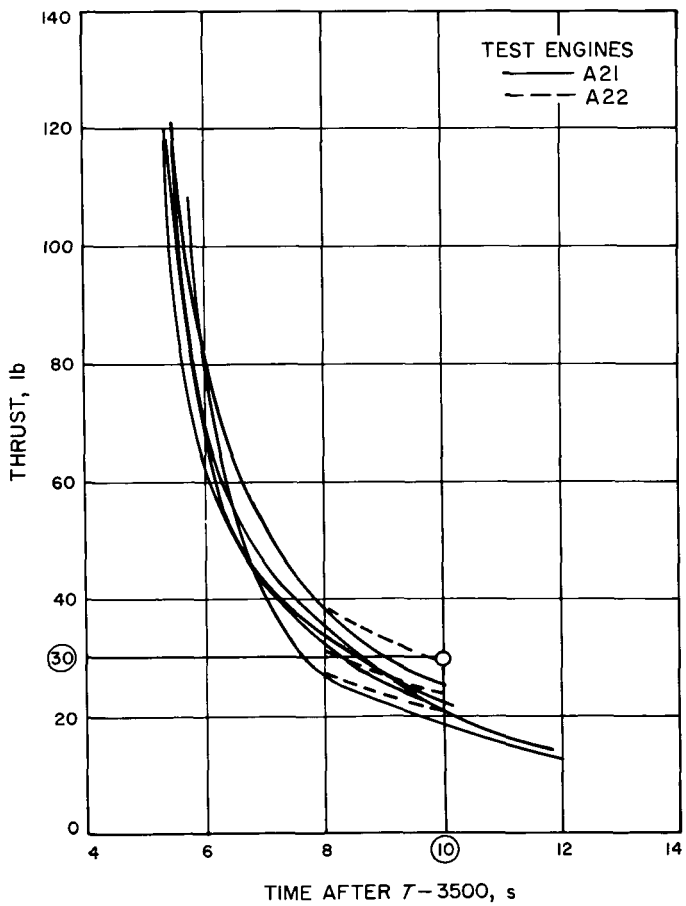

Fig. 2. Retroengine thrust tailoff

by 4%. Results of recent analysis based on the more realistic cross section of the notch and assuming 0.010 in. of liner in the notch predicts a reduction in ultimate strength of 1.1%. Hughes Aircraft Company conducted a similar analysis based on 0.005 in. of liner in the groove, resulting in a reduction of ultimate strength of 1.9%. Based on the most pessimistic model of the liner defect, the strength properties of the case exceed the minimum requirement. The combined analyses and X-ray observations give confidence that the insulation is adequate for flight use.

Based on the findings presented above, the A21-29 retroengine is considered suitable for use on SC-6.

b. Surveyor V. The retroengine was successfully fired September 10. The T-3500 time was 38.56 s or 1.3% less than the predicted 39.06 s. In order to minimize the vernier engine burn time, the thrust tailoff data down to 30 lb of thrust was reviewed (Fig. 2). It was determined that if the vernier engines went to high thrust between 8.5 and 10.0 s after T-3500, separation between the retroengine and spacecraft could occur. The tailoff data also helped fix the lowest retroengine burnout altitude, which, in turn, influenced the delay time between altitude marking radar mark and retroengine ignition. A longer delay time meant a shorter vernier engine burn time. The actual burnout altitude, approximately 4500 ft, compares well with predicted values.

c. SC-6. The flight engine for SC-6 is A21-29. Flight preparation included only checking the safe and arm device since the engine was previously X-rayed, thermally wrapped, and aligned for *Surveyor V*.

The original spare engine, A22-11, was rejected for flight use, and engine A22-12 will serve in its place for SC-6. The rejection of A22-11 was based on the extensive insulation separation, noted in X-rays, when the engine was conditioned to 20°F. It should be noted that a bulk temperature of 20°F is more severe than the temperature gradient experienced in flight. In order to evaluate whether this separation at the low 20°F temperature was caused by a design deficiency or a processing error, three additional engines, A22-5, A21-16, and A21-20, were X-rayed at ambient 40° and 20°F. These X-rays indicated separation at ambient 40° and 20°F for A22-5 and separation of A21-16 and A21-20 only at 20°F. To obtain a correlation between X-ray anomalies and actual separation, engine A22-5 was then dissected. The samples obtained confirmed the suspected separated condition of engine A22-5, and it was concluded that the suspected areas in A22-11 are indeed propellant separations.

As a result of the X-ray program and A22-5 dissection, it was concluded that a design deficiency existed for low temperature conditions and that all engines would probably separate when subjected to 20°F. During the development and qualification program eleven retroengines were subjected to 20°F temperature conditioning and subsequently successfully static fired. Although none of these engines were X-rayed for propellant bond integrity, it is now suspected that all contained some degree of propellant separation induced by the low temperature exposure. However, since A22-11 was exposed to the minimum specification value of 20°F and since there is no way to verify that this separation is a worse or nominal condition than previously tested, A22-11 was rejected.

Propellant separations had appeared in three X-ray views of engine A22-12. In order to add confidence that this engine was acceptable for flight, a special X-ray examination of the engine was conducted after thermally conditioning it to a temperature gradient equivalent to the flight condition. The size of the separations did not increase from the condition seen at the ambient temperature. Therefore, an increase in the size of the separations would not be expected when the engine was subjected to flight temperatures or operating conditions. The engine was considered acceptable.

Because the present design may be marginal for flight conditions, engine A22-13, being processed to replace A22-11 will incorporate a slightly modified case insulation. The insulation was locally thickened in the area of the separation. Photoelastic models of the area indicated a local high stress concentration in the propellant adjacent to the liner. Thus, in thickening the insulation in that area, the stress concentration is now located within the stronger insulation material rather than in the propellant. The adequacy of the design change will be determined by X-raying the engine after thermally conditioning it to a temperature gradient equivalent to the flight condition.

d. SC-7. Retroengine A22-13 was delivered to AFETR October 6. This retroengine is assigned as the SC-7 spacecraft flight engine, with SN A22-12 as the spare backup.

3. Vernier Propulsion System

a. System analysis.

Consent documentation. Inputs were provided for blue ribbon committee meetings and for the *Surveyor V* consent-to-launch, SC-6 consent-to-ship, and SC-7

consent-to-ship meetings. Additionally, closures of all B action items for *Surveyor V* and SC-6 were generated and submitted.

Spacecraft performance analysis command. Two A series and one operational readiness test were supported by propulsion spacecraft performance analysis and command (SPAC) personnel. Additionally, SPAC propulsion handbooks were updated for the *Surveyor V* mission. From September 8 through 10, the mission was supported on a 24-h basis by propulsion SPAC personnel.

During Mission E, all propulsion parameters were normal except for a helium regulator anomaly that appeared immediately upon release of the helium gas prior to performance of the midcourse correction. Subsequent to the apparently normal midcourse shutdown, the helium tank pressure was noted to be dropping at a rate of approximately 10 psi/min. It also appeared that the oxidizer or fuel relief valves were venting. This condition was indicative of a failure of the regulator to lock up the propellant tank pressures. The suspected cause of the problem was that foreign material had lodged on the helium seat, thus preventing regulator lockup, with the result that helium was leaking through the regulator into the propellant tanks and increasing the propellant tank pressure to the relief valve cracking level. A technical review team was formed immediately of JPL and HAC personnel.

Surveyor V data review. A committee comprised of HAC and JPL engineering and quality assurance personnel reviewed the data from *Surveyor V* and the associated quality records. It was concluded that, while the helium regulator attempted to lock up near the expected value, the regulator probably was prevented from sealing securely by a particle of contaminant damage to the seat. A review of the quality records associated with the construction of the *Surveyor V* vernier propulsion system leads to the following conclusions:

(1) The *Surveyor V* helium regulator is functionally identical with the regulators used on *Surveyors I* through *IV*.

(2) The processes employed in cleaning, flight acceptance testing (FAT), assembling, and handling were unchanged on *Surveyor V* and were considered adequate.

(3) No manufacturing test or quality discrepancies were detected in the records or hardware of the helium tank and valve assembly on SC-6, -7, or SP-2.

Minor recommendations were made and implemented for SC-6 flight checkout at AFETR. These include the following:

(1) The test sequence was modified.

(2) Regulator flow and lockup tests were performed last in the vernier propulsion system functional (VPSF) test.

(3) The VPSF test was modified to incorporate millipore analysis following regulator flow test.

(4) The lockup test was extended to 6 h.

(5) Positive procedural changes were implemented to preclude any back flow through the regulator. This change was not implemented for the first test so the regulator did have back flow. In a subsequent test the correct procedure was used with only a forward flow taking place.

No hardware changes were recommended.

Extensive comparative tests, including multiple squib firing, regulator function testing and millipore analysis, substantiated the equivalency of the A21 and A21-E regulators and the adequacy of their design and processing specifications.

b. Spacecraft servicing, HAC.

SC-6. The SC-6 propulsion system was deserviced during this period.

Following VEV, the shipping engines and the vernier propulsion system pressurization assembly were installed and the helium tank pressurized to shipping pressure.

SC-7. The propulsion system was prepared for solar thermal vacuum (STV) during this period. As a result of the propellant tank leakage problems on *Surveyor V*, leg 1 and 2 oxidizer tanks were changed. Additionally, leg 3 oxidizer tank was changed when the thermostat failed to pass a hi-pot test. All three of the new oxidizer tanks were equipped with higher quality O-rings.

c. Spacecraft servicing, AFETR.

Surveyor V. Following the VPSF test (which resulted in replacement of the oxidizer check and relief valve assembly and leg 1 fuel tank), the system was loaded and the high pressure test performed. During this test, a liquid leak was noted at leg 2 oxidizer tank flange. This tank was replaced and the high pressure test repeated. Leg 1 oxidizer tank flange developed a leak

during this test; and, subsequently, this tank also was changed.

Solvents were reloaded to repeat the pressure decay test and leakage of liquid was noted at FVV4. All fuel tanks were offloaded and leak tested, and leg 2 and 3 tanks were determined to have leaky bladders. These two tanks were then changed, the system reloaded with solvents, and the high pressure and pressure decay test performed with no further problems. After solvents were offloaded, a composite bladder leak test was performed on the tanks with satisfactory results. Propellants were loaded and a titration test performed following loading. Results of the titration test indicated all tank bladders were good. A high pressure test (725 psig) was performed, and no leakage was noted in the system. The titration test was repeated and again indicated no propellant leakage through the bladders. These tests ensured suitability of the system for flight.

SC-6. Following arrival at AFETR, the propulsion system was subjected to the VPSF test with satisfactory results. Included in this test series was a 6-h regulator lockup test to verify that no leakage occurred during lockup.

d. Propellant tanks. Tests have been performed at the Placerita Canyon test site to determine the feasibility of a bladder integrity check after the postpropellant load, 750-psig flange seal leak check. The test procedure involves: (1) directing the effluent gases from the 750 to 300 psig depressurization through a cold trap; and (2) taking two additional samples by reapplication of 350 psig followed by bleed to 300 psig through cold traps. Tests were carried out for both fuel and oxidizer with good sets of bladders and for sets wherein one tank contained a high leak rate bladder. In both cases, the quantity of propellant collected in the samples was several times greater for the set having one bad bladder. This type of integrity check will be carried out on SC-6 and -7. The first phase of this integrity check (collecting the 750 to 300 psig effluent) was carried out successfully on *Surveyor V*. The level of propellant collected indicated good bladders on *Surveyor V*.

Failure analysis has continued on the torn bladders removed from *Surveyor V* legs 1 and 2 fuel tanks at AFETR. The vendor is conducting dimensional checks, physical properties tests, and photoelastic and cross-sectional (microtome) analysis. As of this writing, no cause for the failures can be positively assigned.

Failure analyses on O-rings from three oxidizer tanks removed from *Surveyor V* at AFETR have shown the cause of leak to be excessive mold offset. Examination of O-rings from other lots has traced the offset problem to one particular lot. The SC-7 leg 2 oxidizer tank, which had O-rings from the same lot that failed on *Surveyor V*, was replaced. A second leg 1 oxidizer tank was also removed from SC-7; this tank had a questionable O-ring which had been dispositioned "use as is."

A penalty test has been conducted on the blistered bladder from *Surveyor V* leg 1 fuel tank which was removed after indicating a leak rate slightly over allowable at AFETR.

The bladder was subjected to the following tests:

(1) Simulated systems high pressure leak check and pressure decay tests.

(2) Vacuum dry and bladder leak check.

(3) FAT vibration (Z-axis).

(4) Vacuum dry and bladder leak check.

(5) 70°F, 95% expulsion with isopropyl alcohol.

(6) Vacuum dry and leak check.

(7) 20°F, 95% expulsion with fuel.

(8) Vacuum dry and bladder leak check.

At the completion of all tests, the bladder leak rate had increased only 100 cm^3/h over the value at the start of testing. It was concluded that a blistered bladder would have survived all servicing, systems tests, and performed the mission with ample safety margin.

e. Check and relief valve high temperature type approval test. The helium check and relief valves for the vernier propulsion system were type approval tested. The type approval tests covered a temperature range of 0° to 125°F under a combined thermal vacuum environment after propellant exposure, vibration, and shock. This testing simulated the flight environment as predicted at that time.

Due to an over-temperature exposure of the *Surveyor* V check and relief valves during spacecraft STV testing, a special test program was undertaken to extend the high temperature range of the type approval test.

Four valves were functionally tested at 70° and 125°F to establish base line data; the following test program

was then performed to expose the valves to a more rigorous propellant and temperature environment than the initial type approval test program.

(1) Expose to referee fluid for 5 days at ambient temperature.

(2) Vacuum dry for 5 h at 70°F with all ports opened.

(3) Exposure to propellant-saturated helium for 14 days.

(4) Perform nonfunctional vibration testing to the FAT specification requirements with two valves vibrated in the Z-axis only, and each of the other two valves vibrated in the X-axis only, and one in the Y-axis only.

(5) Exposure to propellant-saturated helium gas at 300 psig for 66 h at 150°F. Functionally test once at 150°F after the 66-h exposure with propellant-saturated helium.

(6) Subject each valve to five relief cycles with saturated helium at temperatures of 140°, 150°, 160°, 165°, and 170°F.

(7) Perform functional tests on each valve at 70° and 125°F after the exposures outlined above.

Valve performance at the conclusion of extended exposure testing was within specification requirements at 70° and 125°F. Also, the extended exposure testing did not appear to change any valve components or the outside finish of the valves.

Performance of the valves at the higher temperatures is considered satisfactory, based on a comparison with the valve design requirements and the predicted valve temperatures of 130°F on *Surveyor V* and following spacecraft.

All valves performed within specification requirements at 140°F with a maximum crack pressure of 823 psig and a minimum reseat pressure of 800 psig recorded.

4. Thrust Chamber Assembly[2]

The program for *Surveyor* vernier engine [Reaction Motors Division of Thiokol Chemical Corporation (RMD) model TD-339] evaluation continued with twenty engine firings and miscellaneous flow and storage tests. Table 1 summarizes these activities.

[2]Prepared by JPL Technical Section 384.

Table 1. Vernier engine evaluation test summary

Group	Test	Test date	Purpose
50	DD-239, -240, -242, -243, -248	June, July	Bracket strain gage tests
51	DY-131 to -136	June, July	Lunar hopper tests
52	F-36, -39, F-41 to -46	July, August, September	Lunar storage tests Static firing tests
53	FB-257 to -287 DY-139 F-47 to -54	September, October	Dupont PR 250AC Lubricant tests
54	DY-142 to -145 FB-280 to -284	October	Helium inlet filter tests
54	DD-253 FB-246	July, October	SC-2 failure analyses tests
55	FB-266 FB-267	September	SC-5 supporting tests

a. Engine bracket strain gage evaluation. Initial tests (DD-173 and -176) of the engine flight bracket and SC-1 flight data indicated 0.5 to 1.0 lb/s of thrust decay in the strain gage readout during a 20-s firing at the midthrust level. To improve thrust measuring accuracy, HAC redesigned the strain gage installation. Three firing tests (DD-203, -204, and -205 reported in SPS 37-44, Vol. I, p. 24) were made in December 1966, to evaluate the redesigned circuits. The test data indicated a thrust decay similar to that experienced in the SC-1 midcourse correction. The strain gage circuitry was reviewed by JPL during early 1967.

In June, two engine firing tests (DD-239 and -240) were performed to evaluate two alternate bridges. The data from test DD-239 indicated that relocation of the four strain gages to the internal surfaces of the leg two/three bracket side members provided a marked reduction in thermal decay. Additional tests (DD-242, -243, and -248) were performed in mid-July to provide confidence that such a bridge relocation would improve thrust measuring accuracy. The same improvement was obtained in these latter tests.

The data were presented to HAC personnel, and discussions were held as to the factors involved in implementing a change in the bridge circuitry for SC-6 and -7. It was decided that a change in the strain gage circuitry was not justified at such a late date in the program.

b. Lunar hopper tests. A series of tests was performed from June 20 to July 3, 1967 to verify the spacecraft capability to perform the hopper (lunar lift-off and translation) experiment. Following several preliminary tests (DY-131 to -133) two successful single-engine closed-loop tests (DY-134 and -135) were performed June 27. Test DY-134 was a 10-s test at ambient temperature; test DY-135 was a repeat test at a simulated lunar temperature of 250°F. The firings were performed in the vacuum facility at Edwards Test Station (ETS) with throttle valve current commands controlled by the HAC analog computer at El Segundo, California. Engine response (chamber pressure) was linked to the computer using data phones and commercial telephone lines. Engine "on-off" commands originated at ETS. The response characteristics of the other two engines were simulated electrically at El Segundo. The firing profile for the two closed-loop tests called for 0.2 s operation at maximum thrust, followed by about 9.5 s at minimum thrust.

The sixth test (DY-136), an open-loop high temperature (250°F) test with an abbreviated dynamic test profile, was successfully conducted July 3. The test was 5 s in duration and included two pulse trains as well as a step from minimum to maximum thrust.

All data in analog form were transmitted to the HAC flight control group for analysis. The ambient closed-loop test verified that a satisfactory lunar lift-off and translation experiment could be performed with an engine temperature of 100°F or up to a temperature at which performance and response do not change materially from the 100°F characteristics. The 250°F closed loop test showed that, with *one* engine thermally degraded, anomalous spacecraft performance can be expected.

The results of the subject test series (together with the results of other high temperature tests performed in 1966 at ETS) show that thrust can be expected to be erratic, and either higher or lower than the flight acceptance test (FAT) commanded level. The largest thrust increment (actual thrust less FAT thrust at the same command) measured in the high temperature tests was 19 lb. This occurred in test DY-136, immediately following a downthrottle to $-80\ \Delta$ mA.

Comparing the data from the last 7 s of ambient test DY-134 with comparable data from test DY-135 (constant throttle valve current command level of about $-70\ \Delta$ mA over this time interval), the average thrust increment was 10.1 lb.

At the higher temperatures, thrust chamber assembly (TCA) throttling performance is dominated by vaporization or partial vaporization of the oxidizer, causing:

(1) Higher than FAT thrust output for a low thrust command.

(2) Lower than FAT thrust output for a high thrust command.

(3) Slower dynamic response.

c. Lunar survival and static firing tests.

Shutoff valve lunar survival. One of the constraints imposed on a lunar hopper or lunar static firing test is the marginal nature of the nylon seat in the shutoff valve when exposed to high temperature fuel for several days. Tests of small discs of the nylon seat material have indicated that fuel chemical attack causes severe degradation at temperatures between 230 and 280°F when the material is exposed for more than a few days. Mission B lunar survival tests (SPS 37-43, Vol. I, p. 7, tests DD-143 to -145, September 1966) did indicate, however, that a nylon poppet could survive 3 days of storage in the 220 to 250°F temperature range together with three valve actuations (engine firings) in this time period. Posttest inspection of the poppet revealed severe degradation with a loss of the poppet tip, although the seating surface was solid enough to seal.

The marginal nature of the nylon material indicated the need for additional testing, so that the risk associated with firings on the lunar surface could be better evaluated. A test program, involving the storage of three shutoff valves in contact with fuel in a temperature controlled box for 11 days under conditions simulating the SC-3, leg two temperature profile, was successfully conducted in July and August. Test results are as follows: (1) the nylon seat in valve one survived two actuations on the third day at 260°F; (2) the nylon seat in valves one and two failed in actuations on the seventh day (fuel leakage and severe degradation/erosion of the nylon); (3) the nylon seat in valve three survived the lunar day (no actuations performed) and four actuations following cooldown to ambient temperature.

Lunar static tests. Having demonstrated in two test series that a nylon poppet may survive a certain number of valve actuations over 3 days of high temperature exposure to the fuel, the engine and its valves were further evaluated in a high temperature storage and firing program. This program was an extension of the work described above, with particular reference to the plans for a mission E lunar static test.

A sea level engine, equipped with a new nylon poppet, was subjected to a simulated lunar storage and firing program for 48 h during the last week of August 1967. Six firings, each for 0.6 s at a throttle valve current command level of -80Δ mA, were planned at 24-h intervals over a 2-day storage period. The storage and firing program were initiated August 30 with two firing tests (F-41 and -42) at ambient temperature (100°F). Following these tests, oven temperature was raised to 220°F and maintained at this level for 24 h. Two tests (F-43 and -44) were performed within ½ h of each other at the end of the 24-h period. Again, oven temperature was raised and maintained at 250°F for 24-h. The final two tests (F-45 and -46) were performed September 1 with the engine conditioned at 250°F.

The thrust behavior of the engine in the first two ambient tests was normal, exhibiting a constant 24.0 lb (equivalent vacuum thrust) over the firing period. The firing tests with the engine conditioned to 220°F produced nearly identical thrust-time records. In each test, thrust peaked at about 35 lb at 0.15 s from fire signal and fell gradually to about 32 lb prior to shutdown. The behavior of the engine in the final two tests at 250°F differed from that of the previous tests. In test F-45, a sharp thrust peak of 29 lb developed at 0.10 s from fire signal, diminished rapidly to 19 lb at 0.20 s, and gradually decreased to 14 lb prior to shutdown. In test F-46, thrust reached a peak value of 30 lb at 0.40 s from fire signal, and then decayed rapidly to 19 lb prior to shutdown.

The variability in thrust for tests F-45 and -46 is attributed to the fact that the MON-10 contained in the line within the conditioning box could have existed in either the gas or liquid phase prior to engine firing. The MON-10 was probably entirely in the gaseous phase in the feed line in test F-45 (the vapor pressure of MON-10 at 250°F is about 800 psi) following some 17 h of storage at this temperature. This firing test then caused a certain amount of liquid MON-10 to be drawn from the system at ambient temperature outside the conditioning box. Thus, a heterogeneous mixture of liquid and vapor probably existed in the line at the time of test F-46 (½ h soak between tests F-45 and -46), and produced the rather erratic operation in the latter test.

Pressure measurements in the oxidizer circuit downstream of the throttle valve indicated that a much higher pressure exists at this point in the circuit during high temperature operation than in ambient tests. These higher pressures reflect the fact that MON-10 has a high vapor pressure and is partially in the vapor phase as it exits from the throttle valve.

From an analyses of these data as well as prior short-duration firing tests DD-143 (½ s firing at 220°F) and DD-145 (½ s firing at 250°F), it appears that the *largest* thrust increment is developed when the temperature of the propellants entering the engine is about 220°F. Tests in the 250°F range have either shown a smaller thrust increment or a thrust decrement when compared with ambient temperature firings. Comparing the results of these F-stand tests with test DY-136 (subsection 4b), it is concluded that engine performance and magnitude of the thrust increment at 250°F is influenced by the type of firing profile demanded of the engine.

It is of interest to compare the thrust-time relationships obtained in these high-temperature ground tests with the thrust recorded during the SC-5 lunar static firing. SC-5 engine temperatures were 118, 272, and 138°F for legs one, two and three, respectively, at the time of the lunar firing. Thrust developed by the leg two engine during the lunar static test was about 17 lb, based upon two data bits. This compares favorably with the previously discussed data of test F-45. The thrust developed by leg one and three engines in the lunar static firing was in the range of 24 to 26 lb. This thrust level is in good agreement with the thrust developed in tests F-41 and -42 and the FAT thrust (26 ± 0.5 lb) expected from the SC-5 engines when fired at a throttle valve current level of -80Δ mA.

d. Lubricant evaluation. The *Surveyor* engines on SC-1 through -5 all used Kel-F 90 as a lubricant for the seals of the shutoff valve assembly. In the course of engine buildup and testing at RMD in 1966, certain deficiencies in this lubricant became apparent. These appeared to be related to the reactivity of Kel-F 90 with the fuel. The development of reaction products resulted in galled threads and sluggish response of the valve in dynamic tests. These same products were found in one fuel regulator, causing it to stick closed.

Engine firing experience of JPL with Kel-F 90 over the past 3 years has resulted in only one failure (fuel poppet would not close) directly attributable to the development of reaction products. This took place with SN 538 TCA in November 1966, after about 1½ years of testing with this engine at ETS.

Laboratory work at RMD indicated that the lubricant Dupont PR 240AC offered superior qualities; RMD recommended in mid-1966 that it be used in all engine rework.

As a result of this recommendation, the engines to be installed on SC-6 and -7 will contain this lubricant in the shutoff valves. Dupont lubricant is also planned by JPL for use in all engine rework at ETS. At the same time special tests were devised and carried out to develop confidence that this material is qualified for use in the flight engines. The paragraphs following describe JPL's experience with Dupont lubricant.

Laboratory tests. During the months of July and August 1967, laboratory tests were performed at JPL to determine the compatibility of the Dupont PR 240AC lubricant with the *Surveyor* propellants and solvents. The tests involved immersing the lubricant in the fluid within a test tube, heating the contents, and storing at temperature for a selected period of time. The tests with isopropyl alcohol, Freon-113 and MMH • H_2O involved temperatures in the range of 76° to 100°C and storage for 24 h. Storage tests with MON-10 and N_2O_4 (results from the N_2O_4 would be expected to be similar to the MON-10 used on *Surveyor*) were performed at ambient temperature for 24 h and 154 h, respectively. The only evidence of an interaction between the lubricant and the fluid was in the tests with N_2O_4. The grease turned mildly yellow and appeared to be somewhat soluble in the oxidizer.

Engine firing tests. Serial number 506 TCA, lubricated with the Dupont PR 240AC, successfully performed seven simulated midcourse plus retroengine descent missions (tests DD-122 to -128) with no evidence of lubricant degradation. Details of the test program are presented in SPS 37-46, Vol. I, pp. 38 to 48.

Serial number 525 TCA, lubricated with Dupont PR 240AC, successfully performed two simulated midcourse plus retroengine descent missions again (tests DY-142 to -145) with no evidence of lubricant degradation. Solvent flow tests, before and after the engine firing tests, showed no change in engine start and shutdown characteristics. These tests were a part of a type approval test (TAT) program to evaluate a helium inlet filter for the engine and are discussed in Subsection 4e of this article.

Compatibility tests. Special tests were performed to compare the compatibility of the two lubricants with *Surveyor* fuel. The test program involved disassembling, cleaning and lubricating the seals of a shutoff valve. The initial buildup of the valve was performed with Kel-F 90 lubricant. About ½ cm^3 of MMH • H_2O was injected into the valve actuation cavity. The valve was then placed in an oven, heated to 150°F, and stored for 20 h. Since the fuel would be in contact with the lubricated fuel piston seals, the development of reaction products should manifest itself by a change in valve timing during the opening/closing cycle. Solvent flow test FB-258, performed prior to storage, indicated normal valve response. Flow test FB-259 following storage revealed the presence of reacted products. While the movement of the fuel poppet was sufficient to establish flow, the oxidizer poppet failed to move in the first actuation, moved sluggishly in the second actuation, and finally moved normally in the third actuation.

Inspection of the interior of the valve following test revealed a brownish stain on the cylinder wall adjacent to the fuel shaft quad-ring and a minute quantity of reacted (Kel-F/MMH) material on the quad-ring itself. It is believed that the pressure forces acting on the fuel piston in the opening cycle were large enough to move the fuel poppet off its seat but could not overcome the oxidizer poppet spring force together with the added friction created by the reacted products on the quad-ring.

The same shutoff valve was then recleaned and lubricated with Dupont. Following response test FB-261, ½ cm^3 of MMH•H_2O was injected into the valve actuation cavity. The valve was then placed in a 150°F oven and stored for 90 h. Flow test FB-264 following storage indicated no change in valve timing. No reaction products were noted upon disassembly and inspection.

Flight qualification tests. Upon completion of the tests described above, a program was developed for testing the Dupont PR 240AC lubricant under the conditions to which this material would be exposed in the many operations at RMD, HAC and ETR. This program was to serve as the basis for certifying the lubricant as flightworthy for *Surveyor* missions.

The test program involved buildup of a shutoff valve assembly with new seals (lubricated with the Dupont PR 240AC) and installation of the valve on overhauled sea-level engine SN 531. The engine was then to be subjected to a series of operations including: (1) acceptance firing test; (2) solvent flow tests; (3) water flow test; (4) deservicing; (5) storage with solvents; (6) storage with propellants; (7) firing tests following storage; and (8) disassembly and inspection. The record of valve response and pressure changes in the valve assembly during solvent flow and engine firings was to be the major indicator of lubricant suitability. Chamber pressure records in engine firings would be a secondary indicator of these transients.

The program was initiated during the first week of September 1967 and was completed October 9. The operations performed on the valve assembly included: three

engine firings, nine solvent flow tests, one water flow test, six engine deservices (gas purge; vacuum dry), 1 wk of storage with solvents at 150°F, 10 days of storage with propellants at 150°F, and final disassembly and inspection.

The solvent flow data were the primary indicators of valve transient response throughout the program. Transient response was defined as the time interval between command signal to the valve to the start of fuel or oxidizer valve inlet pressure change. Tests at the "0" Δ mA level indicated essentially no change in valve timing. Start and shutdown times ranged from 10 to 34 ms. Solvent flow tests at −80 Δ mA, while indicating essentially no change in dynamic start response (start times ranged from 10 to 18 ms), showed a small change in shutdown response on the oxidizer side of the valve. Initial flow tests (FB-72) at −80 Δ mA produced a sharply reacting pressure change (shutdown times ranged from 16 to 20 ms) in both sides of the valve at shutdown. The final flow tests (FB-287) indicated the same fast response in the fuel circuit but a slowly reacting pressure change in the oxidizer circuit. If one measured from shutdown signal time to the point of intersection of a 45-deg tangent with the gradually increasing oxidizer pressure trace, shutdown time was 50 to 58 ms. If one considered the normal definition of shutdown time (time to the start of pressure change), the first change in oxidizer pressure occurred 20 to 25 ms following the voltage signal to the valve. Fuel pressure in this final series of flow tests continued to react sharply; the shutdown times in this circuit were 16 to 17 ms.

Start and shutdown times for the three firing tests were normal. Shutdown times at 0 Δ mA ranged from 9 to 34 ms. The chamber pressure confirmed these shutdown times.

Valve inspection at the start of the test program indicated all bore and shaft dimensions to be within design tolerances. Valve inspection at the end of the test program revealed no defects. The shafts were unscored and easily removed from the valve body. No discoloration or evidence of reacted products was observed.

The small change in the shutdown behavior of the valve during the testing program is believed to be caused by a small amount of washing of the Dupont PR 240AC lubricant by the Freon in flow tests. Laboratory tests have indicated that Freon tends to dissolve the Dupont PR 240AC lubricant. Considering the large number of solvent flow tests performed in this program (more than normally performed on a flight engine) it is probable that there is a small and progressive increase in sliding friction between the oxidizer piston and the Teflon omniseal as a result of some removal of lubricant in this area. This effect may be compounded by the fact that, at the low flow rate associated with a −80 Δ mA shutdown, the oxidizer pressure forces (added to the spring force during shutdown) are small. For the extreme condition of a complete loss of lubricant in this area of the shutoff valve, friction would tend to be low because of the lubricating qualities of the Teflon itself. This is exemplified by the results of actuation tests (FB-257) performed with dry seals in the shutoff valve. Shutdown transient times were 30 to 38 ms up to 50 actuations. Thereafter, the shutdown time became progressively longer (80 ms on the ninety-sixth actuation). The valve failed to close on the ninety-seventh actuation due to deterioration of the quad-ring in the helium piston cavity. This ring is normally lubricated and is not normally exposed to the propellant or solvents.

Considering the results of the engine firing tests, the compatibility tests, and the flight qualification tests described above, it is concluded that Dupont PR 240AC is a suitable lubricant for the *Surveyor* engine.

e. Helium inlet filter tests. SPS 37-46, Vol. I, pp. 38 to 48, described the results of tests at ETS to evaluate the TRI-DOT filter produced by Mectron Industries. The tests indicated that a 10-μm filter can be substituted for the present fitting at the helium inlet port of the shutoff valve with no effect on valve actuation timing.

During this report period the Mectron TRI-DOT filter assembly was tested and qualified for use on the spacecraft. One section of the TAT specification called for the qualification of the filter in engine firings. Two filter configurations were involved, one a union-type filter assembly for the leg one engine, the other a reducer-type assembly for the leg two/three engines. The test program consisted of solvent flow tests and mission simulation firing tests. The solvent flow tests were to be performed before and after the engine firings to provide start transient engineering data. The engine firings constituted the formal part of the TATs. Acceptance criteria for each filter were based upon the firing start transient chamber pressure data which were to be within the starting limits called out in Thiokol acceptance test specification 15124.

Each filter configuration was subjected to two engine firing tests. The first test in each series consisted of a simulated midcourse of 50-s duration at the midthrust level. The second test was a simulated maximum-duration terminal descent firing. Prior to each midcourse firing, 1 cm^3 of $MMH \cdot H_2O$ was placed in a section of the line immediately upstream of the filter assembly to demonstrate that its presence (possibility of fuel condensate in

the spacecraft helium actuation line) would not affect the engine start characteristic.

The solvent flow test (FB-280 to -284) data indicated that the start transient time interval (previously defined) for the two filter configurations was in the range of 15 to 18 ms and was essentially unchanged by the engine firings. The engine firing data (tests DY-142 to -145) produced start transients which met the requirements of the Thiokol AT specification. There was no indication from the data obtained in this program that the 10-μm helium inlet filter affected the engine start characteristic.

f. SC-2 failure analyses tests.

Restriction tests. Previous articles have discussed the attempts to simulate the failure mode of the leg three engine during its second burn, this burn having been selected as representative of the 2-s firings made during the SC-2 flight and in addition having exhibited less zero shift in the thrust data. SPS 37-43, Vol. I, pp. 7 to 11, reported on the results of tests DD-178 to -183 in which the movement of the oxidizer poppet was restricted. Thrust data from test DD-182 provided the closest simulation with the spacecraft telemetered strain gage data. Flight data had indicated a uniformly low level of thrust (about 2 lb), lasting from 4 to 5 s. Thrust in test DD-182 ranged from 6.4 lb at the start to 0.7 lb at shutdown. The oxidizer flow rate averaged about 0.005 lb/s.

The poor simulation noted above prompted additional tests (DD-223 to -226) described in SPS 37-46, Vol. I, pp. 38 to 48. In this second group of tests, the restriction was provided by a needle valve located alternately at the inlet and the outlet of the throttle valve. Simulation again was poor, all tests exhibiting an initially high thrust (8 to 15 lb) followed by a reduction to a low level. The data indicated that the most likely point of restriction to produce the thrust-time relationship exhibited by the SC-2 leg three engine would be located at or near the injector orifices.

From May to September 1967, attempts were made to induce plugging (by the formation of nickel salts) of the injector to the degree that the oxidizer flow rate passing through the orifices would be about 0.007 lb/s, which is the estimated oxidizer flow rate during burn two of the leg three engine. All attempts to obtain the desired amount of plugging were unsuccessful. To obtain some indication of the effect of blockage in the general area of the injector orifices, it was decided to replace the filter element (located at the interface between the shutoff valve and the injector) with a sharp-edged restricting orifice (peened-80 drilled-hole). To further simulate the effect of injector manifold blockage, a few pieces of stainless steel drill rod were placed in the injector port. Flow tests of the oxidizer circuit with these modifications resulted in a MON-10 flow rate of about 0.01 lb/s. This flow rate, though higher than desired for simulation, corresponded to about the lower limit for recording flow with the existing turbine type flow meter.

Test DD-253 resulted in an initial thrust of about 12 lb, rising to about 14 lb at the end of the test. Although thrust was again higher than that indicated by flight data, the buildup of thrust was more gradual than in previous tests. In this respect, a better simulation of the flight data was obtained. It is believed that, with a restriction in this location and a reduction of MON-10 flow rate to about 0.007 lb/s, thrust would be of the order of that experienced in flight.

From the thrust data obtained in these SC-2 failure analyses tests, it is concluded that the most likely point of restriction in the SC-2 leg three engine was at or near the injector orifices. A restriction at the injector orifices could have developed from the formation of nickel salts.

Gas phasing tests. As indicated previously, the data from the SC-2 failure analyses tests have shown that the oxidizer flow rate to the leg three engine (SN 544) during midcourse was approximately 0.007 lb/s. A review of pertinent AFETR documents for this engine indicated that an acceptable solvent flow test had been performed prior to installation of the engine on the spacecraft. Subsequently, a gas leak was found in one of the flare tube connectors of the oxidizer tubing leading from the throttle valve to the shutoff valve. The leak was corrected by replacing the conical seals. Following this operation, a gas flow test (normal check of proper phasing) of the oxidizer circuit of each engine was performed. No appreciable difference in the phasing flow data for the three engines was noted. The solvent flow test was not repeated following replacement of the conical seals.

It was considered important to know whether the gas phasing test could have detected a restriction of a size that would limit the MON-10 flow rate to 0.007 lb/s. To answer this question, the SC-2 gas phasing tests were repeated at ETS. The metering equipment used by HAC at AFETR was shipped to ETS in August 1967 for this determination. The equipment consists of a flow circuit having two orifices connected in series to the oxidizer bleed port of the shutoff valve assembly. Two pressure gages, mounted on each side of the upstream (metering) orifice, indicate

the pressure drop across this orifice during flow with helium gas. The downstream orifice simply provides the proper back pressure for the metering orifice. For the ETS test, a needle valve was installed in the oxidizer line connecting the throttle valve and the shutoff valve to provide a means for simulating the MON-10 flow restriction. Serial number 520 TCA, a representative sea-level engine, was a part of the flow system.

Flow test results at ETS are briefly described in the following paragraphs.

(1) *Phase 1.* Using a supply pressure of 66 psig, the system (without metering valve) was flow tested in duplication of the AFETR gas phasing test. With this test setup, the AFETR flow ΔP data were reproduced at ETS. Pressures on each side of the metering orifice were within 1 psi of the values measured on SC-2. The orifice pressure drop in these unrestricted tests ranged from 13 to 16 psi for throttle valve settings of +8, +56 and −80 Δ mA.

(2) *Phase 2.* A metering valve was installed in the oxidizer line between the throttle valve and the shutoff valve and adjusted to simulate a restriction in this circuit. Flow tests were made with Freon-TV at selected metering valve restrictor settings and at a throttle valve current setting of +80 Δ mA. Maximum flow achieved with the valve wide open was 0.0343 lb/s (equivalent MON-10 flow rate), which corresponds to about 15% of full oxidizer flow rate. Flow tests at other metering valve settings resulted in flow rates of 0.0252 and 0.0125 lb/s, corresponding to 11.3 and 5.6% of full oxidizer flow rate, respectively.

(3) *Phase 3.* With the metering valve adjusted to each of the settings established in phase 2, gas phasing tests were again performed at three throttle valve settings (+8, +56, and −80 Δ mA). Pressures on each side of the metering orifice were recorded. In these restricted gas phasing tests, the orifice pressure drop was about one-half the unrestricted value when the metering valve was adjusted to give 15% of full oxidizer flow rate. With the metering valve restricted to 5% of full flow, no orifice pressure drop could be measured with the particular gages that were supplied with the equipment.

In summary, the tests performed at ETS indicated that the presence of a restriction in the oxidizer circuit of the TCA of such a size as to limit flow to 15% of full flow or less would definitely have been detected by the gas phasing tests performed on the spacecraft at AFETR.

g. SC-5 supporting tests. Special solvent flow test (FB-266 and -267) were performed at ETS September 8 and 9, 1967 in support of the SC-5 retroengine descent firing. It was assumed at this time that spacecraft tank pressures (helium and propellant) would stabilize at about 815 psia, a pressure corresponding to the setting of the relief valve. The characteristics of the engine when operating under lower than normal tank pressures were to be determined. Two engines (SNs 506 and 535) were flow tested over a tank and helium actuation pressure range from 594 to 438 psia. The tests indicated that engine operation would be essentially normal at a tank pressure of 594 psia. As tank pressures were reduced below this level, fuel flow was gradually throttled by the action of the fuel regulator and was completely stopped when tank pressure had decayed to about 448 psia.

Tank pressures at SC-5 touchdown were about 575 psia. Thus the engines probably operated at a mixture ratio only slightly higher than normal.

F. *Surveyor* Solar Panel (SC-5, -6, and -7)[3]

Progress in preflight preparation of solar panels developed for *Surveyor* SC-5, -6 and -7 was: (1) completion of the type approval (TA) drop test program; (2) delivery of the panel for SC-6 and field testing at the Air Force Eastern Test Range (AFETR); and (3) preliminary analysis of the SC-5 flight data. Work at the solar panel contractor has diminished to the point of: panel clean up; final Table Mountain calibration; and processing for shipment to AFETR. This type of work should be concluded by the end of 1967.

1. Type Approval Drop Test Panel Program

Solar panel serial number (SN) 006, commonly referred to as the S-9 drop test panel, was fabricated in accordance with JPL drawing J 143284 and is shown in Figs. 3 and 4. The figures show the front and back view of the solar panel after successful completion of the qualification tests. This solar panel is only partially celled, having approximately 40% of its area covered with active solar cells. The remaining area is covered with aluminum chips to simulate mass loading effects. The active solar cells were placed where maximum degradation (if any) was anticipated for the drop test conducted by HAC. In other respects the drop test panel is considered to be representative of a flight panel for qualifying the design.

Following fabrication, the S-9 panel was subjected to a normal flight acceptance environment test sequence. The electrical performance requirements were appropriately scaled to account for the fact that the panel was partially

[3]Prepared by JPL Technical Section 273.

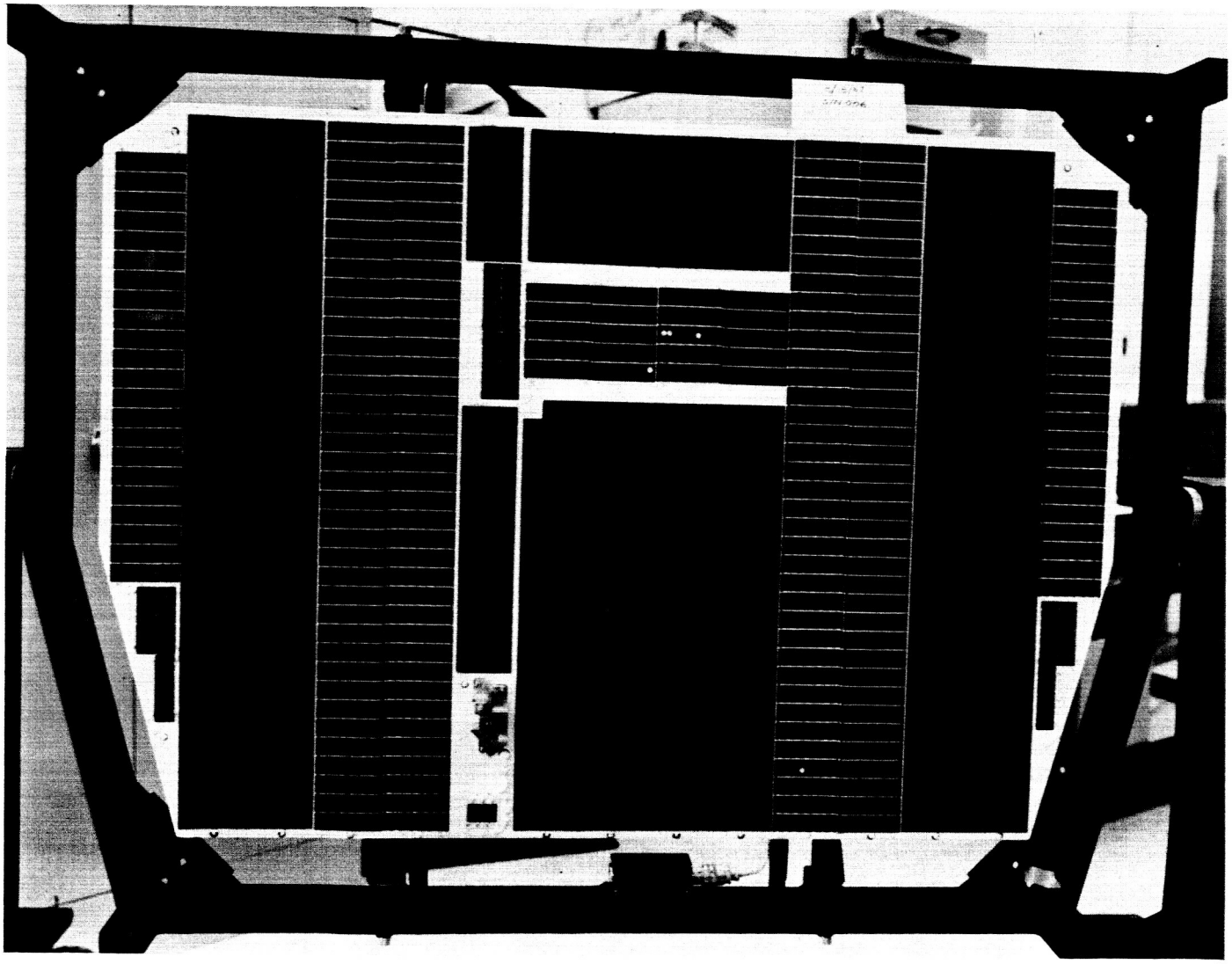

Fig. 3. Surveyor, S-9 TA drop test solar panel, SN 006 front view (in handling frame)

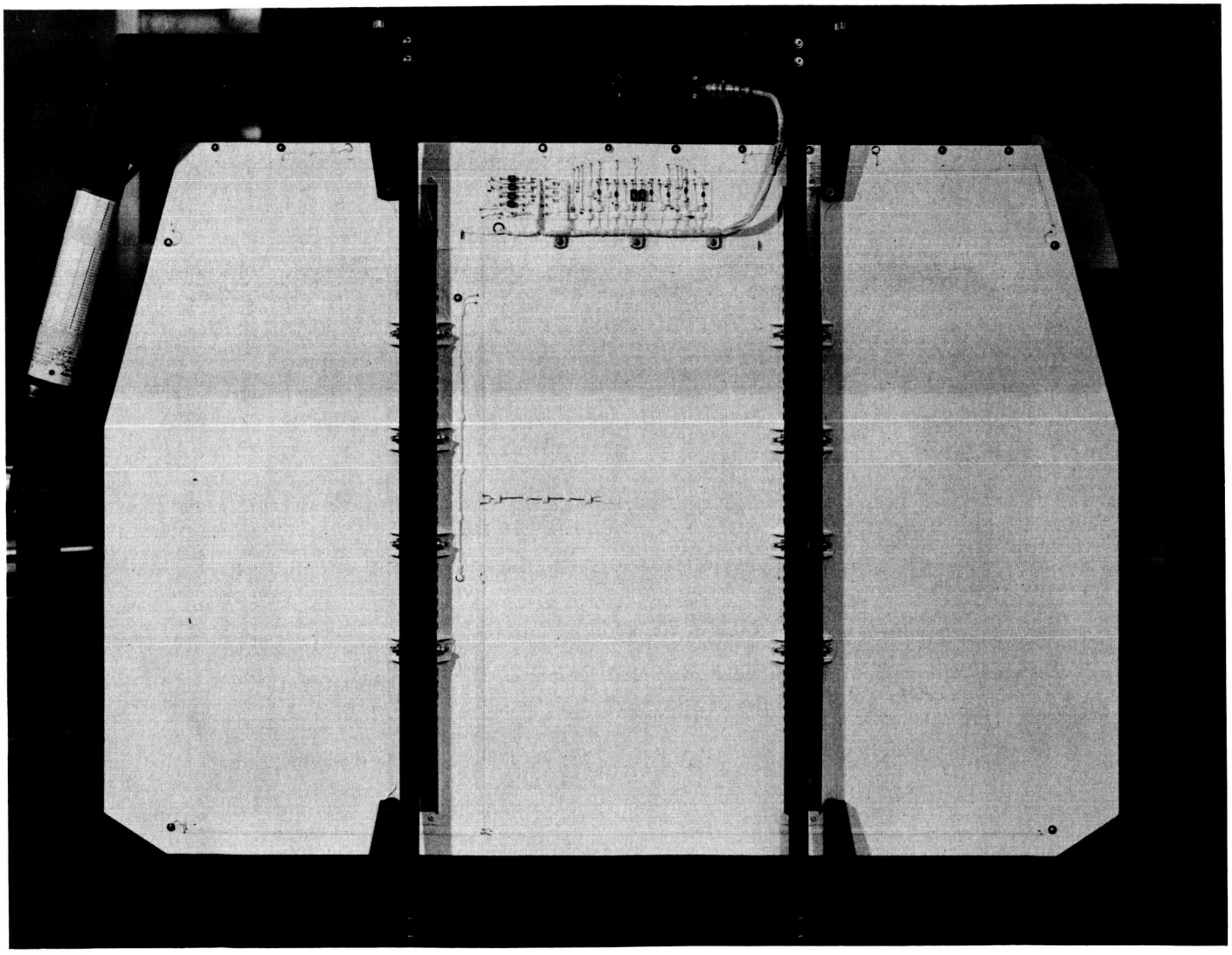

Fig. 4. *Surveyor*, S-9 TA drop test solar panel, SN 006 rear view (in handling frame)

celled. It was then delivered to HAC where it was mounted on the *Surveyor* S-9 vehicle for the drop test sequence. This test completed the TA sequence required by the solar panel interface specifications.

Since the original TA solar panel fabrication and test sequence had included an abnormal amount of rework and retest the confidence in the results of the temperature test was low. A modified TA temperature sequence was then run on the S-9 panel. The results of this test, which cycled the panel to a low temperature of −260°F and a high temperature of +235°F, were satisfactory and the SC-5, -6, -7 configuration panel met the requirements of the *Surveyor* program.

2. Status of SC-6 Solar Panel Assembly

Flight solar panel SN 002 and flight spare SN 005 were delivered to spacecraft operations at AFETR according to schedule. These units underwent successful sunlight testing, cleaning and inspection operations at AFETR during September 1967. Serial number 002 panel has been installed on SC-6.

3. Preliminary Analysis of SC-5 Flight Data

The *Surveyor* mission E (SC-5) was launched successfully September 8, 1967, from AFETR. The solar panel assembly SN 003 performed with no anomalies, as predicted, and supported all the spacecraft power requirements during the transit and first lunar day operations. The panel provided approximately 85 W of usable power to the spacecraft. During the low power cruise mode of the mission, the solar panel supplied all of the load requirements. During the lunar day operation the solar panel power capability was never fully utilized. This resulted in higher than expected lunar environment temperature. However, no degradation to the power capability of the panel was anticipated.

G. Structures, Mechanisms and Spacecraft Integration

1. Introduction

The purpose of the engineering effort outlined herein is to assure the physical integrity of the *Surveyor* spacecraft hardware and mechanical devices, the management of structural test vehicles, and the execution of the test program for these vehicles. Also included are the design, development, and production sustaining activity for the electromechanical devices used on the spacecraft, as well as the basic spaceframe, landing gear, substructure, and harness.

2. Structure, Mechanism

a. Hopper confidence level verification study. Permissible landing velocities were established for the *Surveyor V* lunar liftoff and translation maneuver based on consideration of antenna/solar panel positioner (A/SPP) loads (mode shapes and frequencies were assumed the same as for the 287580 A/SPP), with the solar, elevation, and roll axis unlocked. Boundaries were obtained for two criteria: (1) the moment about any axis must not exceed the yield torque of the drive motor shaft (500 in.-lb); and (2) the motor shaft permanent deformation must not exceed 1.5 deg of twist (600 in.-lb). Velocity boundaries were obtained for vehicle incidences, relative to the surface, up to 8 deg and the on-site slopes not exceeding 15 deg (Fig. 5). The areas under the boundaries in Fig. 5 represent the acceptable velocity combinations for each configuration. Figures 5(a) to 5(c) represent the criteron that the torque of any drive motor shaft must not exceed 500 in.-lb. Figure 5(d) shows, for a 4-deg relative incidence, the boundary obtained using the criterion that the motor shaft permanent deformation must not exceed 1.5 deg. Comparison of this figure with Fig. 5(b) shows the increased capability.

An assessment of nonstandard shock absorbers showed that a 50% internal pressure loss from shock absorbers has a negligible effect on the velocity boundaries, while high temperature shock absorbers (190°F) decrease the regions of allowable landing velocities. Comparison of Fig. 5(e) with Fig. 5(b) shows the effect of high temperature shock absorbers for a 4-deg relative incidence.

b. SC-7 alpha scattering instrument redeployment. On SC-7, the soil mechanics/surface sampler (SM/SS) mechanism will be used to lift the alpha scattering instrument sensor head after it has been dropped to the lunar surface and reposition it to another location. The dynamic effect of the additional mass of the sensor head on the end of the SM/SS arm during operation could cause structural failure of the arm unless certain operational constraints on its movement are met during repositioning. After testing and analyzing the system, the following recommendations were made to ensure the structural integrity of the SM/SS mechanism:

(1) Operation in azimuth and elevation shall be in the fine mode (0.1 s/pulse).

(2) Maximum rotation in azimuth, per pulse, shall be 3.5 deg or less. For nominal operation in the fine mode this constraint is met, but, for nonstandard temperature and voltage, it is possible to exceed it.

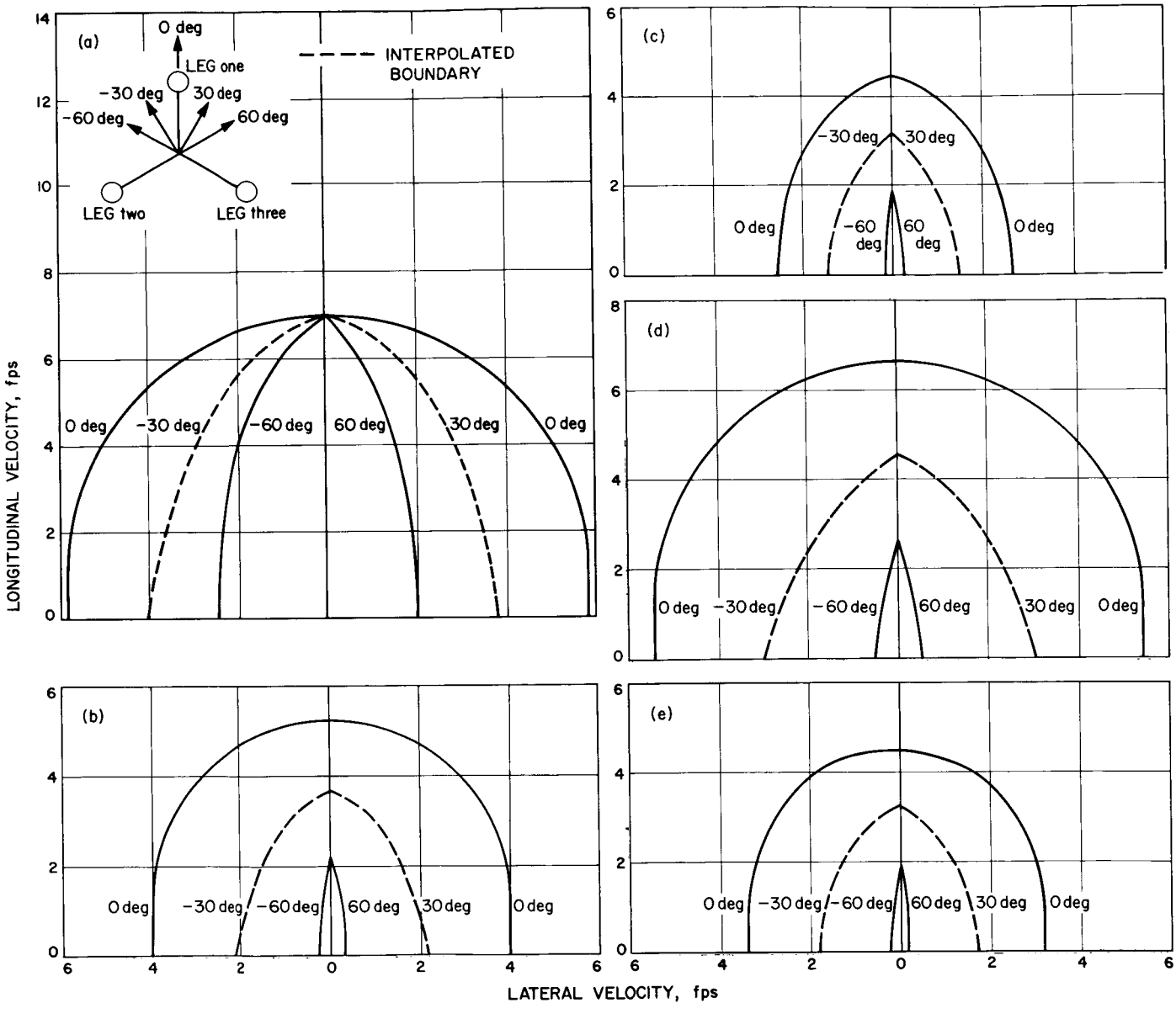

Fig. 5. *Surveyor* lunar translation capability envelope: (a) vehicle incidence relative to slope = 0 deg, torque limit = 500 in.-lb; (b) vehicle incidence relative to slope = 4 deg, torque limit = 600 in.-lb; (c) vehicle incidence relative to slope = 8 deg, torque limit = 500 in.-lb; (d) vehicle incidence relative to slope = 4 deg, torque limit = 500 in.-lb; (e) vehicle incidence relative to slope = 4 deg, torque limit = 500 in.-lb, shock absorbers and block = 190°F

(3) Maximum rotation in elevation, per pulse, shall be 0.5 deg or less. This constraint is met for all operations in the fine mode, nominal or nonstandard.

(4) Time between pulses shall be 5 s or greater to allow damping of oscillation and thus avoid amplitude buildup due to successive pulsing.

3. Integration

The type approval test review committee has accepted *Surveyor V* and subsequent compartments A and B for flight. Approval was based on the test programs the compartments were subjected to and previously approved *Surveyor IV* compartment A and B designs.

Improper handling during service of the SC-7 compartment A was initially thought to have imparted excessive stress into the compartments upper structural members. Followup stress analysis and X-rays established that the structural integrity of the compartment had not been affected and the compartment met flight qualification requirements.

HAC specification 286544 spacecraft structural and electrical integrity verification procedure has been generated and released. This verification procedure serves the purpose of subjecting each spacecraft to a final examination of structure and wiring harnesses by senior cognizant engineering personnel to ensure against mechanical or electrical discrepancies and/or oversights. This is a parallel and redundant inspection recommended by the *Surveyor IV* failure review team. Section A of the procedure was implemented on SC-6. Section B will be accomplished at the end of the report period. Several rivets were found suspect by X-ray during section A inspection, but were approved by analysis and results of previous test programs on similar rivet conditions.

During the pin retention test performed on SC-7, a broken insert in the klystron power supply modulator 38P1 connector was found. An investigation showed a 0.005 interference between insert cavities and contact socket. This is a vendor design problem and is being remedied. An engineering change authorization has been approved to install a washer between the insert halves whenever a subsequent unmating of any connectors reveal this discrepancy.

Engineering was released to upgrade existing compartments A and B and landing gear leg three spares category SP-1 and -2 to be compatible with SC-6 and -7 configurations.

4. Manufacturing

The last report, covering the period of mid-June through mid-August, made known the alternate plans then under study to overcome the A/SPP taper pin disengagement problem. Plan 1, removal of lubricants and application of alodine to the pins and mating surfaces, was selected. This decision lifted a stop order and permitted manufacturing effort to resume on the balance of flight and test pin pullers (SC-6, -7, and spares).

Attaching screws were removed from all A/SPP drive units and replaced with safety wired drilled-head screws.

The SC-6 A/SPP was removed from the vehicle. The solar axis drive was removed from the A/SPP and was checked for end-play of the output shaft; A/SPP potentiometer mounting screw was checked and torqued; pin retention tests were performed; the drive was stall-torque tested; and a flight acceptance test preassurance test, a postassurance test, and a single-axis vibration test were performed. The A/SPP was then returned to the vehicle.

5. Launch Vehicle Integration[4]

a. Completed Surveyor missions. *Surveyors III, IV,* and *V* (missions C, D and E) were successfully launched from Cape Kennedy, Florida April 17, July 14, and September 8, 1967, respectively.

After arrival at the Air Force Eastern Test Range (AFETR) April 13, 1967, *Surveyor III* proceeded through inspection, assembly and preparation for joint compatibility testing with the AC-12 launch vehicle on launch pad 36B. The joint flight acceptance composite test (J-FACT) was performed March 7, 1967. This test includes a simulation of launch events through spacecraft separation and *Centaur* retromaneuver. Spacecraft separation is simulated by manually disconnecting the *Surveyor/Centaur* field joint electrical connector.

During the securing operations after J-FACT, the spacecraft main power bus was momentarily shorted to ground while attempting to remate the connector. To avoid possible damage to the spacecraft, by remating the connector, the spacecraft was demated from the *Centaur* and the RF system calibration test was rescheduled for completion after final mate. As a result of this accidental shorting of the electrical connector a spacecraft/launch vehicle power isolation box was designed and assembled for use during future joint tests both at combined systems

[4]Prepared by JPL Technical Section 291.

test stand (CSTS) in San Diego and at AFETR. Appropriate call-outs have been added to test procedures for operating switches on the box for turning spacecraft power off and on to preclude accidental shorting of the connector during demating and remating operations.

The launch April 17 was delayed 51 min due to a spacecraft problem. It is a notable achievement that the launch vehicle developed no problems during the countdown and was able to hold an extra 51 min with all cryogenics aboard. The *Atlas/Centaur* AC-12 vehicle performance was very satisfactory, providing injection into the desired parking orbit followed by successful *Centaur* restart and accurate injection of the *Surveyor III* spacecraft into the prescribed lunar transfer trajectory which would have resulted in an uncorrected impact of only 466 km from the prelaunch target point. The spacecraft/*Centaur* separation rate of approximately 1 ft/s and the net spacecraft angular rate of 0.56 deg/s was well within the requirements.

Surveyor IV was shipped to the CSTS April 13 and participated in a CST with its booster, SC-11, April 20, 1967. Only minor problems were encountered and the spacecraft was airshipped to AFETR, arriving April 24, 1967. The *Atlas* and *Centaur* were also airlifted to AFETR where the two stages were erected on launch pad 36A May 3 and 6, 1967, respectively.

The *Surveyor IV*/AC-11 J-FACT was performed satisfactorily June 2, including a launch vehicle electromechanical interference test (EMI) between T −120 and T −55 min in the J-FACT countdown. The purpose of the EMI test is to verify spacecraft electrical compatibility with the launch complex and vehicle propellant storage and handling systems in lieu of a cryogenic tanking operation. On-pad calibration of the spacecraft RF system with the service tower in the launch position (removed) and replaced was performed after the J-FACT and prior to demate.

The *Surveyor IV* launch was postponed 1 day in order to tighten and properly ground a loose propellant utilization system connector at the top of the *Centaur* hydrogen tank. The spacecraft was demated, suspended in the service tower while the corrective action was accomplished, then remated and the interface revalidated. The launch on July 13 was delayed 29 s in order to complete liquid hydrogen topping.

All launch vehicle systems performed satisfactorily throughout the power phase of flight; and via direct ascent (one *Centaur* thrust phase), the spacecraft was accurately injected into a lunar transfer trajectory which would have resulted in an impact approximately 176 km from the original target point.

The spacecraft gyro data indicated the following maximum angular rates at separation (deg/s): pitch, −0.42; yaw, +0.16; roll, 0.0. Tip-off rates well within the specification limit of 3.0 deg/s were confirmed by *Centaur* data which indicated virtually simultaneous extension of the three separation springs. Anomalous transients of up to 8 *g* peak-to-peak were discovered in the accelerometer data recorded during the boost phase of flight. The three accelerometers which recorded these transients were located at the column base of each landing leg and recorded on interrange instrumentation group channels 14 and 17.

These transients had relatively large amplitudes compared to anomalous transients recorded from previous flights; and since *Surveyor IV* signal was lost during terminal descent, an intensive investigation to determine the origin of the transients was undertaken by JPL, Lewis Research Center, HAC, and General Dynamics/Convair. It was concluded that the transient shocks were most likely produced by straining or stress relief in the launch vehicle resulting from stresses caused by thermal and dynamic loading; and further, that the effect on the spacecraft was of little importance, since the induced loads are less than normal flight event transients, such as those occurring at *Centaur* insulation panel jettison and *Atlas/Centaur* separation.

The *Surveyor V* mission was the first *Atlas/Centaur* flight to use the new SLV-3C *Atlas*, which has a 51-in. longer tank section and increased thrust, compared to the LV-3C *Atlas* previously used. Spacecraft/launch vehicle compatibility was verified by a CST in the test facility at San Diego June 23, 1967. The space vehicle was then shipped by air to AFETR with the spacecraft arriving June 28, 1967, the *Atlas* on June 30, and the *Centaur* on July 3, 1967.

Mechanical fit, operational tests, and procedure checkout of the alpha scattering experiment dry nitrogen purge system were performed during the CST period. (The alpha scattering experiment was part of the payload for *Surveyor V*.)

The *Atlas* was erected on launch pad 36B July 3 followed by erection of the *Centaur* July 6, 1967; and all systems were prepared for the J-FACT, which was successfully run July 31. Only a minor spacecraft air conditioning problem occurred during the J-FACT and no

spacecraft anomalies were observed during the EMI portion of the test.

On-pad calibration of the spacecraft receivers, with the service tower in place, was performed immediately after the J-FACT. The portion of the receiver calibration with the service tower removed was rescheduled for accomplishment after final mating, due to an electrical storm and a problem with the service tower drive system.

The launch on September 8 was delayed 18 min in order to investigate a launcher stabilization problem and a spacecraft receiver signal strength anomaly.

All vehicle systems performed satisfactorily throughout the powered phases of flight and during a parking orbit of 402.5 sec. The spacecraft was injected into a near perfect lunar transfer trajectory which would have resulted in an uncorrected impact only 45.9 km from the prelaunch target point. Extension of the three spacecraft separation springs was normal and nearly identical producing a separation rate of approximately 1 ft/s. The spacecraft angular rates resulting from the separation event were small and well within the specified maximum acceptable rate of 3.0 deg/s.

b. Surveyor mission F (AC-14/SC-6). Problems associated with the testing of SC-6 at HAC delayed shipment until September 4, 1967, and precluded cycling the spacecraft through a CST at San Diego with AC-14. The spacecraft was shipped, therefore, directly to AFETR. The *Atlas* and *Centaur* arrived by air August 26 and 31, respectively. The *Atlas* and *Centaur* were erected on launch pad 36B September 11—the third day after the launch of *Surveyor V* from the same pad. Replacement of pad burn-off items vehicle checkout, and preparation for the J-FACT progressed concurrently and SC-6 was mated to the *Centaur* September 27, 1967.

The J-FACT and demate of the spacecraft was conducted September 29. The 21-day time span between the launch of *Surveyor V* and the AC-14/SC-6 J-FACT represents a significant reduction in the planning estimates of pad turn-around time and overcame a severe schedule risk. No spacecraft/launch vehicle anomalies occurred during the J-FACT, and the space vehicle is presently proceeding toward its scheduled launch November 7, 1967.

As a result of difficulties in correlating spacecraft receiver calibration data between that obtained during the J-FACT and after final mate, it has been decided to run the entire calibration after final mate for mission G.

c. Surveyor mission G (AC-15/SC-7). *Surveyor* spacecraft SC-7 is presently scheduled to be shipped directly to AFETR November 5, 1967, by-passing a CST at San Diego because of the tight schedule. J-FACT is planned for November 29 and final mate December 31, 1967.

d. Launch pad modifications. Extensive mechanical and electrical modification of the CSTS and launch pads 36A and B were required in order to accommodate the SLV-3C *Atlas*. Modifications to the CSTS began April 24, 1967 immediately after the departure of *Surveyor IV* and its booster AC-11. Alterations to pad 36B began immediately after the launch of *Surveyor III* and those to pad 36A were initiated subsequent to the launch of *Surveyor IV*. Changes in launch pad configuration included replacement of the launcher system, relocation of service tower levels, changes in the launch control, and fueling systems and checkout of the entire complex. The scheduling of *Surveyor* launches on 2-mo centers required pad modifications and erected vehicle checkout to be run concurrently.

e. Spacecraft launch vehicle interface. Beginning with *Surveyor III*, a dry nitrogen purge system was installed for purging the spacecraft vernier engine thrust chamber assemblies after encapsulation, in order to ensure a dry atmosphere and prevent salts forming as a result of any propellant seepage. The plugs and tubing forming the onboard portion of the system are removed at T −175 min in the countdown shortly before the service tower is removed. A procedure has been developed and tested for reinitiation of the nitrogen purge in the event of a delay in a launch of 24 h or more.

Modifications of the payload envelope, indicated by an analysis of possible rotational motions of the nose fairing during jettison have been approved and incorporated on the interface control drawing, JPL 142800. These changes also result in the *Mariner* Mars 1969 and *Surveyor* dynamic clearance envelopes being nearly identical. (*Mariner* Mars 1969 will use the same nose fairing as *Surveyor*.)

Change A to the *Surveyor/Centaur* Interface Control Drawing, JPL 142800, was released September 27, 1967. Changes and additions from the previous issue included numerous pin reallocations, and the addition of extra spacecraft battery charge and sensing lines between the HAC launch control rack and the umbilical tower upper J-box at both launch complex 36A and 36B. This wiring,

installed in time for the AC-11/SC-4 J-FACT, proved to be an acceptable solution to a spacecraft ground power oscillation problem which had hindered on-pad testing.

Revision three of *Surveyor* Project Document 1, Spacecraft/Launch Vehicle Interface Requirements, is in the publication cycle.

H. Payload

1. Soil Mechanics/Surface Sampler Subsystem

a. Introduction. The soil mechanics/surface sampler (SM/SS) subsystem is that part of the *Surveyor III, IV* and SC-7 payload designed to manipulate a portion of the lunar surface near the spacecraft. The subsystem consists of a mechanism, auxiliary electronics and thermal compartment, installation substructure, and wiring harnesses. The mechanism performing operations on the lunar surface is controlled by the auxiliary electronics housed in its own thermal compartment. The auxiliary electronics receives and decodes ground commands, and provides power and signal conditioning for the SM/SS subsystem.

In compliance with a JPL change order, work is in process to add the SM/SS to SC-7.

b. SM/SS payload systems integration. Progress continued during the report period in the integration and testing of the SM/SS experiment subsystem on SC-7.

Electromagnetic interference tests. Electromagnetic interference testing was conducted on SC-7 to determine how the alpha scattering experiment is affected by the operation of the SM/SS experiment. The tests showed that the SM/SS could be operated without affecting the alpha scattering experiment data. During turn-on or -off of the SM/SS, however, the transmitter carrier is shifted, thus requiring retuning of the receiver to the new frequency. Therefore, during turn-on or -off of the SM/SS and the receiver retuning, the alpha scattering experiment data analyzer must be switched off. However, it is unlikely that simultaneous operation will be necessary during actual lunar operations.

Solar thermal vacuum tests. Tests were conducted on the SM/SS experiment on SC-7 during posttouchdown operations of phase B in the solar thermal vacuum (STV) test. Stowage of the instrument was safely accomplished manually after lowering of the end-bell. The decision to repeat phase B prior to reapplication of spacecraft power to the SM/SS required this deviation from normal procedures.

c. SM/SS engineering. Selection of the pickup device for the alpha scattering sensor head was based on extensive tests conducted during this and the preceding report period. The device chosen provides reliable redeployment of the sensor head over the largest area within the operational range of the SM/SS mechanism. This device, shown in Fig. 6, was installed on the alpha scattering sensor head.

d. SM/SS support analysis. The equations that relate the survey camera (TV-3) coordinates with the viewing field at the nominal lunar surface were generated. These equations were solved and results were plotted over the operational area of the SM/SS mechanism. The results of this analysis are given in Fig. 7.

2. Alpha Scattering Experiment Subsystem

a. Introduction. The alpha scattering experiment has been added to SC-6 and -7 for the purpose of analyzing the composition of the lunar surface materials. The presence of all elements, except hydrogen, helium, lithium, and beryllium is detected by irradiating the surface with

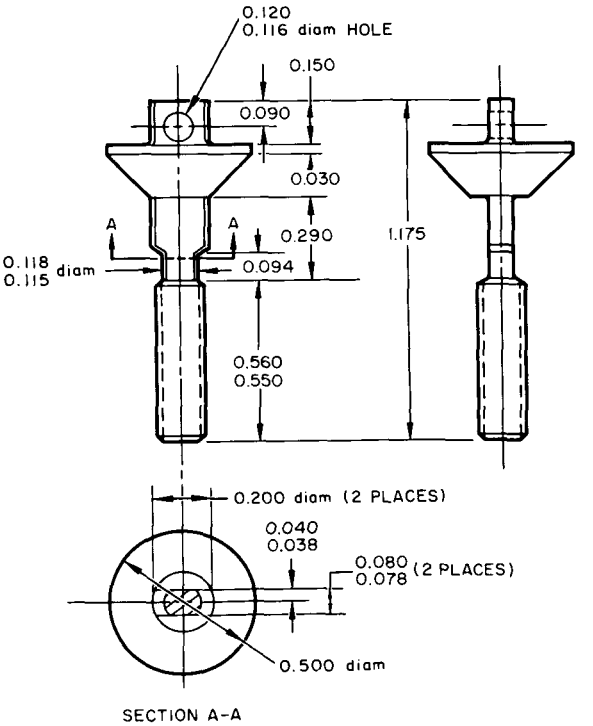

Fig. 6. Eye bolt, sensor head pickup

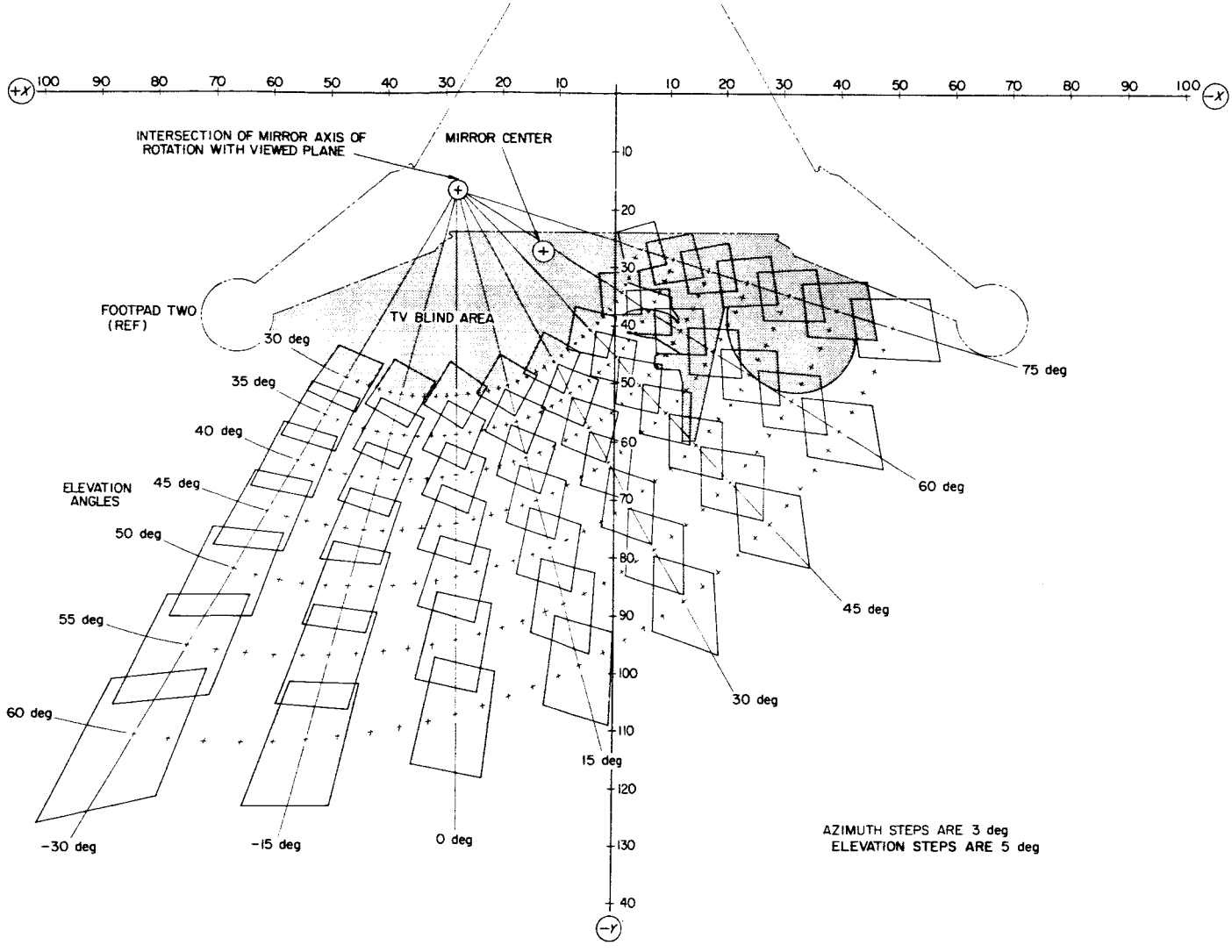

Fig. 7. Partial TV viewing field at nominal lunar surface

6 MeV alpha particles and measuring the return energies and relative quantities of backward scattered alpha and proton particles.

The Government-furnished alpha scattering instrument consists of a sensor head, electronics, and standard sample. Equipment supplied by HAC consists of an auxiliary, compartment C with heater, and deployment mechanism to provide mechanical and electrical interface of the alpha scattering instrument with the *Surveyor* basic bus and for the deployment of the sensor head to the background and lunar surface positions.

The experiment is operated in three positions:

(1) Stowed position utilizing the standard sample for calibration of the system.

(2) Background position for calibration of the solar and surface natural radiation.

(3) Lunar surface position for lunar surface compositional analysis.

b. Alpha scattering experiment. Operation of the alpha scattering experiment on *Surveyor* V was completely successful with over 90 h of lunar surface analysis being accomplished. A brief summary of the operation of the experiment is presented in Table 2. Figure 8 is an early photograph of the sensor head on the lunar surface.

During the flight and operations of the instrument, the essential telemetering data remained within predicted limits except for the sensor head, which ran slightly

Table 2. Alpha-scattering operations on *Surveyor V*

September	Time, h:min	Operation
8	00:57	Launch
8	10:47	Compartment C heater on
8	11:39	Compartment C heater off
9	01:49	Compartment C heater on
9	03:39	Alpha scattering power on, 10 min standard sample operation plus calibration
9	04:28	Alpha scattering power off
9	04:28	Compartment C heater off
10	10:43	Compartment C heater on
10	13:29	Sensor head heater on
10	17:39	Compartment C heater off
10	17:39	Sensor head heater off
10	17:47	Touchdown
10	17:57	Compartment C heater on
10	17:59	Sensor head heater on
11	00:30	Alpha scattering power on. Calibration and 60-min standard sample count
11	03:35	Stowed position operation complete
11	05:15	Sensor head deployed to background position. 160-min background position operation
11	08:36	Sensor head deployed to surface position. 340-min surface position count plus calibration
11	14:56	Initial surface position operation complete
11	23:18	Continue surface position operation. 730-min surface position count plus calibration
12	15:27	Alpha scattering power off
12	22:38	Vernier engines refire
13	01:45	Alpha scattering power on. 550-min surface position count plus calibration
13	13:37	Alpha scattering power off
13	15:47	Alpha scattering power on. 65-min surface position count plus calibration
13	17:16	Alpha scattering analyze off
14	02:00	Alpha scattering analyze on. Special background check
14	02:55	Alpha scattering analyze off
16	11:44	Alpha scattering analyze on. 700-min surface position operation plus calibration
16	16:45	Sensor head heater on due to shading by solar panel
17	13:55	Alpha scattering analyze off
18	01:22	Alpha scattering analyze on. Special background check
18	01:53	Alpha scattering analyze off
18	08:58	Alpha scattering analyze on. 475-min surface position operation plus calibration
18	19:31	Alpha scattering analyze off
19	01:07	Alpha scattering analyze on. 2500-min surface position operation plus calibration
23	10:52	Alpha scattering operations complete

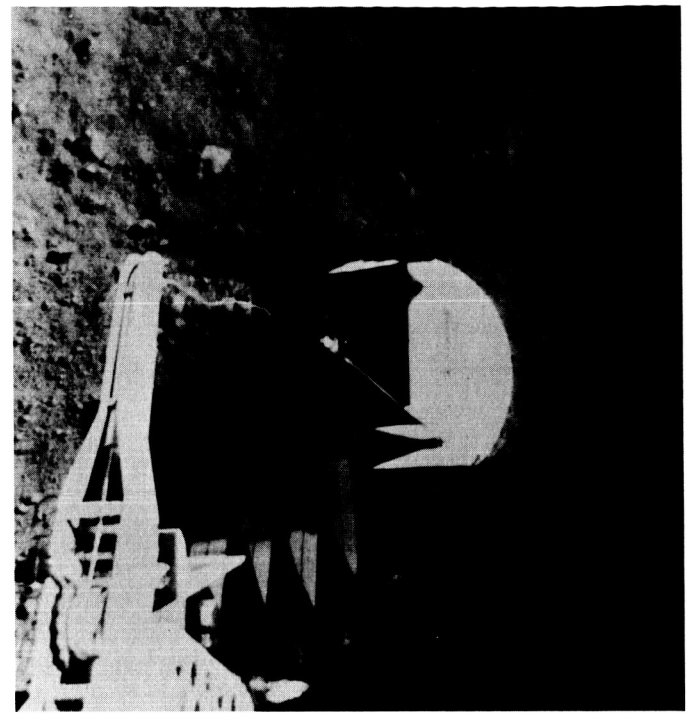

Fig. 8. Alpha scattering head on lunar surface

above the maximum desired operating temperature limit for a short period of time near lunar noon. However, the data were not affected and the detectors remained operable at all times. The guard event monitor, which measures the high energy background radiation, remained approximately near 100 MV, indicating a radiation level about four times as large as that on earth. The +7 and +24 V monitors remained essentially constant throughout all operations.

A second sample of the lunar surface was taken as a result of the vernier engine reburn. The pressure of the expelled gases moved the sensor head approximately 5 in. from the original position. The new position of the sensor head is shown in Fig. 9.

The data taken on the surface indicate the composition of the surface of the moon is similar to basalt, which is found in large areas of the earth. Although the most common elements are oxygen and silicon, some trace of iron was detected.

c. Alpha scattering experiment payload integration. Significant progress has been accomplished during this report period in conducting experiment integration and tests on *Surveyor V*, SC-6, and -7.

Fig. 9. Alpha scattering sensor head repositioned on lunar surface

Surveyor V. The P-4 alpha scattering instrument on *Surveyor V* progressed through the following phases of system tests and preparation for flight:

(1) At the conclusion of the *Surveyor/Centaur* matchmate tests at the Air Force Eastern Test Range (AFETR), which occurred in the preceding report period, the alpha scattering instrument sensor was removed from the spacecraft and special tests were conducted on it to determine if it had been affected during the X-raying of the spacecraft. The sensor was checked in several modes of operation and was found to be operating correctly. During subsequent X-ray operations, the sensor was not installed in order to preclude any possible damage.

(2) After completion of the test to determine the effects of X-ray exposure, the flight sources, Cm^{242}, were installed in the sensor and extensive calibration tests were performed. The sensor was then reinstalled on *Surveyor V*, utilizing the continuous dry nitrogen purging procedure.

(3) A 5-h integration and checkout test was performed on the alpha scattering subsystem after the sensor was reinstalled on the spacecraft. All tests were successful, indicating that the alpha scattering subsystem was flight-ready.

(4) Three subsequent system readiness tests were performed on the spacecraft. The alpha scattering subsystem operation was completely normal.

SC-6. The alpha scattering subsystem on SC-6 has progressed through the following phases of systems tests and preparation for flight:

(1) Vibration

(2) Shipment to AFETR

(3) Performance verification test/systems readiness test (SRT)-A

(4) Encapsulation SRT

(5) Launch pad SRT

(6) Removal of the sensor for installation of flight sources

During postvibration testing of the alpha scattering subsystem, abnormal noise events appeared in the proton spectrum over a 4-min period of operating time. The noise events were the result of a temporary breakdown of one of the proton detectors. Special tests, as reported elsewhere in this article, were conducted on the sensor. The trouble has not recurred during 27 h of subsequent sensor operations, and no corrective action will be taken, as it is believed that the detector breakdown no longer exists.

On several occasions during systems testing, the instrument +7-V power supply has indicated intermittent instability. This instability caused voltage variations which are well within the specified operating limits. No corrective action is required at this time; however, the +7-V monitor will be watched closely throughout the remainder of the testing to assure that the instability does not become progressively worse.

SC-7. Alpha scattering subsystem testing on SC-7 has progressed through the following phases of system tests and preparation for flight:

(1) Mission sequence, run one.

(2) Mission sequence, run two.

(3) Mission sequence, run three.

(4) STV dry run.

(5) STV phases A and B.

During mission sequence three, an alpha scattering SM/SS EMI compatibility test was performed. Operation of the SM/SS did not cause interference in the alpha scattering subsystem. It was determined, however, that when preparing to go into a SM/SS mode of operation when the alpha scattering instrument is operating, it is necessary to stop alpha scattering data accumulation during the period required to reestablish down-link lock when lock is lost due to switching on and off of the SM/SS experiment. All SC-7 tests involving the alpha scattering subsystem have been successful, and the subsystem is operating properly.

3. Television Engineering

The SC-6 and -7 cameras have been retrofitted with vidicon tubes previously survival tested to −310°F. The second spare camera is undergoing retrofit to reduce the video amplifier gain to prevent over-deviation of the transmitter.

During flight acceptance test of the serial number 13 camera, an approximate 1 kHz sinusoidal noise was observed when the camera was tapped or disturbed, such as occurs when a mechanical function is activated several times in succession. This same anomaly was repeatable in several other cameras and spare vidicon tubes.

The problem was found to be capacitive coupling from the G5 mesh (+300 V) to the target (+12 V) within the vidicon tube. As the tube is tapped, the mesh vibrates sinusoidally at an approximate rate of 1 kHz, thus varying the capacitance between G5 and the target. The resultant signal is amplified approximately 1200 times in the 200-line mode (only 200 times in the 600-line mode) and appears as periodic noise in the video. The time for damping of the mesh can be 10 to 12 s.

This noise should not affect the picture quality of the camera since it is noticeable in the 200-line mode only and appears only when some mechanical function is actuated several times in succession. It may represent an operational constraint, and this aspect of the problem is being investigated in the systems area.

Although the noise resulting from this problem has somewhat different characteristics than that reported on the *Surveyor V* camera, it is likely that the *Surveyor V* reported problem is the result of the same G5 capacitive coupling to the target as reported here.

I. Deep Space Network Test, Operations, and Training

This subsection includes all activities associated with the test, maintenance, operations, and Deep Space Network (DSN) personnel training related to hardware peculiar to *Surveyor*. Primary activities relate to the operation and maintenance of HAC-supplied, mission-dependent equipment at the deep space stations (DSS) and to the on-site mission control function.

Mission E operations. Station command and data handling console (CDC) personnel supported *Surveyor* mission E at DSS 11 (Goldstone), DSS 42 (Canberra-Tidbinbilla), DSS 51 (Johannesburg), DSS 61 (Madrid), DSS 71 (Cape Kennedy), and DSS 72 (Ascension Island). Liftoff occurred at 00:39 PDT on September 8.

A nominal midcourse thrusting operation at 18:44 PDT was performed on September 8. Successful touchdown was accomplished at 17:46 PDT on September 10, approximately 16 mi from the original aiming point.

Surveyor V was responsive to approximately 114,000 commands throughout the lunar day, which ended September 16.

The total number of TV pictures taken was 18,006. Extensive use was made of the alpha scattering equipment which accumulated over 83 h of data. Engineering interrogations were performed into the lunar night until critical temperature cutoff levels were reached. The spacecraft was then shut down with all indications that a revival would be possible during the next lunar day.

DSS 11. During the mission, Goldstone provided support for 19 passes, including midcourse maneuver, terminal descent, and lunar day and night operations.

DSS 42. Canberra provided support for 19 passes, including nonstandard midcourse thrusting and commanding for the first 600-line TV pictures.

DSS 51. Johannesburg provided support for three passes, including initial acquisition operations. The station had a limited commitment for this mission but performed a more active part than anticipated.

DSS 61. Madrid provided support for 19 passes, including star acquisition for the first pass.

DSS 71. Cape Kennedy support for this mission consisted of a deep space instrumentation facility (DSIF) spacecraft compatibility test; an operational readiness test; a prelaunch countdown phase; and a postlaunch phase, lasting through the first 40 min of the flight.

DSS 72. Ascension Island provided support for two passes as backup to DSS 51.

Modification kit installations. Eighteen modifications were completed at DSS 11, 42, and 51, and nineteen modifications at DSS 61, 71, and 72. Modifications included those that satisfy the ground rule of keeping all DSIF CDC units as interchangeable as practicable. These modification kits were installed between August 1 and October 1, 1967.

Maintenance and operations transfer. Updated open item sheets (list 11) were issued monthly to document progress on closure of all remaining items.

Command data console patchboard/overlay control. New overlay scales required for mission F are in work. Revision H of CDC decommutator patchboard/telemetry overlay control specification 3023300 was prepared and completed prior to mission E. This revision incorporated changes to spacecraft data channel assignment specification 3023920.

Development tests. The following development test request bulletins (DTRB) were issued during the report period.

(1) DTRB 26—"Interface Signal Levels." This test to be completed after the first *Surveyor V* lunar day by Goldstone.

(2) DTRB 27—"Interface Signal Levels." This test, to be performed by DSS 42 and 51, has not yet been received from JPL.

(3) DTRB 28—"Interface Signal Levels." To be completed at DSS 61, 71, and 72 by October 16, 1967.

Deep space instrumentation facility detailed operating procedures. Required mission E changes to the DSIF detailed operating procedures (DOPs) have been or are in the process of being implemented.

Personnel deployment. Reassignments of station personnel are taking place in preparation for *Surveyor V* second lunar day and mission F.

Surveyor operations chief handbook. Revision D of SSD 68089R, "*Surveyor* Operations Chief Operational Aids Handbook," was completed and distributed for use in mission E. Change pages reflecting corrections and updates for mission F are in preparation.

Deep space net training. Training of DSN personnel for their assumption of CDC maintenance and operations responsibility by HAC was completed, and HAC maintenance and operations personnel returned from the stations. However, with the exception of DSS 42, maintenance and operations responsibility remains with the HAC resident manager.

New work—CDC 10/12 add-on equipment (modification 83). All modification 83 equipment was received at DSS 72 and DSS 61 and was successfully checked out prior to mission E, closing out all action on this "new work" item.

J. Mission Operations Support Equipment

1. Introduction

This work item covers the engineering support of all command and data handling consoles (CDC) and related hardware used in the Deep Space Network (DSN) and of the system test equipment assemblies (STEA).

2. Trouble and Failure Reports

A review of trouble and failure report (TFR) statistics for this period reveals the following:

(1) Sixty new TFRs were received during this 2-mo period, bringing the total to 2735.

(2) Operational support equipment engineering action completed 111 TFRs, leaving 29 to be completed. Engineering completions to date total 2706.

(3) One hundred sixty-one TFRs were closed out during this period by project reliability, leaving 41 to be closed. A total of 2694 TFRs have been closed by project reliability to date.

One new TFR was classified as critical and closed during this period. No CDC critical TFRs remain in the system at this time.

3. Modification Kit, Engineering Change Request and Engineering Change Order Status

Detailed status on specific engineering change requests (ECRs) and engineering change authorizations (ECAs) is

given in the *Surveyor* Project management plan, HAC document 3023333 and in the engineering change management report, both updated monthly.

a. Modification kits. Nineteen CDC modification kits were assembled, shipped, installed, and checked out at the deep space stations prior to mission E. Five kits have been shipped for mission F, making a total of six on site. The sixth kit was on-site for mission E use, but was not approved, and it is not expected to be approved for future missions.

b. Engineering change request and change authorizations. The average ECR and ECA work loads have declined to about 16 and 1 per month, respectively.

4. Operation and Maintenance Manual Upgrade

Interim Data Sheets (IDS) 86 and 87 and formal change notices (FCNs) 14 through 19 were prepared and distributed during the report period.

5. New Work — Alpha Scattering

The alpha scattering CDC equipment was satisfactorily checked out before mission E and performed as designed. Several modifications were added to the basic 133360 installation, the most significant being provision of switchable patch boards for simplifying alpha scattering equipment test and checkout. One of the units shipped for mission F will eliminate amplifier crosstalk in the bit synchronizer equipment.

6. Command Data Console System Test Equipment Assembly Configuration Accounting

Formal release of the equipment indexes ("as-is") for all STEA CDCs was accomplished during the report period. Audits of these indexes are being made utilizing quality assurance records to verify the "as-is" information submitted. Discrepancies will be noted for reconciliation in preparation for STEA CDC selloff.

7. Program Phase-Out

A review of preparation for *Surveyor* program phase-out is being conducted and preliminary steps are being taken to dispose of *Surveyor* property, both contract deliverable and nondeliverable items. Residual property consisting of developmental hardware, unfinished subassemblies and modules, raw stock (such as capacitors, diodes, resistors, and transistors, as well as nut and bolt hardware items) is being transferred to support equipment logistics for appropriate disposition action.

K. AFETR Base Support

Following successful completion of performance verification test 5 (PVT-5) *Surveyor V* was returned to the explosive safe facility (ESF) for fuel loading and final flight preparations. The spacecraft was encapsulated for flight on August 30, 1967 and mated to the *Centaur* launch vehicle September 1. All prelaunch testing proceeded as scheduled, and the spacecraft was successfully launched September 8.

Upon the arrival of SC-6 at the Air Force Eastern Test Range (AFETR), initial performance verification testing was completed. The spacecraft was prepared for the joint flight acceptance composite test (J-FACT), encapsulated, and mated to the launch vehicle (A/C-14) at launch complex 36B. Onstand testing was accomplished as scheduled, and the spacecraft was returned to the spacecraft checkout facility (SCF) where PVT-5 was performed.

The majority of the AFETR base support effort was directed toward *Surveyor V* and SC-6 launch operations. System test equipment assembly and other aerospace ground equipment support continued as required. Logistics, contamination control, and range and launch vehicle phase engineering continued.

L. Reliability

1. Reliability Engineering

The data-based reliability point estimate for the flight and landing mission is 0.73 for SC-6 and 0.74 for SC-7. These estimates are based upon SC-6 and -7 systems test data and applicable *Surveyor I–V* test and flight experience.

Table 3 summarizes subsystem reliability estimates for the current report period. Figure 10 shows successive data-based reliability estimates for SC-6, the initial SC-7 reliability estimate, and, for comparative purposes, past *Surveyor I–V* reliability estimates.

2. Subcontractor Controls

a. Main battery. Results of an on-site reliability audit performed in May 1967 revealed that considerable deterioration had occurred in implementation of the contractor's reliability program. Deficiencies such as incomplete analysis of critical tests, lack of thoroughness in diagnosis of failures and problems, no reliability approval of engineering changes, and lack of an updated reliability plan were noted. Corrective action has been satisfactorily completed on these deficiencies. Monthly

Table 3. Subsystem reliability estimates for flight and landing mission, SC-6 and -7

Subsystem	Reliability	
	SC-6	SC-7
Telecommunications	0.989	0.990
Vehicle mechanisms	0.854	0.857
Propulsion	0.934	0.934
Electrical power	0.986	0.987
Flight controls	0.938	0.940
Total subsystems	0.730	0.735
Systems interaction reliability factor	1.0	1.0
Spacecraft	0.73	0.74

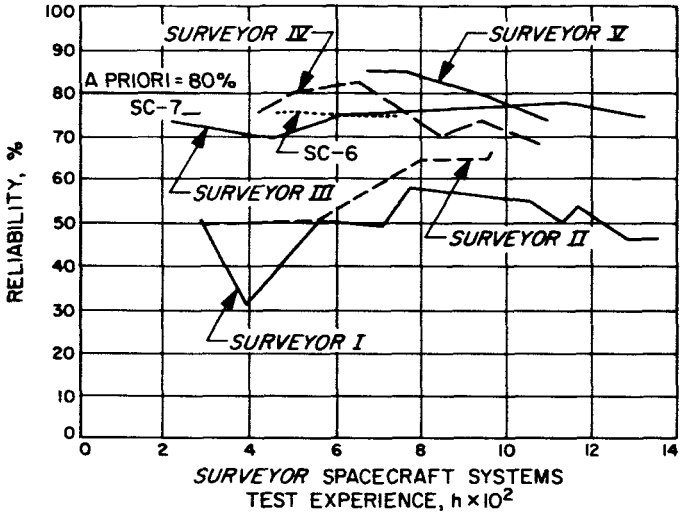

Fig. 10. *Surveyor* reliability estimates—flight and landing mission, September 27, 1967

reliability reports have been upgraded to provide visibility regarding the cause of failures and thoroughness of corrective action.

b. Bladders. Observation of process controls utilized for the manufacture of bladders indicated that satisfactory conditions existed. However, inspection for bladder thickness indicated that measurements were only being made in one diametrical plane. To obtain greater assurance of uniform thickness, it was recommended that measurements be made at 60-deg intervals.

c. Radar altimeter doppler velocity sensor. Evaluation of the trouble and failure report (TFR) and material review record (MRR) system indicated lack of technical followup by reliability personnel. Also, not all troubles or failures were promptly reported. Corrective actions were initiated by project engineering, and dates were established for submittal of complete information.

3. Parts and Materials

A formal failure review board (FRB) was established to investigate five primary failure modes (rotor stoppage, excessive torque, total resistance change, excessive noise, and linearity out of specification) that occurred during qualification tests. Failure review board findings determined the causes of such failures to be reversed bearings, high contact pressure, Kel-F shrinkage, loose slip ring tolerances, debris, slider/housing interference, excessive lubrication, and assembly procedures. The source of such causes were design deficiencies aggravated by extreme temperature and vacuum environments plus handling and assembly techniques.

Examination of performance data indicated that the two most detrimental failure modes (rotor stoppage and excessive torque) could be detected in early use and that sufficient life existed in the worst case to successfully complete a mission. As a result, the FRB concluded that only a minimal risk exists and that such units should be considered acceptable for flight.

4. Trouble and Failure Reports

The TFR count for the report period is given in Table 4.

Table 4. TFR count for report period

Category	Open	Total
Spacecraft mission critical	72	2566
Spacecraft nonmission critical	64	1048
Aerospace ground equipment (AGE)/command data console (CDC)	189	3851
Total	325	7465

Reductions or increases in TFRs from the last report period are given in Table 5.

Table 5. TFR count change

Category	New TFRs	TFRs closed
Spacecraft mission critical	177	196
Spacecraft nonmission critical	44	55
AGE/CDC	227	502
Total	448	753

The blue ribbon group met August 9 through 11 to review open TFRs for *Surveyor V* consent-to-launch and on October 2 through 4 for SC-7 consent-to-ship.

A lost TFR was found which necessitated replacement of several parts in the battery charge regulator on SC-6. As a result, HAC was directed to conduct an audit to determine if there were other lost TFRs that may have required additional action and a B lien was placed on SC-6 for consent-to-launch. A TFR audit was conducted and a report submitted. Twelve TFRs were found, as a result of the audit, and were reviewed and judged to be noncritical. Of the 10,526 controlled TFRs assigned to *Surveyor*, 85 were determined as still lost. Corrective action has been taken to prevent the recurrence of this problem and to help recover the lost TFRs.

5. Quality Assurance[5]

The most significant quality activities that occurred during this report period were directed towards hardware problem investigations and solutions. Some of the more significant activities are described below.

a. SC-4 technical review. Spacecraft inspection practices and procedures were reviewed by quality assurance at the request of the SC-4 technical review board. Improvements resulting from that review are as follows:

(1) The use of an inspection procedure by engineering at specified times during spacecraft operations. Engineering inspection is intended to increase confidence in the spacecraft and is redundant to assembly and quality assurance inspection points.

(2) Modification and amplification of quality assurance inspection points and methods to complement those established for engineering.

After the *Surveyor IV* failure and subsequent investigation by the technical review board, the board recommended that further investigation be conducted with respect to the retroengine. A team composed of JPL, Thiokol Chemical Corporation (TCC), and HAC personnel reviewed records at TCC in their respective specialty areas to determine if the retroengines were being fabricated in a reproducible manner. Static test data, X-rays, process techniques, TFRs, material review boards (MRBs), and pressure vessel design criteria were reviewed in detail.

During the investigations, certain discrepant items were disclosed that could possibly affect the suitability of A21-29 for flight use on SC-6. These items were investigated and conclusions reached, one of which was an extensive investigation in the area of case weld mismatch/and weld quality. The principal element of this investigation was the survey of case manufacturing and performance.

b. Helium regulator review. As part of the in-flight SC-5 helium problem review, a committee comprised of HAC and JPL engineering and quality assurance personnel reviewed the data from *Surveyor V* and the associated quality records. The probable failure of the *Surveyor V* helium regulator, part number 254201-1, serial number (SN) 58, was investigated from the quality assurance standpoint by means of the following:

(1) Review of supplier and HAC quality history and test records, including those of helium tank and spacecraft vernier propulsion system.

(2) Audit of the supplier's facilities to determine adequacy of assembly methods, cleanliness controls, and assembly controls during the manufacture of part number 254201-1 regulators.

(3) Evaluation of HAC facilities, assembly methods, cleanliness control, and assembly controls during assembly of *Surveyor V* and its propulsion subsystem.

A review of the quality records associated with the construction of the *Surveyor V* vernier propulsion system leads to the following conclusions:

(1) The *Surveyor V* helium regulator is functionally identical with the regulators used on *Surveyor I–IV*.

(2) The processes employed in cleaning, flight acceptance testing, assembling, and handling were unchanged on *Surveyor V* and were considered adequate.

(3) No manufacturing test or quality discrepancies were detected in the records or hardware of the helium tank and valve assembly on SC-6, -7, or SP-2.

Recommendations were made and implemented for SC-6 flight checkout at the Air Force Eastern Test Range. These include the following:

(1) The test sequence was modified.

[5]Prepared by JPL Technical Section 151.

(2) Regulator flow and lockup tests were performed last in the vernier propulsion system functional test.

(3) The vernier propulsion system functional test was modified to incorporate millipore analysis following regulator flow test.

(4) The lockup test was extended to 6 h.

(5) Positive procedural changes were implemented to preclude any back flow through the regulator.

No hardware changes were recommended.

Extensive comparative tests performed by Carlton Controls Corporation, including multiple squib firing, regulator function testing and millipore analysis, substantiated the equivalency of the A21 and A21-E regulators and the adequacy of their design and processing specifications.

c. RADVS solder problems. As noted in a previous summary, a special test program was initiated to determine if vibration/temperature exposures affect solder integrity in the dc amplifiers of the signal data converter (SDC). Signal data converter, SN 3, was exposed to the following vibration levels:

(1) 6 g nonoperating 40 to 125 Hz.
2 g nonoperating 125 to 1500 Hz.

(2) 0.002 g^2, white gaussian noise 50 to 1500 Hz.

Examination of the solder joints did not indicate any change resulting from vibration.

The SDC, SN Y1, which has just now completed type approval testing, and its converter boards were utilized to determine temperature affect on solder joints. The temperature exposures were as follows:

(1) + 75°F — unit stabilized.

(2) + 15°F — unit stabilized.

(3) +122°F — unit stabilized.

(4) + 77°F — unit stabilized.

(5) − 45°C — cold soak for 4 h.

Since this special test has just been concluded, a thorough review and analysis of the results has been completed by a special team, familiar with the previous proceedings.

Inspection of the Y1 system revealed a major failure mode and a serious potential failure mode. It was also noted that a process fabrication change was included in these units—a reduction in amount of bonding material used to hold cordwood module to the circuit board.

The nature of the failure encountered involved dc amplifier units which are encapsulated, and very heavy as compared to others. Observed failure showed evidence of broken bonding between dc amplifier modules and circuit cards at the fiber washers. Additionally, through wires joining dc amplifiers to the circuit boards were torn loose and pulled part way through the solder joints. Extensive fracturing of the solder was also noted in the dc amplifiers themselves. This condition was observed on circuit board number 500619-G1 SN 01113 and one other. At the time of this inspection another card removed from the SDC SN 6 subsystem was brought in for failure analysis. This board exhibited the same characteristics as the above noted. This board was subsequently found to have been removed from system Y2. It was installed in the SN 5 system to replace a faulty board. In both cases, extensive rework will be necessary; probably involving removal of the dc amplifier from the circuit card. The SN 5 SDC failure is documented on TFR 65363. This subsystem is designated as spare 1 for SC-6 and SC-7.

In both cases these failures occurred following vibration. The units did not actually fail in vibration, but became noisy in subsequent bench tests. All of these boards are, or could become flight units, as there is very little difference between flight acceptance and type approval testing on the SDC.

d. Spacecraft inspection procedure. Specification 286544 Spacecraft Structural and Electrical Integrity Verification Procedure has been generated and released. This verification procedure serves the purpose of subjecting each spacecraft to a final examination of structure and wiring harnesses by senior cognizant engineering personnel to ensure against mechanical or electrical discrepancies and/or oversights. This is a parallel and redundant inspection recommended by the *Surveyor IV* failure review team. Section A of the procedure was implemented on SC-6 on September 6, 1967. Section B will be accomplished at the end of the report period. Several rivets were found suspect by X-ray during Section A inspection, but were approved by analysis and results of previous test programs on similar rivet conditions.

e. Connector pin design deficiency. During the pin retention test performed on SC-7, a broken insert in the klystron power supply modulator 38P1 connector was found. An investigation showed a 0.005 in. interference between insert cavities and contact socket. This is a vendor design problem and is being remedied. An engineering change authorization has been approved to install a washer between the insert halves whenever

a subsequent unmating of any connectors reveal this discrepancy.

f. JPL Surveyor QA status report. The JPL *Surveyor* QA monthly status report was issued for the last time due to the decline in hardware manufacture and the resultant change in emphasis towards spacecraft testing activities.

M. Spaceflight Operations

This subsection concerns spaceflight operations project engineering, spaceflight planning and documentation, spaceflight operations systems design, and spaceflight operations rehearsals, flight, and lunar operations. The primary activity covered by this work item is in the spacecraft performance analysis and command (SPAC) function. Effort during the report period consisted mainly of the following:

(1) Support of mission E operations at the space flight operations facility (SFOF) at JPL.

(2) Preparation of mission E spaceflight operations reports and inputs to the *Surveyor* final report.

(3) Premission E and F planning activities and preparation of supporting documentation.

(4) Participation in SFOF tests for missions E and F.

1. Mission Operations

The following is abstracted from the SPAC director's section of mission E spaceflight operations report.

This discussion presents a comprehensive report of SPAC activities, including real-time analysis and decisions, and includes a summary of spacecraft performance as determined during conduct of the mission. In addition, significant operational capabilities demonstrated and problem areas encountered are summarized.

Under the direction of project management and the trend and failure analysis (T&FA) group of SPAC, a nonstandard terminal descent timing sequence was generated. Over a period of some 47 h, the task force performed: (1) extensive subsystem and system analysis in the spacecraft performance analysis area of the SFOF in Pasadena, (2) extensive flow tests on the complete propulsion system on a spaceframe at the Hughes Placerita test facilities, (3) thrust chamber assembly flow tests at JPL, Edwards test station, (4) terminal descent timing sequences on SC-6 at Cape Kennedy, and (5) extensive simulation runs on the flight control analog simulator at HAC facilities. The resulting nonstandard terminal sequence was successfully implemented.

The flight of *Surveyor V* starting from launch pad 36B at Cape Kennedy and culminating in a soft landing in a crater in the Sea of Tranquility on the moon, was accomplished between the morning of September 8 and the night of September 10, 1967. The landing, characterized by leg 1 striking the lunar surface first, followed by legs 2 and 3 striking nearly together, was so gentle that Goldstone (DSS 11) did not lose phase lock, and the spacecraft shock absorber strain gages indicated a low level of force and a touchdown velocity of some 12 fps. Table 6 is a timetable indicating the times major milestones were accomplished during mission E.

The flight was characterized by the following:

(1) A seemingly critical helium pressure leak.

(2) Demonstration of the usefulness and effectiveness of the SPACE-T&FA group.

(3) Largest volume of specialized SPAC technical tasks beyond normal mission spacecraft monitoring, analyses, and command control requirements yet conducted during an unmanned mission, including the following: six separate midcourse corrections, with the first three conducted in an unprecedented time block of 50 min; an additional 360-deg yaw maneuver intended to more precisely determine the spacecraft rotational rate; an alpha scattering experiment checkout during transit, with attendant telecommunications analyses; intensive redesign of spacecraft command sequences of event for earth orbit as well as lunar soft landing with retroengine burnout at 4500 ft (instead of the nominal 38,000 ft) from the surface of the moon; and additional command sequence design to prepare TV and alpha scattering experiments for use after achievement of earth orbit.

During transit, sun acquisition, solar panel deployment, DSIF acquisition, initial commanding and interrogations, star acquisition and verification, and the midcourse maneuvers were all executed and successfully completed with no difficulties observed until a few moments after midcourse thrusting. At that time, a helium leak was reported by propulsion. The mission was thought to be lost until project management presented three possible terminal descent sequences that might still effect a soft lunar landing. A T&FA subgroup was quickly formed to study the possibilities and select a desired terminal sequence for a soft landing.

Table 6. *Surveyor V* mission milestones

Event	September 1967	Time	
		PDT	After launch
Launch	8	00:57:01	
Injection (end of second burn)	8		
Separation			
Electrical disconnect	8	01:16:20	$00^h19^m19^s$
Mechanical	8	01:16:25	$00^h19^m24^s$
Automatic sun acquisition completed	—	—	—
Spacecraft visibility at Johannesburg station begins		01:25:10	$00^h28^m09^s$
Initial deep space instrumentation facility (DSIF) acquisition (two-way lock) confirmed	8	01:29:00	$00^h31^m59^s$
First ground command sequence initiated	8	01:37:00	$00^h39^m59^s$
Canopus verification started	8	07:10:02	$06^h13^m01^s$
Canopus verification completed	8	07:27:52	$06^h30^m51^s$
First premidcourse attitude maneuver initiated	8	18:32:57	$17^h35^m56^s$
Midcourse thrust executed (14.25 s in $-\dot{U}_3$ direction)	8	18:45:02	$17^h48^m01^s$
Sun reacquired	8	18:55:02	$17^h58^m01^s$
Second engine burn executed (10.05 s along sun line)	8	19:12:02	$18^h15^m01^s$
Third engine burn executed (23.05 s anti-sun line)	8	19:39:51	$18^h42^m50^s$
Fourth engine burn sequence initiated (12 s, 0.5 s, and 0.5 s burns—separated by 1 s intervals)	8	21:18:48	$20^h21^m47^s$
Fifth engine burn sequence	9	01:24:04	$24^h27^m03^s$
Sixth engine burn sequence (final midcourse correction)	9	16:30:58	$39^h33^m57^s$
Canopus reacquired	9	16:46:35	$39^h49^m34^s$
First terminal descent attitude maneuver initiated	10	17:12:15	$64^h15^m14^s$
Retroengine thrust direction properly positioned	10	17:19:24	$64^h22^m23^s$
Altitude marking radar mark generated	10	17:44:40	$64^h47^m39^s$
Vernier engine ignition	10	17:44:52	$64^h47^m51^s$
Retroengine ignition	10	17:44:53	$64^h47^m52^s$
Retroengine separation (initiated by ground command)	10	17:45:38	$64^h48^m37^s$
Radar control initiated (initiated by ground command)	10	17:45:40	$64^h48^m39^s$
Touchdown (based on strain gage recording)	10	17:46:44	$64^h49^m43^s$
First 200-line TV	10	19:00:45	$66^h03^m44^s$
Earth/sun acquisition completed	10	22:29:00	$69^h31^m59^s$
First 600-line TV	10	22:40:00	$69^h42^m59^s$

The performance analysis (PA) group was directed by the SPAC director to design specific command sequences to implement each of the three possible sequences. The PA group also provided two team members to the T&FA subgroup. It soon became clear in PA that one of the three solutions had distinct operational advantages over the other choices. In a meeting with project management, the SPAC director recommended and justified the selection of the most operationally preferred sequence. Project management concurred with the recommended sequence and implementation was begun. Tight coordination was established between all SPAC groups and flight path analysis and command (FPAC), with T&FA being the primary FPAC interface.

It was decided that the desired time between the emergency altitude marking radar (AMR) mark command and the predicted time of AMR mark would be established by FPAC in their computation of the time for sending the emergency AMR mark command, which they normally provide to SPAC.

Provided with the outputs of the T&FA and PA groups, the command preparation group went to work approximately 11 h prior to predicted touchdown. After approval of the terminal maneuvers at 11:25 a.m., the first trial command tape message was formatted on cards and constructed with a *Surveyor* command preparations computer program (SCPS) run interfacing with the FPAC midcourse and terminal guidance system program output. Shortly thereafter, the nonstandard terminal sequence was modified to include the vernier engine high thrust command prior to sending the emergency start programmed thrust command, and the basic timing between commands was also changed. This required reformatting of the SCPS program input cards to ensure

the correct sequence of the actual commands and the correct number of delay characters which would be punched on the tape to maintain the required basic timing.

Within minutes after completing the second trial command tape message, the basic timing between the desired execution of the emergency AMR mark signal command and the execution of the emergency retroengine eject command was reduced by ½ s to 54 s; this required another message to be formatted on cards and constructed with the computer program. A card input error on this third computer run necessitated another run at 1:58 p.m.

The final terminal descent calculations were completed by the FPAC team at 3:37 p.m., about 2 h before touchdown. At that time, the final command tape message was constructed. The command verify/transmit (CVTS) program was run at 3:51 p.m. to prepare the message for teletype transmission to the Goldstone tracking station. The actual transmission of the message took place at 4:00 p.m., and the command tape was punched at the Goldstone facility using the *Surveyor* on-site computer program in conjunction with their on-site data processor. The SPAC check of the Goldstone tape was completed at 4:20 p.m., and the tape was installed on the Goldstone tape reader ready for use only 20 min ahead of its scheduled use.

Since all automatic events during the *Surveyor* terminal descent are based on the AMR mark, which occurs at a nominal 60-mi slant range from the lunar surface, this was the basic cue time selected to start the command tape. For operational simplicity, it was decided to calculate the time at which the emergency AMR mark should occur relative to the predicted AMR mark signal. The taped commands would start at this time so that the timing of the events would be as accurate as operationally possible. The command "emergency AMR mark" would then be sent from the tape instead of from the keyboard as had been done in previous missions. The T&FA and SPAC calculations and command techniques were then perfectly implemented via SPAC command control and the Goldstone *Surveyor* operations team. The change that this nonstandard sequence represented from the normal premission planning is shown in Fig. 11.

It can be noted that, although the special terminal descent sequence did initiate the doppler steering phase approximately 4 s earlier than normal, it did not begin this phase while the retroengine was still burning (reflecting the results of tests which indicated that it would not be feasible to attempt initiation of the doppler steering phase prior to retroengine burnout due to saturation of the acceleration loop). Three other points of interest regarding this sequence are as follows:

(1) The sequence was based on the normal automatic initiation of the vernier engine ignition, retroengine ignition, and RADVS turnon by the AMR triggered at a slant range of 60 mi from the surface.

(2) The commanded delay time between the generation of AMR mark and vernier engine ignition was increased to adjust the retroengine ignition altitude (and range) to the desired lower values.

(3) The time at which the emergency AMR mark command was sent to the spacecraft was significantly delayed from its normal time to ensure that the probability of sending it too soon was negligible.

The difference between the planned sequence timing (AMR mark to retroengine eject) and the actual sequence was 0.32 s, i.e., the planned time between the AMR mark and retroengine eject was 61 s; the actual time was 61.32 s. The components of this time are shown in Fig. 12.

The standard retroengine eject and vernier engine high thrust commands were interchanged to save fuel and provide separation of the retroengine from the spacecraft as soon as possible. The planned 9½ s from the 3½ *g* point to start RADVS control was 4½ s less than the nominal sequence. The planned 4½ s saving was very important in terms of accomplishing spacecraft operations in sufficient time to acquire the descent curve and to achieve a soft landing within the engine burn constraint imposed by the available helium pressure.

In addition to confirming spacecraft performance parameters, mission E was instrumental in further demonstrating the following unique operational capabilities:

(1) Rapid and accurate response to project management instructions not occurring on previous missions.

(2) Rapid playback of data by the SCCF 1219 computer system at HAC El Segundo, for point-by-point plotting in the SPAC area. This capability greatly increases the near real-time analysis capability of the SPAC team.

(3) Six midcourse corrections were accurately executed by SPAC during the *Surveyor V* mission, with the first three firings executed within an unprecedented time block of 50 min.

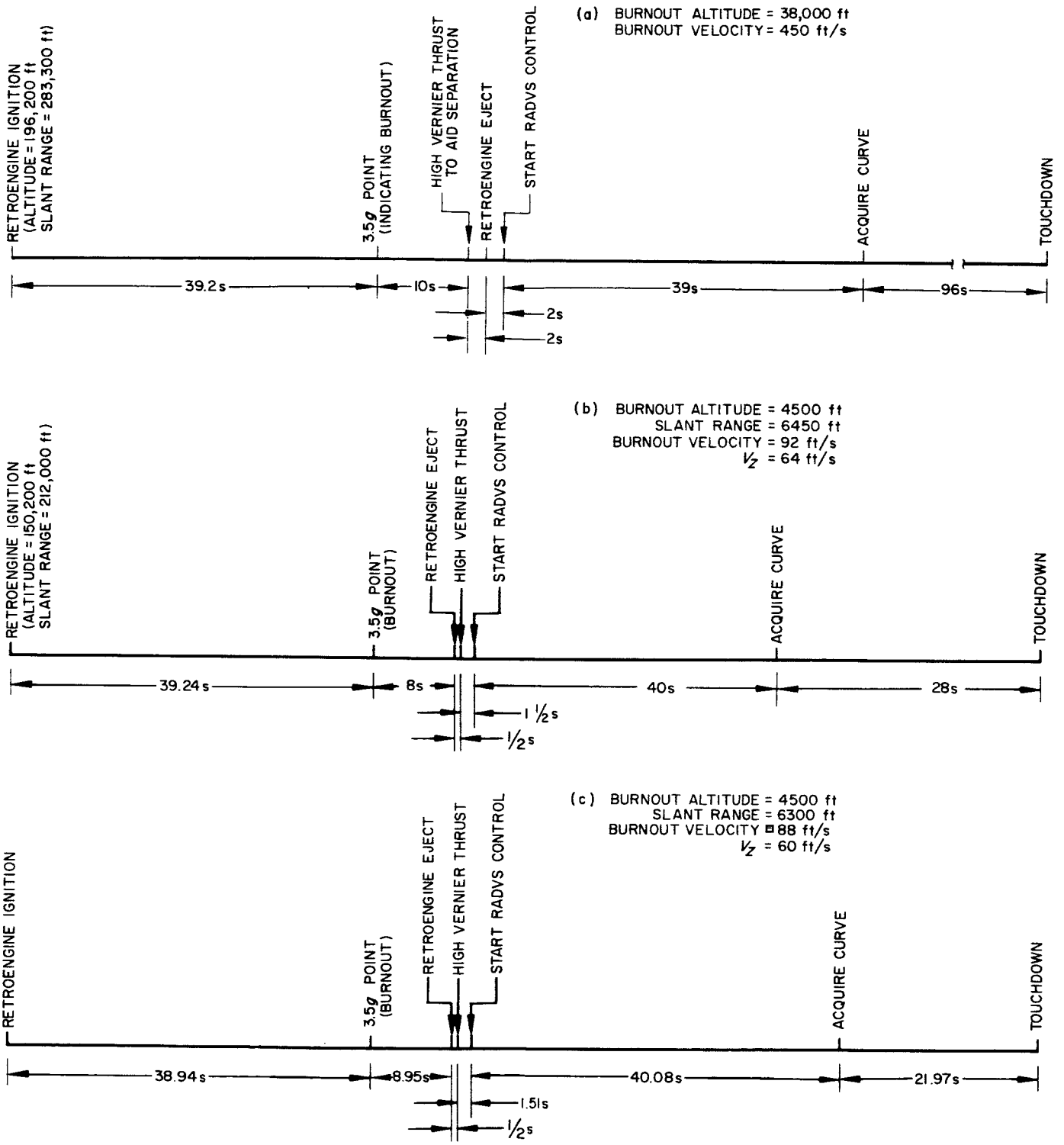

Fig. 11. Terminal descent comparison: (a) premission nominal descent sequence controlled entirely by spacecraft; (b) planned descent to account for limited vernier engine burn time due to helium leak—retroengine eject, vernier high thrust and start radar altimeter and doppler velocity sensor (RADVS); (c) quick look report real time preliminary assessments of actual descent—retroengine eject vernier high thrust and start RADVS control initiated by ground command

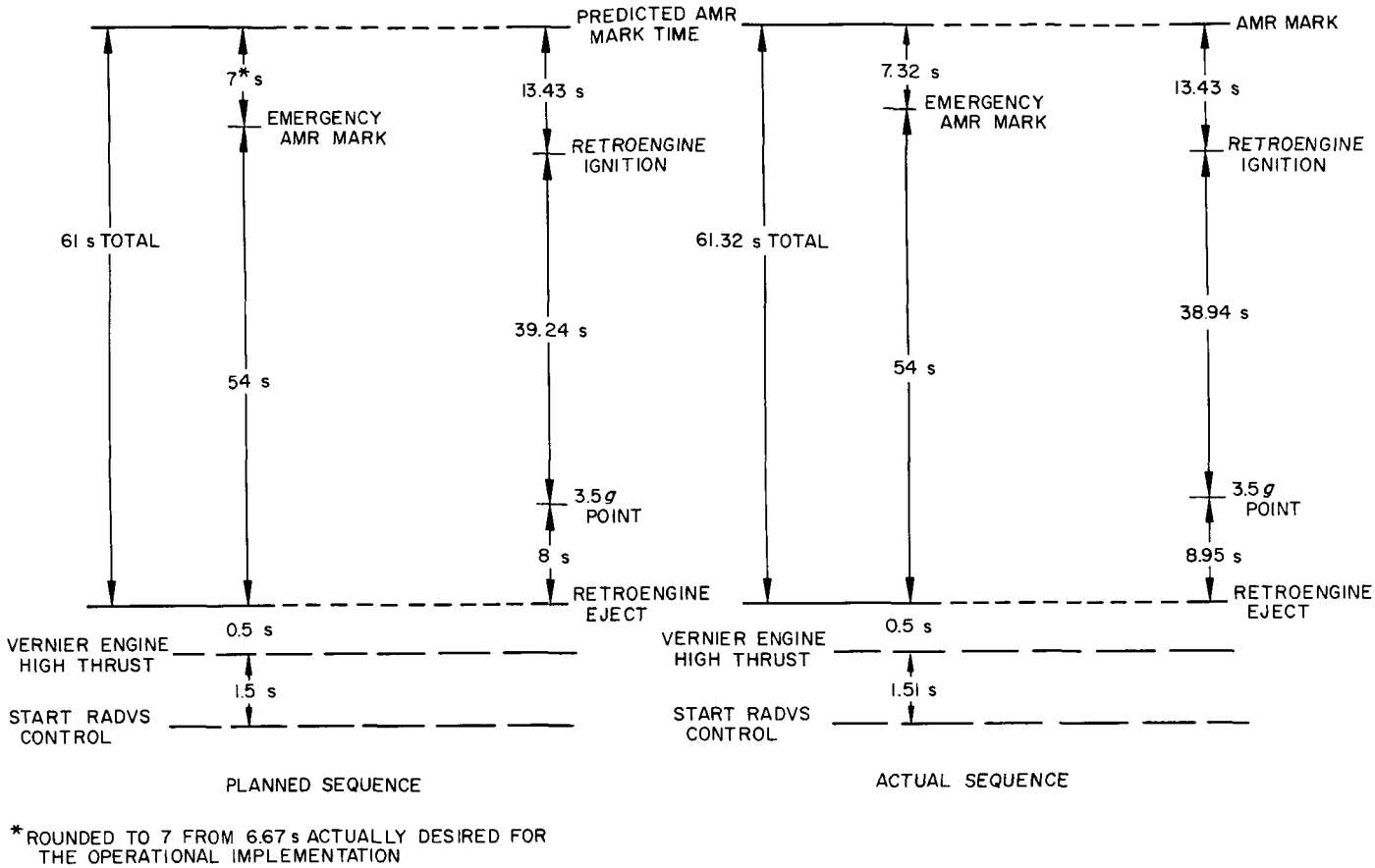

Fig. 12. Comparison of planned and actual descent sequences

(4) Command tape transmission time accuracy was demonstrated not only during complex engine firings but during terminal descent where critical commands were received at the spacecraft within 0.32 s of their intended time.

(5) The SPAC "man-in-the-loop" team succeeded in taking advantage of the inherent flexibility of the spacecraft design to achieve a soft landing at the target location in spite of a seemingly disastrous pressure leak in the vernier engine helium system. This was the first mission where the T&FA group was afforded an opportunity to contribute to mission success and demonstrate their technical excellence.

N. A Study to Preclude Spacecraft Motion During Static Firing[6]

Relationships of vernier engine thrusts, local slope, and two different spacecraft roll orientations are developed and graphically presented. The spacecraft motions considered are those which could result from sliding acceleration or angular acceleration. Of course, it is the intent of the static firing experiment not to move the spacecraft.

Graphical results are presented parametrically to aid in approximating the possibility of spacecraft motion for the static firing experiment. These graphs are based upon preliminary predictions of lunar thermal conditions, the spacecraft roll orientation, and a range of assumed local slopes.

To improve the predictions for spacecraft motion equations are developed for use in real time analysis after having obtained information about spacecraft attitude, roll orientation and thermal data on the vernier engine. The roll orientation and thermal data provide information with regard to which vernier engine(s) will be hot and how much thrust to expect out of each engine. The post-landed spacecraft attitude determination accuracy allows for more accurate prediction of spacecraft motion, if any, during static firing.

[6]Prepared by JPL Technical Section 292.

1. Sliding

For sliding to occur during the static firing of nominal engines, the following conditions are required:

(1) Spacecraft resting on a slope.

(2) No spacecraft footpads embedded in lunar surface material.

With high thrusting engines, sliding may occur even though the footpads are embedded in the lunar surface by first lifting the spacecraft out of the embedded footprints. Of course, this condition could be classified primarily as "liftoff" instead of sliding.

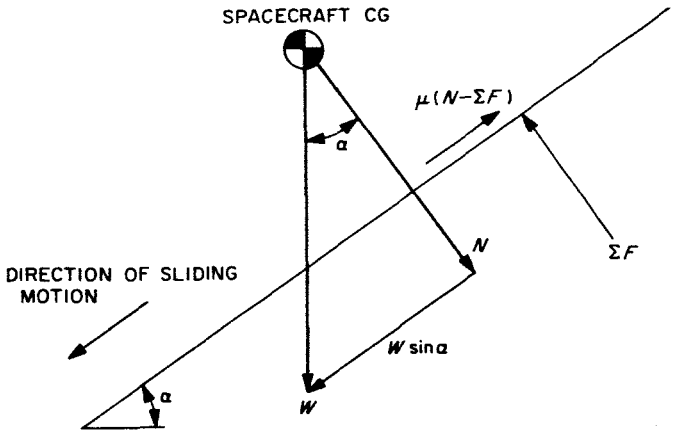

Fig. 13. Spacecraft sliding forces

From the sum of the forces equation (Fig. 13) the equation for sliding acceleration during burn is

$$\frac{W}{g} a_b = W \sin\alpha - \mu (N - \Sigma F) \tag{1}$$

$$a_b = g(\sin\alpha - \mu\cos\alpha) + \mu\frac{\Sigma F}{m}$$

a_b = sliding acceleration during burn

ΣF = total thrust of the three vernier engines

μ = coefficient of friction of local lunar surface ($0.4 \leq 0.8$)

g = lunar gravitational constant (5.32 ft/s^2)

m = spacecraft mass (20.42 slugs)

α = local slope

The values for the downhill sliding acceleration during static firing are shown in Fig. 14 for different values of ΣF, μ, and α.

Total thrust required to initiate spacecraft sliding as a function of α and μ is

$$0 = g(\sin\alpha - \mu\cos\alpha) + \mu\frac{\Sigma F}{m}$$

$$\Sigma F = \frac{-mg}{\mu}(\sin\alpha - \mu\cos\alpha) \tag{2}$$

By substituting values for μ and α the total thrust required to initiate sliding is approximately

$$\Sigma F\ (\mu = 0.4, \alpha = 10\ \text{deg}) = 80\ \text{lb}$$

$$\Sigma F\ (\mu = 0.4, \alpha = 20\ \text{deg}) = 10\ \text{lb}$$

$$\Sigma F\ (\mu = 0.8, \alpha = 10\ \text{deg}) = 95\ \text{lb}$$

$$\Sigma F\ (\mu = 0.8, \alpha = 20\ \text{deg}) = 54\ \text{lb}$$

For the nominal engine (90 lb minimum total thrust) only the third case will not initiate spacecraft motion.

If spacecraft motion is initiated, the total distance the spacecraft will travel is

$$S = S_b + V_{max}\, t_2 + \frac{1}{2} a_2 t_2^2 \tag{3}$$

where

$V_{max} = a_b t_b$ is the velocity achieved during burn

t_b = engine burn time (0.55 s)

$a_2 = -g(\sin\alpha - \mu\cos\alpha)$ is the acceleration (deceleration) of the spacecraft after engine shutdown and is negative

t_2 = required time for spacecraft to come to rest after engine shutdown

$S_b = V_0 t_b + \frac{1}{2} a_b t_b^2$ is the distance the spacecraft moves during burn. $V_0 = 0$ for the initial velocity of the spacecraft

The time t_2 is solved by differentiating Eq. (3) and setting it equal to zero (i.e., the spacecraft comes to rest).

$$\frac{dS}{dt} = V_{max} + a_2 t_2$$

$$0 = a_b t_b + a_2 t_2$$

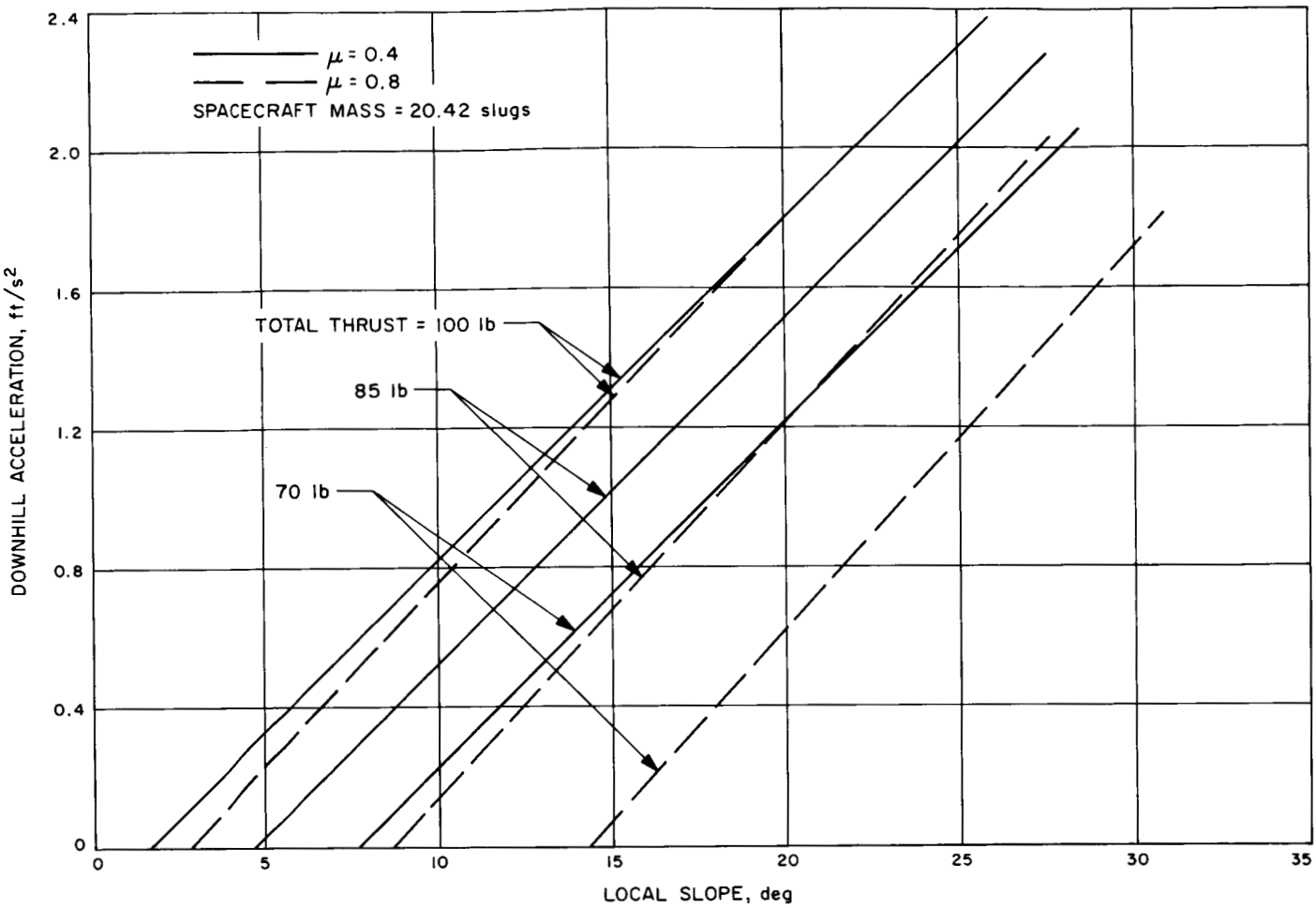

Fig. 14. Downhill sliding acceleration during static firing

substituting for a_b and a_2 and simplifying

$$t_2 = \left(1 + \frac{\mu \Sigma F}{mg\,(\sin\alpha - \mu\cos\alpha)}\right) t_b \qquad (4)$$

substituting V_{max}, S_b, and a_2 in Eq. (3) and simplifying

$$S = a_b\left(\frac{t_b^2}{2} + t_b t_2\right) - \frac{1}{2}\left[g\,(\sin\alpha - \mu\cos\alpha)\right] t_2^2 \qquad (5)$$

2. Rotation About Two Footpads

If spacecraft rotation occurs during a static firing, the most likely rotational axis is that connecting two footpads which are closest to being perpendicular to the downhill direction. Due to spacecraft symmetry, the equations developed for spacecraft motion about this axis apply for any roll orientation, provided two footpads are downslope. Spacecraft geometric values are noted in Fig. 15.

From the sum of the forces equation the equation for angular acceleration ($\ddot{\theta}_b$) during burn is

$$I_A\ddot{\theta}_b = L_1F_1 + L_2F_2 + L_3F_3 - L_4\,mg\cos\alpha + Z\,mg\sin\alpha$$

$$\ddot{\theta}_b = \frac{L_1F_1 + L_2F_2 + L_3F_3 + (Z\sin\alpha - L_4\cos\alpha)\,mg}{I_A} \qquad (6)$$

F_1, F_2, F_3 are the vernier engine thrusts and I_A (moment of inertia about the axis of rotation A) is

$$I_A \approx I_{CG} + m\,[(L_4)^2 + (Z)^2]$$

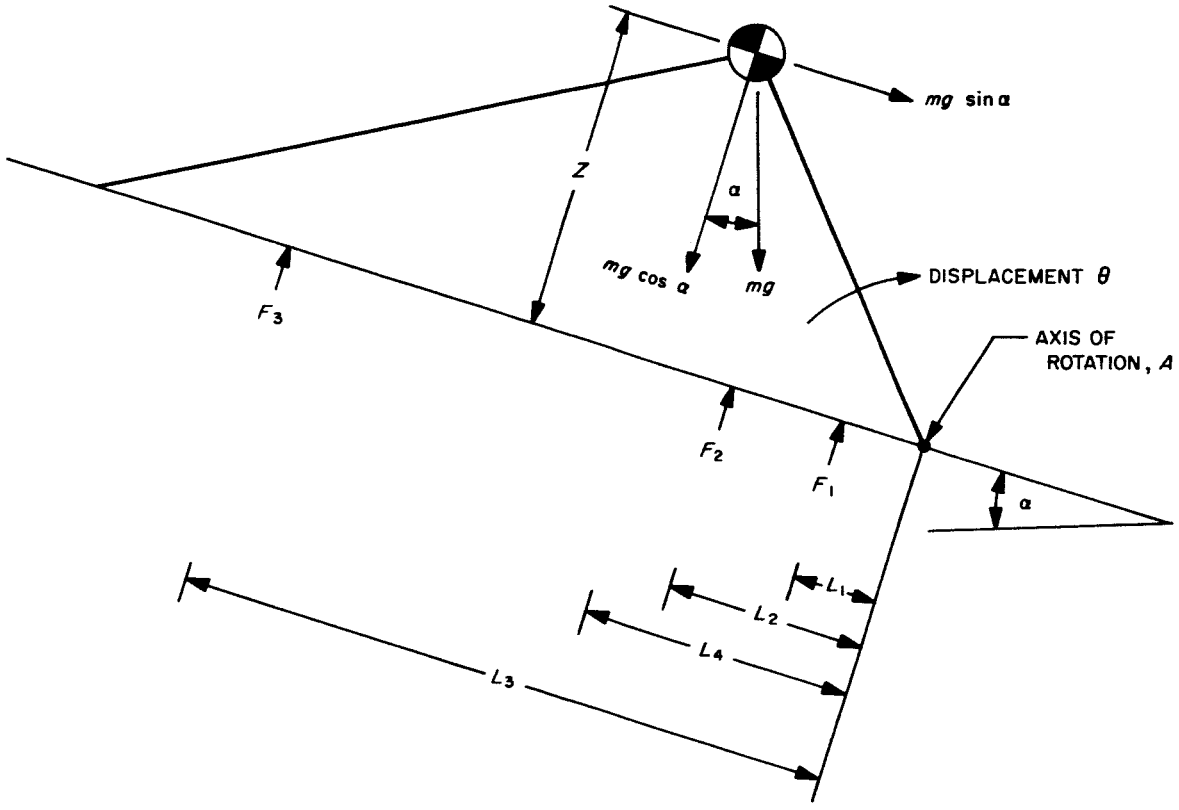

LOCATION OF ENGINES WITH TWO FOOTPADS DOWNHILL = $\begin{cases} L_1 \text{ (0.80 ft)} \\ L_2 \text{ (2.82 ft)} \\ L_3 \text{ (6.16 ft)} \end{cases}$

DISTANCE FROM ROTATIONAL AXIS TO CG IN $x-y$ PLANE = L_4 (3.19 ft)

HEIGHT FROM FOOTPAD TO CG = Z (2.95 ft)

ANGULAR DISPLACEMENT OF THE SPACECRAFT ABOUT THE ROTATIONAL AXIS $A = \theta$

APPROXIMATE VALUE FOR MOMENT OF INERTIA ABOUT AXIS OF ROTATION $A = I_A$ (531) slug-ft^2

Fig. 15. Rotation about two footpads

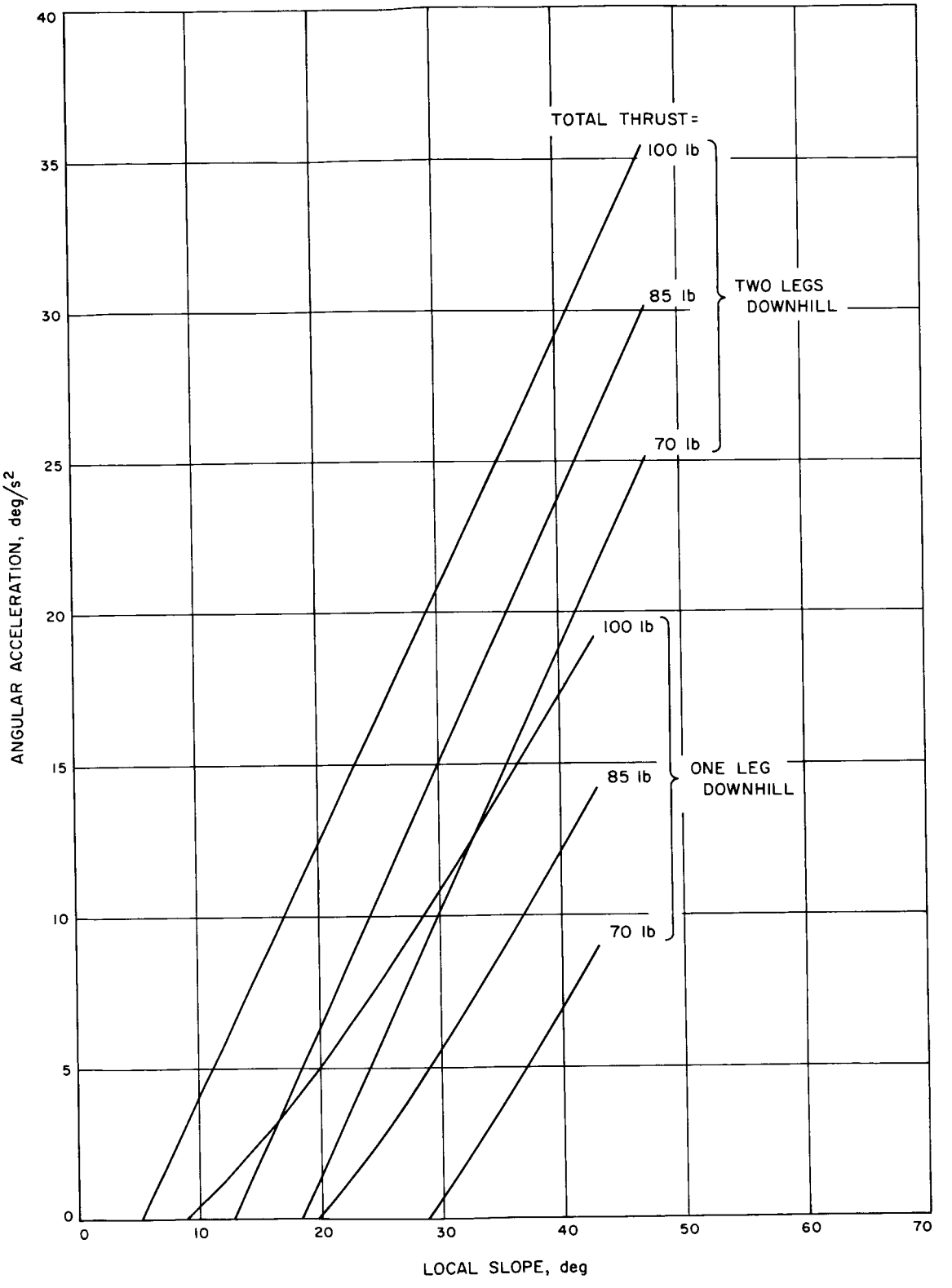

Fig. 16. Initial overturning angular acceleration

The values for the overturning angular acceleration during static fire are shown in Fig. 16 for two legs downhill for different values of ΣF and α.

Total thrust required to initiate spacecraft rotation about an axis through two footpads in the downhill direction is shown in Fig. 17 for different values of α. Equation (7) is used to calculate this total thrust.

$$0 = L_1F_1 + L_2F_2 + L_3F_3 - L_4\,mg\cos\alpha + Z\,mg\sin\alpha \tag{7}$$

Let $F_1 = F_2 = F_3$, then F (per engine)

$$= \frac{mg\,(L_4\cos\alpha - Z\sin\alpha)}{L_1 + L_2 + L_3}$$

where $3 \times F$ = total thrust required as α is varied.

For the nominal engines (90 lb minimum total thrust) spacecraft rotation will occur for α values greater than 10 deg for two legs downhill, as indicated in Fig. 17. If spacecraft rotation is initiated, the maximum angular travel is

$$\theta_{max} = \theta_b + \dot{\theta}_{max}\,t_2 + \frac{1}{2}\,\ddot{\theta}_2\,t_2^2 \tag{8}$$

$\dot{\theta}_{max} = \ddot{\theta}_b t_b$ is the angular velocity achieved during burn.

$\theta_b = \dot{\theta}_0 t_b + 1/2\,\ddot{\theta}_b t_b^2$ is the angle the spacecraft moves through during burn. $\dot{\theta}_0 = 0$ for the initial angular velocity of the spacecraft.

$$\ddot{\theta}_2 = -\left(\frac{(Z\sin\alpha - L_4\cos\alpha)\,mg}{I_A}\right)$$

is the acceleration (deceleration) of the spacecraft after engine shutdown and is negative.

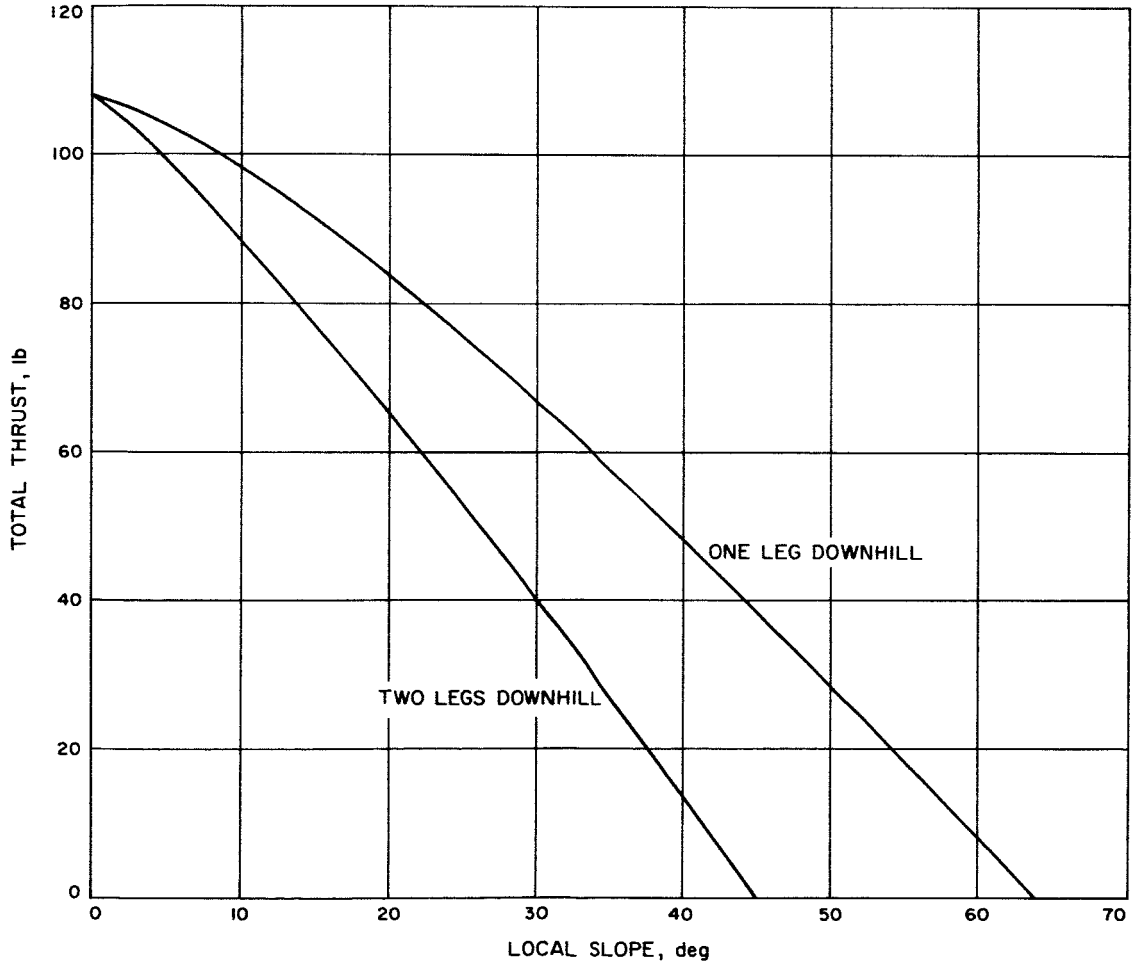

Fig. 17. Total thrust required to start downhill rotation

t_2 = required time for spacecraft to reach maximum angle after engine shutdown.

t_b = engine burn time (0.55 s).

The time t_2 is solved by differentiating Eq. (8) and setting it equal to zero (i.e., the spacecraft angular velocity is zero at maximum angular rotation).

$$\frac{d\theta}{dt} = \dot{\theta}_{max} + \ddot{\theta}_2 t_2$$

$$0 = \ddot{\theta}_b t_b + \ddot{\theta}_2 t_2$$

Substituting for $\ddot{\theta}_b$ and $\ddot{\theta}_2$ and simplifying

$$t_2 = \left[1 + \frac{(L_1F_1 + L_2F_2 + L_3F_3)}{(Z \sin \alpha - L_4 \cos \alpha)\, mg}\right] t_b \tag{9}$$

Substituting θ_b, $\dot{\theta}_{max}$, and $\ddot{\theta}_2$ in Eq. (8) and simplifying, the maximum angular travel is

$$\theta_{max} = \ddot{\theta}_b \left[\frac{t_b^2}{2} + t_b t_2\right] - \frac{1}{2}\left[\frac{(Z \sin \alpha - L_4 \cos \alpha)\, mg}{I_A}\right] t_2^2 \tag{10}$$

The above equations considered all engines terminating thrust simultaneously. If one or two engines continue thrusting, Eq. (6) can be used with appropriate values of thrust.

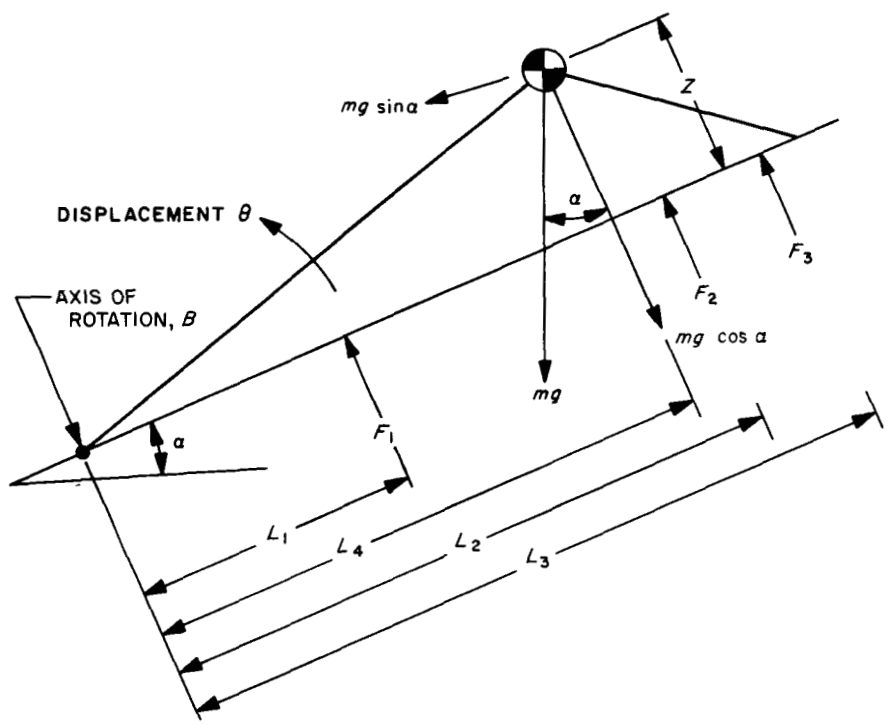

LOCATION OF ENGINES WITH TWO FOOTPADS DOWNHILL = $\begin{cases} L_1 \text{ (3.41 ft)} \\ L_2 \text{ (6.95 ft)} \\ L_3 \text{ (8.77 ft)} \end{cases}$

DISTANCE FROM ROTATIONAL AXIS TO CG IN $x-y$ PLANE = L_4 (6.38 ft)

HEIGHT FROM FOOTPAD TO CG = Z (2.95 ft)

ANGULAR DISPLACEMENT OF THE SPACECRAFT ABOUT THE ROTATIONAL AXIS A = θ

APPROXIMATE VALUE FOR MOMENT OF INERTIA ABOUT AXIS OF ROTATION = I_B (1155 SLUG-ft^2)

Fig. 18. Rotation about one footpad

3. Rotation About One Footpad

If a single leg is almost directly downhill, the rotation may take place about one axis perpendicular to this leg. This is perhaps a less likely occurrence than the previous example, where the spacecraft had two legs downhill, from a stability standpoint. Due to spacecraft symmetry, the equations developed for spacecraft motion about this axis apply for any roll orientation, provided one footpad is downslope. Specific geometric values are noted in Fig. 18.

From the sum of the forces equation the angular acceleration during burn is

$$I_B \ddot{\theta}_b = L_5F_1 + L_6F_2 + L_7F_3 - L_8\, mg \cos \alpha + Z\, mg \sin \alpha \quad (11)$$

where I_B (moment of inertia about the axis of rotation B) is

$$I_B \approx I_{CG} + m\,[(L_8)^2 + (Z)^2]$$

The rest of the equations are developed similarly as for the spacecraft rotation about two footpads.

The geometric values for the spacecraft model with one leg downhill is shown in Fig. 18. The initial overturning angular acceleration ($\ddot{\theta}_b$) and the total thrust required to start downhill rotation for one leg downhill is compared to values calculated for two legs downhill in Figs. 16 and 17.